
Aus der Medizinischen Klinik und Poliklinik IV
Klinikum der Ludwig-Maximilians-Universität München
Vorstand: Prof. Dr. Martin Reincke

**Micro- and macroadenomas causing primary
aldosteronism: molecular and biochemical studies**

Dissertation
zum Erwerb des Doktorgrades der Medizin
an der Medizinischen Fakultät der
Ludwig-Maximilians-Universität zu München

vorgelegt von
Yuhong Yang

aus
Nanchang, China

2021

Mit Genehmigung der Medizinischen Fakultät
der Universität München

Berichterstatter: Prof. Dr. Martin Reincke

Mitberichterstatter: PD Dr. Dr. Urs Lichtenauer
Prof. Dr. Michael Ritter
PD Dr. Georg Vlotides

Mitbetreuung durch den
promovierten Mitarbeiter: Dr. Tracy Ann Williams

Dekan: Prof. Dr. med. Thomas Gudermann

Tag der mündlichen Prüfung: 25.11.2021

Affidavit



Affidavit

Yang, Yuhong

Surname, first name

Street

Zip code, town, country

I hereby declare, that the submitted thesis entitled:

Micro- and macroadenomas causing primary aldosteronism: molecular and biochemical studies

is my own work. I have only used the sources indicated and have not made unauthorized use of services of a third party. Where the work of others has been quoted or reproduced, the source is always given.

I further declare that the submitted thesis or parts thereof have not been presented as part of an examination degree to any other university.

Nanjing, 26.11.2021

place, date

Yuhong Yang

Signature doctoral candidate

Table of contents

Table of contents	1
List of abbreviations.....	2
List of publications	3
1. Introduction.....	5
1.1 Human adrenal cortex and aldosterone	5
1.1.1 Steroidogenesis	5
1.1.2 Aldosterone synthase	5
1.1.3 Histology of human zona glomerulosa.....	6
1.2 Primary aldosteronism	6
1.2.1 Prevalence	6
1.2.2 Subtypes.....	6
1.2.3 Subtype differentiation	7
1.2.3.1 Computed tomography.....	7
1.2.3.2 Adrenal venous sampling.....	7
1.2.3.3 Steroid profiling	8
1.2.4 Treatment and outcomes.....	9
1.2.5 Genetic causes of primary aldosteronism.....	9
1.2.6 Histopathology	12
1.2.7 Transcriptomics.....	12
1.2.8 <i>In vitro</i> cell models	13
1.3 Specific aims of the thesis.....	14
2. Methods and results	15
3. Summary	18
4. Zusammenfassung.....	20
5. Significance and perspectives.....	22
6. Contribution to the publications	23
7. Paper I.....	25
8. Paper II.....	43
9. Paper III.....	70
10. References	85
Acknowledgements	94

List of abbreviations

CT	computed tomography
CYP11B1	11 β -hydroxylase
CYP11B2	aldosterone synthase
CYP17A1	17 α -hydroxylase/17,20 lyase
H&E	hematoxylin-eosin
LC-MS/MS	liquid chromatography tandem mass spectrometry
zF	zona fasciculata
zG	zona glomerulosa
zR	zona reticularis

List of publications

Publications summarized in the thesis

Paper I

Title: Classification of microadenomas in patients with primary aldosteronism by steroid profiling

Authors: Yang Y*, Burrello J*, Burrello A, Eisenhofer G, Peitzsch M, Tetti M, Knösel T, Beuschlein F, Lenders JWM, Mulatero P, Reincke M, Williams TA

Journal: Journal of Steroid Biochemistry and Molecular Biology

Year: 2019

Volume: 189

Pages: 274-282

DOI: 10.1016/j.jsbmb.2019.01.008

*Authors contributed equally to the work

Paper II

Title: *BEX1* is differentially expressed in aldosterone-producing adenomas and protects human adrenocortical cells from ferroptosis

Authors: Yang Y, Tetti M, Vohra T, Adolf C, Seissler J, Hristov M, Belavgeni A, Bidlingmaier M, Linkermann A, Mulatero P, Beuschlein F, Reincke M, Williams TA

Journal: Hypertension

Year: 2021

Volume: 77

Pages: 1647-1658

DOI: 10.1161/HYPERTENSIONAHA.120.16774

Paper III

Title: Primary aldosteronism: *KCNJ5* mutations and adrenocortical cell growth

Authors: Yang Y, Gomez-Sanchez CE, Jaquin D, Prada ETA, Meyer LS, Knösel T, Schneider H, Beuschlein F, Reincke M, Williams TA

Journal: Hypertension

Year: 2019

Volume: 74

Pages: 809-816

Further publications during doctoral study

Yang Y, Reincke M, Williams TA. Prevalence, diagnosis and outcomes of treatment for primary aldosteronism. *Best Pract Res Clin Endocrinol Metab* 2019; 34: 101365

Yang Y, Reincke M, Williams TA. Treatment of unilateral PA by adrenalectomy: potential reasons for incomplete biochemical cure. *Exp Clin Endocrinol Diabetes* 2019; 127: 100-108

Williams TA, Jaquin D, Burrello J, Philippe A, **Yang Y**, Rank P, Nirschl N, Sturm L, Hübener C, Dragun D, Bidlingmaier M, Beuschlein F, Reincke M. Diverse responses of autoantibodies to the angiotensin II type 1 receptor in primary aldosteronism. *Hypertension* 2019; 74: 784-792

Aristizabal Prada ET, Castellano I, Susnik E, **Yang Y**, Meyer LS, Tetti M, Beuschlein F, Reincke M, Williams TA. Comparative genomics and transcriptome profiling in primary aldosteronism. *Int J Mol Sci* 2018; 19: 1124

Awards/prizes during doctoral study

- 2019 **Basic Science Meeting Grant**
 21st European Congress of Endocrinology - Lyon
- 2018 **Brownie Schwimmer Young Investigator Prize**
 18th Adrenal Cortex Conference - Munich

1. Introduction

1.1 Human adrenal cortex and aldosterone

1.1.1 Steroidogenesis

The adrenal cortex is a primary source of steroid production. The human adrenal cortex comprises three concentric zones: the zona glomerulosa (zG, outermost), zona fasciculata (zF, middle) and zona reticularis (zR, innermost) [1] that produce mineralocorticoids, glucocorticoids and androgens, respectively [2].

The zona glomerulosa is the predominant site of aldosterone synthesis, which is the primary mineralocorticoid. Aldosterone is derived from cholesterol which is transported from the outer to the inner mitochondrial membrane by steroidogenic acute regulatory protein (encoded by *STAR*). Cholesterol side chain cleavage enzyme (encoded by *CYP11A1*) then catalyzes cholesterol to pregnenolone, that diffuses to the endoplasmic reticulum and pregnenolone is then converted to progesterone by 3 β -hydroxysteroid dehydrogenase (encoded by *HSD3B2*), followed by conversion to 11-deoxycorticosterone by 21-hydroxylase (encoded by *CYP21*). The final steps in the biosynthesis of aldosterone are mediated by aldosterone synthase (*CYP11B2*, encoded by *CYP11B2*) at the inner mitochondrial membrane via three consecutive reactions of 11 β -hydroxylation, 18-hydroxylation and 18-oxidation [3]. The process of steroidogenesis in the human adrenal cortex is summarized in **Figure 1**.

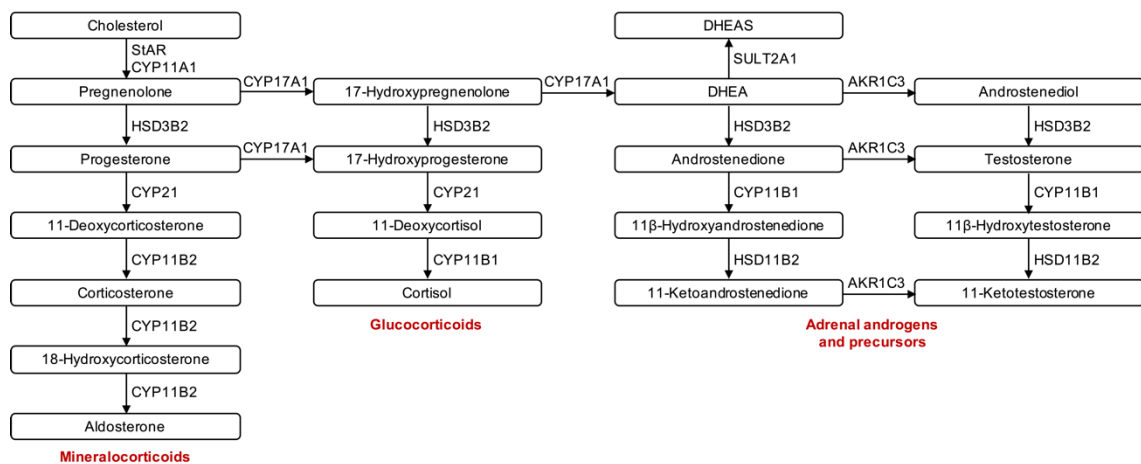


Figure 1. Steroids and enzymes involved in steroidogenesis. DHEA, dehydroepiandrosterone; DHEAS, dehydroepiandrosterone sulfate.

1.1.2 Aldosterone synthase

Aldosterone synthase (referred to as *CYP11B2*) is a member of the cytochrome P450 superfamily, which is a heme-containing protein family that receives electrons from NADPH (reduced nicotinamide adenine dinucleotide phosphate) via electron transfer proteins to perform enzymatic reactions [3]. *CYP11B2* is 95% and 93% homologous to 11 β -hydroxylase (*CYP11B1*) at the cDNA and amino acid levels, respectively [4]. *CYP11B2* and *CYP11B1* are tandemly located in chromosome

8 (with 40 kbp separating the two genes) [5]. Unlike CYP11B2, which is expressed in the zG, CYP11B1 is expressed in the zF and zR [6].

1.1.3 Histology of human zona glomerulosa

Hematoxylin-eosin (H&E) staining is a conventional method for morphological assessment of resected tissue sections. In H&E-stained human adrenal slices, zG cells are small and compact; in contrast, zF cells are larger, and have a clear appearance due to their lipid-rich content.

The specific monoclonal antibody against human CYP11B2 generated in 2014 has enabled the visualization of the likely source of aldosterone production [7]. In human adrenals from young individuals, especially aged under 10, CYP11B2-positive cells form a continuous layer throughout the zG [8]. With aging, the continuous zG layer is replaced with clusters of cells with CYP11B2 expression [8]. These nests of cells, originally called aldosterone-producing cell clusters [9], are now referred to as aldosterone-producing micronodules following a recent international histopathology consensus which standardized the nomenclature for the histopathology of primary aldosteronism [10]. Aldosterone-producing micronodules are CYP11B2-positive lesions (diameter <10 mm) that are situated just beneath the capsule of the adrenal gland [10], which, unlike a nodule, are morphologically indistinguishable with H&E staining.

1.2 Primary aldosteronism

1.2.1 Prevalence

Primary aldosteronism, due to autonomous aldosterone production by the adrenal gland, was initially reported in 1955 in a woman presenting severe hypertension, hypokalemia, temporary paralysis, muscle spasms, mild hypernatremia and metabolic alkalosis [11]. The wide application of a screening test to measure the plasma aldosterone-to-renin ratio (the ratio between plasma aldosterone concentration and plasma renin activity or direct renin concentration) has dramatically increased the detection rate of primary aldosteronism [12], leading to an estimate of 2.6-12.7% in hypertensive patients in primary care centers and 0.7-29.8% in referral centers [13, 14]. Spontaneous hypokalemia is present in 0-38% of patients with primary aldosteronism in primary care centers and 0-67% in tertiary hypertension units [13]. Primary aldosteronism is now regarded as the most prevalent cause of endocrine hypertension and is characterized by aldosterone excess and suppressed plasma renin. Compared with essential hypertension, primary aldosteronism carries an increased risk of cardiovascular and cerebrovascular events, diabetes and metabolic syndrome [15].

1.2.2 Subtypes

Primary aldosteronism is either hereditary (familial hyperaldosteronism types I-IV), which accounts for <5% of cases of the disease [16], or arises sporadically. The sporadic forms are classified into unilateral and bilateral forms based on the source of aldosterone overproduction. Aldosterone-producing adenoma is the most common unilateral form that comprises ~30% of primary aldosteronism [16]. Other unilateral forms are rarely detected, including unilateral hyperplasia (2%) and aldosterone-producing carcinoma (<1%) [16]. Bilateral adrenal hyperplasia is the bilateral form of primary aldosteronism constituting ~60% of primary aldosteronism [16].

1.2.3 Subtype differentiation

1.2.3.1 Computed tomography

In adrenal computed tomography (CT), typical radiographic findings of primary aldosteronism include adrenals with a normal appearance, unilateral adrenal limb thickening, unilateral microadenoma (diameter <10 mm), unilateral macroadenoma (diameter ≥10 mm), and bilateral micro or macroadenoma (or a combination of both) [17]. However, CT scanning often has insufficient sensitivity to identify micro aldosterone-producing adenomas [17]. Many studies have reported that imaging alone has a low accuracy for subtype differentiation of aldosterone-producing adenoma from bilateral adrenal hyperplasia, ranging from 58-80% [18-21]. However, CT is nonetheless diffusely used for subtype classification due to its wide availability. CT scanning is mandatory in patients with newly confirmed primary aldosteronism to exclude an aldosterone-producing carcinoma (usually >40 mm in diameter) [17]. In addition, CT is a reliable method for subtype differentiation in a restricted subgroup of patients: young patients aged below 35 years with CT appearance of a large nodule (diameter >10 mm) and normal contralateral adrenal gland, high plasma aldosterone concentration (>30 ng/dL) and spontaneous hypokalemia [17, 21]. CT scanning can also help visualize adrenal veins, which is helpful for cannulation in adrenal venous sampling [17].

1.2.3.2 Adrenal venous sampling

Adrenal venous sampling is recognized as the “gold standard” for subtype differentiation of primary aldosteronism. A successful adrenal venous sampling requires the correct bilateral catheterization of adrenal veins via percutaneous femoral vein for blood sampling and a peripheral vein for the measurement of aldosterone and cortisol concentrations [17]. The interpretation of adrenal venous sampling results requires two major indices, the selectivity index and the lateralization index. The selectivity index, the ratio of cortisol concentrations in the adrenal vein and a peripheral vein, is used to demonstrate the correct cannulation of the adrenal veins. Most centers adopt a selectivity index > 2 to 3 in unstimulated adrenal venous sampling and > 3 to 5 in adrenal venous sampling stimulated with adrenocorticotrophic hormone [22, 23]. The lateralization index, the aldosterone/cortisol ratio of the ipsilateral (dominant) adrenal vein divided by the same ratio of the contralateral (non-dominant) vein, is used to determine the source of hyperaldosteronism. A lateralization index cut-off of 2 has been recommended for unstimulated adrenal venous sampling and 4 for adrenal venous sampling stimulated by adrenocorticotrophic hormone [22].

Adrenal venous sampling relies on the overproduction of aldosterone and as such CT undetectable micro aldosterone-producing adenomas that cause lateralized aldosterone production can be detected using this approach. Moreover, non-functional macroadenomas will not be mistaken for aldosterone-producing adenomas by adrenal venous sampling which is the case with approaches that rely on nonfunctional imaging.

However, adrenal venous sampling has limitations. Adrenal venous sampling is an invasive and technically-demanding procedure with various protocols and criteria for result interpretation. Moreover, some patients receiving successful cannulation and stringent evaluation of lateralization index (ranging from 4.4-10) can still display hyperaldosteronism after surgery, indicating pre-surgical bilateral primary aldosteronism [24]. The concomitant cortisol secretion from the ipsilateral adrenal gland may decrease the ratio of aldosterone/cortisol of the ipsilateral side. In contrast, it may increase the same ratio of the contralateral side due to a contralateral suppression of cortisol. It may result in a false diagnosis of bilateral adrenal hyperplasia instead of aldosterone-

producing adenoma [25]. Alternative approaches for subtype differentiation of primary aldosteronism have been intensively sought to reduce or even replace adrenal venous sampling.

1.2.3.3 Steroid profiling

Steroid profiling has a potential future application for subtype differentiation. Efforts have been made to identify steroid biomarkers of primary aldosteronism subtypes, since the identification of elevated levels of C-18-oxygenated steroids in a patients with aldosterone-producing adenomas [26]. The subsequent studies found that the levels of 18-hydroxycortisol [27-29] and 18-oxocortisol [27, 29] were higher in patients with aldosterone-producing adenomas, compared with patients with bilateral adrenal hyperplasia. However, it was not feasible to use these steroids for subtype differentiation because of the lack of diagnostic accuracy [29] and the insufficient accuracy of radioimmunoassays [17].

Liquid chromatography tandem mass spectrometry (LC-MS/MS), an innovative analytical technology, opens a new dimension for the specific and quantitative measurement of steroids. Prior to LC-MS/MS, sample preparations are necessary to eliminate proteins that would otherwise block injectors and column frits [30]. Based on the theory that steroids are a heterogeneous mixture of compounds with distinct chemical properties, five major LC-MS/MS processes have been established for the separation and detection of steroids. The first step is the generation of ions by, e.g. electrospray ionization technique, followed by the selection of ions within a vacuum based on their mass-to-charge values. Then selected ions are transported into collision cell containing argon or nitrogen for fragmentation. Fragmented ions are later transported and selected by variable radiofrequency settings, with the final detection of ions by a tandem mass spectrometer. Two consecutive rounds of selection allow multi-analyte quantification in parallel and achieve very high specificity [31]. The panels of steroids are measured differently among centers by LC-MS/MS. Twenty-one steroids have been measured in the clinical studies focusing on primary aldosteronism: aldosterone, cortisol, cortisone, corticosterone, 18-oxocortisol, 18-hydroxycortisol, 11-deoxycortisol, 21-deoxycortisol, 11-deoxycorticosterone, progesterone, pregnenolone, 17-hydroxyprogesterone, androstenedione, 11 β -hydroxyandrostenedione, 11-ketoandrostenedione, dehydroepiandrosterone, dehydroepiandrosterone sulfate, testosterone, 11 β -hydroxytestosterone, 11-ketotestosterone, and 16 α -hydroxyprogesterone [32-34].

A Japanese study firstly utilized LC-MS/MS technology to measure the levels of peripheral plasma 18-oxocortisol and 18-hydroxycortisol in patients with primary aldosteronism. After excluding micro aldosterone-producing adenomas in the study cohort, they identified that 18-oxocortisol measured by LC-MS/MS in combination with plasma aldosterone concentration achieved an accuracy of 84% in subtype differentiation [35]. However, this remarkable accuracy was not reproducible in European centers potentially due to different frequencies of somatic mutations in aldosterone-producing adenomas. Subsequent studies took advantage of the multi-analyte quantification of LC-MS/MS and found that a combination of multiple steroids in peripheral plasma achieved a more satisfactory accuracy in subtype differentiation [32-34]. Steroid profiling is therefore one of promising approaches for subtype differentiation of primary aldosteronism, especially is beneficial to centers without access to adrenal venous sampling. Nevertheless, the utility of steroid profiling in identifying CT-undetectable micro aldosterone-producing adenomas has not been investigated. It is worthwhile to evaluate the utility of peripheral plasma steroid profiling in subtype classification of primary aldosteronism to provide an alternative, supplement, or even substitute method to adrenal venous sampling in the routine diagnostic algorithm.

1.2.4 Treatment and outcomes

Unilateral primary aldosteronism is surgically correctable if appropriate adrenalectomy removes all sources of hyperaldosteronism. Conversely, patients with bilateral adrenal hyperplasia require the life-long medical therapy by mineralocorticoid receptor antagonists [17].

The Primary Aldosteronism Surgical Outcome (PASO) study has established a set of standardized criteria for assessing clinical and biochemical outcomes in patients diagnosed with unilateral primary aldosteronism undergoing surgical treatment [24]. The clinical and biochemical outcomes are classified into complete (cure), partial (improvement) and absent (failure) success based on blood pressure, dose of antihypertensive drugs, plasma potassium concentrations, plasma aldosterone concentrations, and renin concentrations or activities [24]. In this study, which included 705 patients with primary aldosteronism, the majority of patients (94%, 656/699) achieved complete biochemical success, whilst 37% (259/705) of patients achieved complete clinical success after surgical treatment [24]. Incomplete (partial and absent) biochemical success indicates that these patients display asymmetrical bilateral aldosterone excess rather than unilateral primary aldosteronism, and should be administered with medical treatment [24].

The risks of target organ damage have been investigated in medically treated patients with primary aldosteronism. Compared with patients with essential hypertension with comparable risk profiles, medically treated patients with primary aldosteronism have higher risks of mortality, diabetes, atrial fibrillation and cardiovascular events if their renin activities remain suppressed ($< 1 \mu\text{g/L}$ per hour). In contrast, the incidence of cardiovascular and metabolic disease are similar between patients with primary hypertension and patients with primary aldosteronism with unsuppressed renin ($\geq 1 \mu\text{g/L}$ per hour) [36]. The Primary Aldosteronism Prevalence in Hypertension study has also identified that medically treated patients with primary aldosteronism showed a lower atrial fibrillation-free survival rate relative to that of patients with essential hypertension [37].

1.2.5 Genetic causes of primary aldosteronism

Whole-exome sequencing of genomic DNA from aldosterone-producing adenomas and paired blood samples has led to the discovery of somatic and germline mutations in patients with primary aldosteronism and has dramatically advanced our understandings of the pathophysiology of primary aldosteronism.

Germline mutations causing all four forms of familial hyperaldosteronism occur in an inherited autosomal dominant fashion. A chimeric gene combining the adrenocorticotrophic hormone-responsive regulatory sequences of *CYP11B1* with the coding sequence of *CYP11B2* is the genetic cause of familial hyperaldosteronism type I, resulting in ectopic *CYP11B2* expression in zF under the regulation of adrenocorticotrophic hormone [38, 39]. Germline mutations in *CLCN2* (encoding the chloride channel protein 2), *KCNJ5* (encoding KCNJ5, potassium inwardly rectifying channel subfamily J member 5), and *CACNA1H* (encoding the voltage-gated T-type calcium channel) are the genetic causes of familial hyperaldosteronism type II [40, 41], type III [42], and type IV [43], respectively. *De novo* germline mutations in *CACNA1D* (encoding the voltage-gated L-type calcium channel, Ca_v1.3) have been identified in patients with primary aldosteronism with seizures and neurological abnormalities (PASNA, primary aldosteronism with seizures and neurological abnormalities) that cause such a severe form of disease that the mutation has not been inherited and is generally not referred to as a familial form of the disease [44].

The surgically removed aldosterone-producing adenomas have been used for the discovery of somatic mutations in genes encoding ion channels (*KCNJ5* [45], *CACNA1D* [44, 46], *CACNA1H*

[47], *CLCN2* [48]) and ion transporters (*ATP1A1* [encoding Na⁺-K⁺-ATPase] [46, 49] and *ATP2B3* [encoding calcium ATPase type 3] [49]). These mutations disturb intracellular homeostasis, activate calcium signaling, and increase *CYP11B2* expression and aldosterone production [47, 50]. The prevalence of somatic mutations has reached 88-96% using the next-generation sequencing approach guided by *CYP11B2*-immunohistochemistry of paraffin-embedded adrenals [51-54].

KCNJ5 mutations are the most prevalent genetic alterations (34-73%) in aldosterone-producing adenomas [51-54], with considerable variations between sex and among different ethnicities. A meta-analysis included 13 studies and 1636 patients with aldosterone-producing adenomas and reported that patients with *KCNJ5* mutations were more often women than men (67% versus 44%) [55]. The prevalence of *KCNJ5* mutations is almost two-fold higher in patients from East Asia (63-73%) compared with European (35-44%) [51, 53-55] and African-American patients with primary aldosteronism (34%) [52]. Compared with patients with *KCNJ5* wild-type, patients with *KCNJ5*-mutated aldosterone-producing adenomas are younger and have adenomas of a larger size [55].

KCNJ5-L168R and G151R were the first reported mutations by Choi et al. in 8 out of 22 aldosterone-producing adenomas using exome sequencing [45]. These two hotspot mutations are the most prevalent *KCNJ5* mutations in aldosterone-producing adenomas (L168R: 23-44%; G151R: 44-79%) [51-54, 56, 57]. Other *KCNJ5* variants are rarely detected in aldosterone-producing adenomas (0-16%) [51-54, 56]. T158A, one of the rare mutations in aldosterone-producing adenomas, was the first mutation described in patients with familial hyperaldosteronism type III with early-onset hypertension, massive adrenal hyperplasia, and resistance to medical treatment [45]. The germline G151R mutation is similarly associated with the severe phenotype of familial hyperaldosteronism type III [42]. Conversely, patients carrying G151E exhibit an absence of massive adrenal hyperplasia and respond to medical therapy [42, 58]. These mutations are located within (G151R/G151E) or close to (L168R/T158A) the selectivity filter of the *KCNJ5* channel that confers potassium selectivity, thereby causing the loss of ion selectivity and increases sodium permeability [42, 45] (**Figure 2**). Increased sodium conductance leads to membrane depolarization and enhances calcium influx via voltage-gated calcium channels. The subsequently activated calcium signaling increases the activity of the *CYP11B2* promoter and stimulates aldosterone overproduction [45]. *In vitro* studies have confirmed that *KCNJ5* mutations induce *CYP11B2* expression and increase aldosterone production in human adrenocortical cells [50]. Unexpectedly, *KCNJ5* mutations cause cell lethality or a decrease in cell proliferation [50, 59], an effect that is sodium-dependent [42]. Compared with G151R, G151E results in a much larger sodium conductance and a more marked lethality in human embryonic kidney cells, coherent with the phenotype-genotype associations between *KCNJ5* mutations and severity of primary aldosteronism [42]. Macrolide antibiotics have been identified as novel selective inhibitors of *KCNJ5* mutations, rather than *KCNJ5* wild-type, by ablating the *KCNJ5* mutation-induced cell lethality and blunting *CYP11B2* expression and aldosterone production in human adrenocortical cells expressing *KCNJ5* mutations [59] and in aldosterone-producing cells isolated from aldosterone-producing adenomas with *KCNJ5* mutations [60].

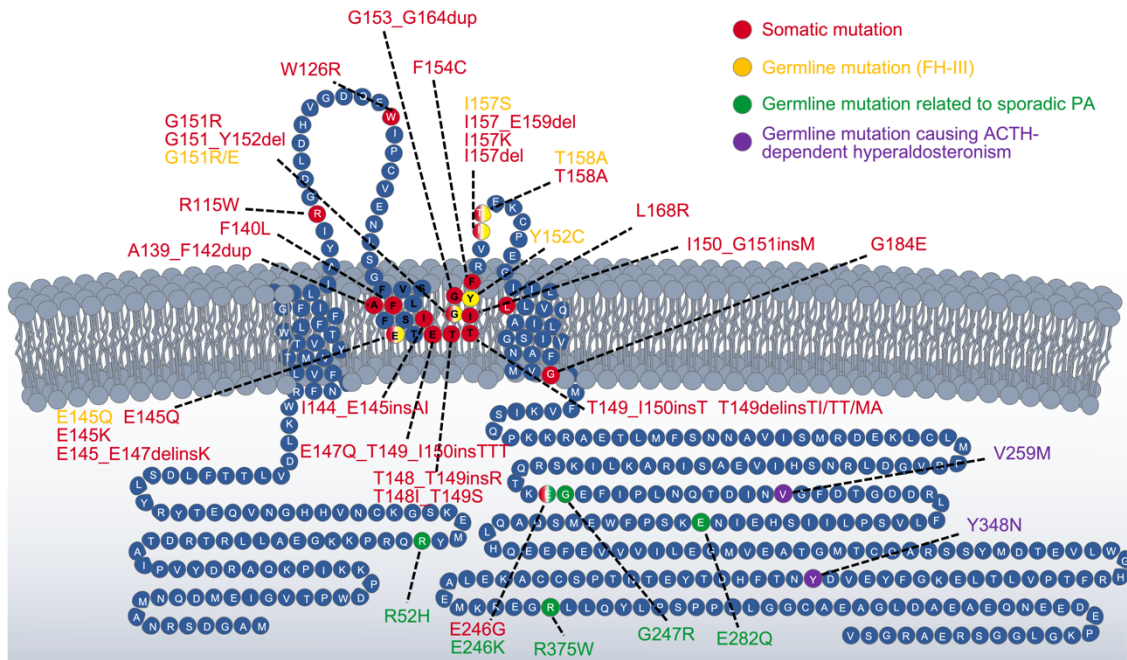


Figure 2. *KCNJ5* germline and somatic mutations causing different forms of primary aldosteronism. Amino acids marked in black and bold indicate the selectively filter of the channel. ACTH, adrenocorticotropic hormone; FH-III, familial hyperaldosteronism type III; *KCNJ5*, gene encoding potassium inwardly rectifying channel subfamily J member 5; PA, primary aldosteronism.

CACNA1D mutations display the second highest mutational frequency (14-27%) in patients with aldosterone-producing adenomas [51, 53, 54] except in a cohort of African-Americans who displayed a higher prevalence of *CACNA1D* mutations (42%) than *KCNJ5* mutations (34%) [52]. *CACNA1D* mutations are more frequent in older and male patients [61], and aldosterone-producing adenomas carrying *CACNA1D* mutations are generally micro aldosterone-producing adenomas [46, 61]. *CACNA1D* encodes the $Ca_v1.3$ calcium channel. The *CACNA1D* mutations cause a shift in voltage-dependent gating of the channel to more negative voltages and suppress channel inactivation, thereby increasing intracellular calcium concentrations, *CYP11B2* transcription and aldosterone production [44, 46].

In addition to *CACNA1D* mutations, the next generation sequencing guided by *CYP11B2* immunohistochemistry has increased the detection of mutations in *ATP1A1* (5-17%) and *ATP2B3* (4-10%) [51-54]. Like *CACNA1D* mutations, *ATP1A1* and *ATP2B3* mutations are more frequent in older and male patients [49, 53], and are detected in aldosterone-producing adenomas of a smaller tumor size compared with aldosterone-producing adenomas with *KCNJ5* mutations [46]. *ATP1A1* mutations cause a substantial reduction in potassium affinity, an inappropriate membrane depolarization and the subsequent activation of calcium signaling and *CYP11B2* transcription [46, 49, 57]. *ATP2B3* mutations impair the capacity of the channel to export calcium, thereby leading to the activated calcium signaling and *CYP11B2* transcription [49].

Somatic mutations in *CTNNB1*, encoding β -catenin, have been reported at a low prevalence in aldosterone-producing adenomas (2-5%) [62, 63]. All *CTNNB1* mutations observed in aldosterone-producing adenomas alter serine/threonine residues (p.Thr41 and p.Ser45) encoded in exon 3 [63]. The corresponding mutated forms of β -catenin bypass phosphorylation and degradation causing activation of WNT/ β -catenin signaling and hyperplastic transformation [64, 65]. Despite the low frequency of *CTNNB1* mutations, 70% of aldosterone-producing adenomas exhibit an

activation of WNT/ β -catenin signaling [66], implicating other factors which induce the activation of this signaling pathway.

1.2.6 Histopathology

Aldosterone-producing adenoma is classically depicted as a single, well circumscribed macronodule consisting of compact, eosinophilic cells (“zG-like”), or lipid-rich, clear cells (“zF-like”), or a combination of both, which can be evaluated by H&E staining [67]. The application of specific monoclonal antibodies against CYP11B2, CYP11B1 [7] and 17 α -hydroxylase/17,20 lyase (CYP17A1) [68] in the immunohistochemistry of pathological adrenal specimens has significantly advanced our knowledge of the histopathological features of primary aldosteronism. CYP11B2 immunoreactivity is highly heterogeneous in aldosterone-producing adenomas, while CYP11B1 tends to be diffuse [69]. Aldosterone-producing adenomas carrying *KCNJ5* mutations display a predominance of clear cells (71%) [70] and cells expressing CYP11B1, with fewer cells expressing CYP11B2 and higher CYP17A1 expression, compared with aldosterone-producing adenomas with other mutations [53, 71, 72]. In *KCNJ5*-mutated aldosterone-producing adenomas, a number of cells express both CYP11B2 and CYP17A1, more compared with aldosterone-producing adenomas with other mutations [53]. This observation likely explains the higher production of 18-oxocortisol and 18-hydroxycortisol in patients with *KCNJ5*-mutated aldosterone-producing adenomas [73], because the synthesis of these steroids requires the enzymatic activities of both CYP11B2 and CYP17A1 [73].

Multiple aldosterone-producing nodules and micronodules, and aldosterone-producing diffuse hyperplasia have also been identified in the resected adrenals [10]. These lesions are more frequently present in patients with primary aldosteronism with absent or partial biochemical success, indicating presurgical bilateral primary aldosteronism in these patients [74].

Aldosterone-producing micronodules are frequently observed in the zG of patients with primary aldosteronism. Sequencing of aldosterone-producing micronodules has demonstrated that most aldosterone-producing micronodules have *CACNA1D* mutations, with a lower frequency in *ATP1A1* and *ATP2B3* mutations [53, 75]. To date, few cases of *KCNJ5* mutations have been identified in aldosterone-producing micronodules [53].

Aldosterone-producing micronodules have been proposed as a potential origin of aldosterone-producing adenomas [76]. The two-hit theory is an alternative hypothesis for the pathogenesis of aldosterone-producing adenomas: one hit causes cell proliferation and the other hit triggers aldosterone excess [77]. It is unclear if these theories are correct and consistent with the real mechanisms driving the formation and growth of aldosterone-producing adenoma.

1.2.7 Transcriptomics

The transcriptome is the product of genome expression, including coding and non-coding RNA. The primary purpose of transcriptomics profiling is to identify differentially expressed genes representing transcriptional responses of the genome to environmental stimuli or physiological or pathological processes [78]. Two major approaches have been established: hybridization-based microarray methods and next generation RNA sequencing-based methods. In microarrays, thousands of transcripts are simultaneously quantified by fluorescence readouts of hybridization between complementary probe sequences and cDNA synthesized from RNA of cells or tissues [78]. Microarrays were widely used until the advent of next generation sequencing. The most common

platform for next generation sequencing-based RNA sequencing is the HiSeq series of sequencers from Illumina [78]. In next generation sequencing-based RNA sequencing, library preparation is the initial step comprising poly A selection (identifying mRNA) or rRNA-depletion (identifying both coding and non-coding RNA), RNA fragmentation, cDNA synthesis, ligation and cleanup steps [79]. The amplified RNA sequencing library with eligible quality is then preprocessed and mapped to the reference genome or undergoing *de novo* transcriptome assembly, followed by quantification and bioinformatics analysis [80]. RNA sequencing provides several advantages over microarray: improved sensitivity and specificity, minimal background, and identification of novel transcripts, isoforms and single nucleotide polymorphisms [80].

Previous transcriptome studies of aldosterone-producing adenomas have identified numerous differentially expressed genes in aldosterone-producing adenomas with different genotypes or between aldosterone-producing adenomas and normal adrenals or incidentalomas. Nevertheless, the majority of studies have used the microarray technique [81]. In these studies, potential molecular effectors involved in the calcium pathway [82, 83], G protein-coupled receptor signaling [84, 85], PI3K/Akt signaling [86] and the Wnt/ β -catenin pathway [66, 87] have been demonstrated to promote or suppress aldosterone production *in vitro*. Although these signaling cascades are all known for a role in cell proliferation or apoptosis, evidence in support of these molecular effectors in modulating adrenocortical cell growth is scarce [81]. Therefore, the mechanisms underlying the pathogenesis of aldosterone-producing adenomas remain largely unresolved.

1.2.8 *In vitro* cell models

Several human adrenal cell lines have been developed, including SW13, CAR47, ACT-1, RL-251, SV40, and NCI-H295 and its substrains [88]. The NCI-H295 cell line, an immortalized cell line with steroidogenic potential, was established from an adrenocortical carcinoma of a female patient [89]. NCI-H295 cells show slow cell growth and an appearance of loosely attached cell clusters [89]. After isolating monolayer strains from the parental NCI-H295 cells, H295A and H295R cells were developed, with the latter displaying a better response to angiotensin II [88, 90]. Three strains of H295R cells were termed based on the serum supplemented in growth medium: H295R-S1 (5% Nu-Serum), H295R-S2 (2.5% Ultrosor-G), and H295R-S3 (10% Cosmic calf serum) [88, 90]. However, the H295R cell line does not show significant response to adrenocorticotrophic hormone, and its steroidogenic phenotype was not stable during the extended cell culture [91]. Therefore, a new subclone HAC15 cell line was derived from H295R cells. HAC15 cells respond well to angiotensin II, potassium and adrenocorticotrophic hormone, and exhibits more stable steroidogenesis [92]. HAC15 cell line represents the optimal *in vitro* adrenal model to date to examine molecular and biochemical mechanisms contributing to pathophysiological and pathogenic processes of primary aldosteronism.

In addition to common physiological events including cell proliferation and apoptosis, human adrenocortical cells undergo a specific type of regulated cell death named ferroptosis under the stimulation of ferroptosis inducer (1*S*, 3*R*)-RSL3 (the inhibitor of glutathione peroxidase 4) with a remarkable sensitivity [93, 94]. Ferroptosis is an iron-dependent form of cell death characterized by accumulated lipid hydroperoxides. Glutathione peroxidase 4 and ferroptosis inhibitors, e.g. Liproxstatin-1 can specifically reduce lipid peroxidation, thereby suppressing ferroptosis (**Figure 3**) [95]. Ferroptosis occurs independently of caspases and manifests with a necrotic morphotype including mitochondrial shrinkage and reduced cristae [96].

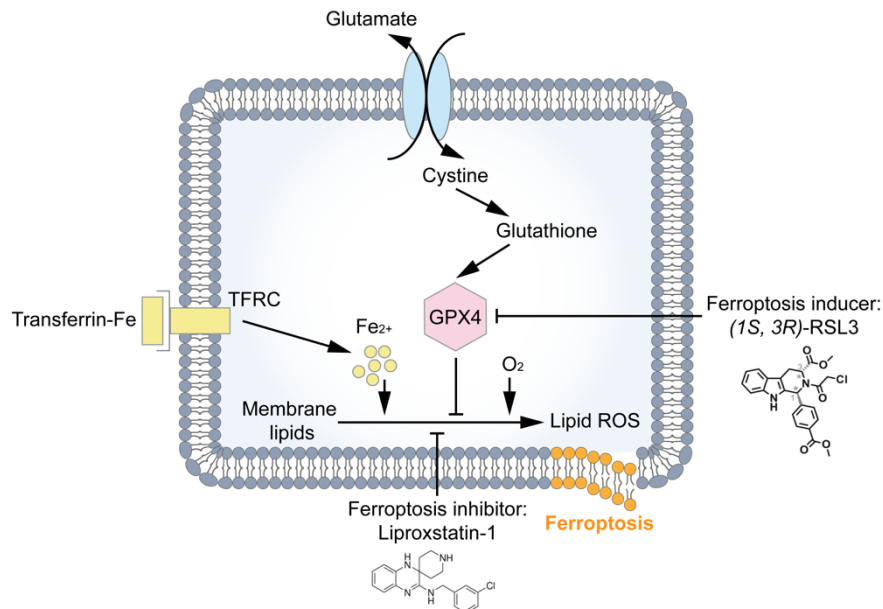


Figure 3. Schematic diagram of ferroptosis pathway. Fe₂₊, iron; GPX4, glutathione peroxidase 4; ROS, reactive oxygen species; TFRC, transferrin receptor.

1.3 Specific aims of the thesis

The overall objective of this thesis is to gain deeper insight into the pathophysiology and pathogenesis of primary aldosteronism by comparing steroidobolomics and transcriptomics of micro and macro aldosterone-producing adenomas to identify biomarkers and biological mechanisms associated with dysregulated cell growth in aldosterone-producing adenoma. The thesis has the following specific aims:

1. Investigate the steroid profiles of micro and macro aldosterone-producing adenomas in primary aldosteronism (Paper I)
2. Investigate the transcriptome profiles of micro and macro aldosterone-producing adenomas in primary aldosteronism (Paper II)
3. Establish functional role of potential modulators (*BEX1* and *KCNJ5* mutations) in deregulated cell growth of adrenal cells in aldosterone-producing adenoma (Paper II & III)

2. Methods and results

To achieve the first specific aim, we included 197 patients diagnosed with primary aldosteronism according to the Endocrine Society Clinical Guideline [17] from two referral centers, differentiated into aldosterone-producing adenoma (n=128) and bilateral adrenal hyperplasia (n=69) by adrenal venous sampling. Micro (n=33) and macro aldosterone-producing adenomas (n=95) were defined based on the diameter of the largest nodule at pathology. The outcomes of surgically treated patients with aldosterone-producing adenomas were assessed in accordance with the criteria established by the Primary Aldosteronism Surgical Outcome study [24]. Steroid profiles of peripheral venous plasma of the included patients were measured by LC-MS/MS. A panel of 15 steroids was measured: aldosterone, 18-hydroxycortisol, 18-oxocortisol, cortisol, 21-deoxycortisol, 11-deoxycortisol, cortisone, corticosterone, 11-deoxycorticosterone, pregnenolone, progesterone, 17-hydroxyprogesterone, androstenedione, dehydroepiandrosterone, and dehydroepiandrosterone sulfate.

Patients with micro aldosterone-producing adenomas showed a lower rate of complete biochemical success (84.8% versus 96.8%, $P=0.023$) but a higher rate of absent biochemical success (9.1% versus 1.1%, $P=0.036$) compared with patients with macro aldosterone-producing adenomas. Overall, there were 8 patients with partial or absent biochemical success after surgery. Therefore, adrenal venous sampling-based management achieved a diagnostic accuracy of 95.9%.

Steroid profiling highlighted distinct concentrations of aldosterone, 18-oxocortisol, 18-hydroxycortisol, and dehydroepiandrosterone sulphate between patients with micro- versus macro aldosterone-producing adenomas or patients with macro aldosterone-producing adenomas versus bilateral adrenal hyperplasia. Analyzed by the random forest algorithm using steroid concentrations, steroid profiling classified the 3 groups (micro aldosterone-producing adenomas, macro aldosterone-producing adenomas, and bilateral adrenal hyperplasia) with 83.2% (163/196) of accuracy albeit with low specificity for micro aldosterone-producing adenomas (33.3%, 11/33). The hypothetical diagnostic algorithm that combines steroid profiling, CT and adrenal venous sampling limited to patients with incongruent steroid profiling and CT results would have elevated the rate of correct classification of micro aldosterone-producing adenomas to 67.9% (19/28), reduced the proportion of adrenal venous sampling procedures by 82.7% (163 of 197 patients would have been assumed to have accordant steroid profiling and CT results) and improved the overall predictive accuracy (92.4%, 182/197).

We further compared the transcriptome profiles of aldosterone-producing adenomas of distinctly different sizes (12 adenomas of diameter ≤ 10 mm versus 9 adenomas of diameter ≥ 30 mm) by mRNA sequencing analysis. Sanger sequencing of genomic DNA from these adenomas for the hot spot mutations of *KCNJ5*, *ATP1A1*, *ATP2B3*, *CACNA1D* and *CTNNB1* classified these 21 adenomas into 2 genotype groups: *KCNJ5* mutations (n=11) or no mutations detected (n=10). No significant differences in the known duration of hypertension were detected in patients with aldosterone-producing adenomas categorized by small (≤ 10 mm) and large (≥ 30 mm) sized adenomas.

Differential expression of 348 and 155 genes was identified between small and large sized aldosterone-producing adenomas with no mutation detected or *KCNJ5*-mutated aldosterone-producing adenomas, respectively. Gene ontology enrichment analysis identified different patterns of differentially expressed gene sets in each genotype group (no mutation detected versus *KCNJ5*-mutated), with cell death as the most significantly enriched biological process in aldosterone-producing adenomas with no mutation detected ($P=6.4 \times 10^{-8}$). The biological processes related to Wnt

signaling, and the cell cycle and division were enriched in the no mutation detected and *KCNJ5* mutations groups, respectively.

We validated the differential expression of 10 genes with a known function in cell death and proliferation by real-time polymerase chain reaction in an expanded sample set of 71 aldosterone-producing adenomas categorized into micro and macro aldosterone-producing adenomas according to a cut-off diameter of 10 mm (13 micro and 58 macro aldosterone-producing adenomas). The *BEX1* gene was upregulated in micro- compared with macro aldosterone-producing adenomas (2.76-fold, $P < 0.001$), and was upregulated in aldosterone-producing adenomas with no mutation detected compared with adenomas with *KCNJ5* mutations (2.31-fold, $P < 0.0001$). The *BEX1* gene expression level was linearly negatively correlated with adenoma diameter in the no mutation detected group ($r = -0.501$, $P = 0.007$).

We established human adrenocortical cells (HAC15) stably expressing BEX1 with a DYKDDDDK tag demonstrated by Western blot and immunofluorescence. Stable BEX1 expression in human adrenocortical cells did not alter cell cycle progression or sensitivity to apoptosis, but conferred protection from ferroptosis under the treatment of ferroptosis inducer (1*S*, 3*R*)-RSL3 ($P < 0.01$), compared with control cells expressing empty vector. These *in vitro* data suggest a role for BEX1 in the pathogenesis of aldosterone-producing adenomas. We hypothesize that the gene expression patterns of *BEX1* reflect the requirement for anti-ferroptotic mechanisms during tumor development.

The validation of transcriptome profiles failed to identify candidate genes to explain the pathogenesis of aldosterone-producing adenomas with *KCNJ5* mutations, because the absent correlation of the validated gene expression levels with adenoma diameter in the *KCNJ5* group. Besides, *KCNJ5* mutations have been proposed to play a role in cell proliferation despite not demonstrated *in vitro*. Therefore, we hypothesized that *KCNJ5* mutations might be the cause of deregulated cell growth in these aldosterone-producing adenomas.

To demonstrate this hypothesis, we included a total of 72 adrenal tissues resected from patients with unilateral primary aldosteronism, and determined their genotypes by Sanger sequencing: *KCNJ5* (n=39), *ATP1A1* (n=3), *ATP2B3* (n=2), *CACNA1D* mutations (n=5), and no mutation detected (n=23).

Patients with *KCNJ5*-mutated aldosterone-producing adenomas had a prevalence of female (82% versus 30%, $P < 0.001$), and displayed a larger adenoma size (17 mm [14-24] versus 12 mm [8-25], $P = 0.019$) compared with patients with aldosterone-producing adenomas with no mutation detected.

The proliferation index by Ki67 immunostaining was determined and quantified. We demonstrated that the Ki67 proliferation index was linearly positively correlated with adenoma diameter in aldosterone-producing adenomas with *KCNJ5* mutations ($r = 0.4347$, $P = 0.0072$). In contrast, the Ki67 index was inversely correlated with adenoma diameter in aldosterone-producing adenomas with no mutation detected ($r = -0.5484$, $P = 0.0226$). No correlation of the proliferation index and adenoma diameter was detected in the group with other mutations combined (*CACNA1D* + *ATP1A1* + *ATP2B3*).

We established human adrenocortical HAC15 cells with cumate-inducible expression of *KCNJ5* with various genotypes (*KCNJ5* wide-type, *KCNJ5* L168R, G151R, G151E, T158A) using the selection marker puromycin. Compared with empty vector control cells, a low induction level of T158A (1 $\mu\text{g/mL}$ cumate) induced a higher level of cell viability after 24 hours ($P = 0.0094$), while a high level of induction (10 $\mu\text{g/mL}$ cumate) ablated this difference. A decreased cell viability was

identified in HAC15 cells with KCNJ5 G151E and L168R mutations ($P < 0.0001$). Higher levels of apoptosis were identified in cells expressing KCNJ5 G151R ($P < 0.0001$), G151E ($P = 0.0078$) and L168R ($P < 0.0001$) mutations compared with control cells (1 $\mu\text{g/mL}$ cumate), while expression of the KCNJ5 T158A mutation had no effect on apoptosis under the same conditions.

We developed a novel specific monoclonal antibody against KCNJ5 and use it for immunohistochemistry on the included adrenal tissues. Semi-quantitative assessment of KCNJ5 immunostaining showed a decreased expression of KCNJ5 in *KCNJ5*-mutated aldosterone-producing adenomas compared with aldosterone-producing adenomas with no mutation detected or carrying mutations other than *KCNJ5* ($P < 0.0001$). It also highlighted a decreased expression of KCNJ5 (assessed by immunostaining) in adenomas with *KCNJ5* mutations relative to the paired adjacent cortex, whereas most aldosterone-producing adenomas with no mutation detected or other mutations displayed either a similar or increased KCNJ5 immunostaining in the adenoma. CYP11B2 and KCNJ5 were colocalized in aldosterone-producing adenomas. A decrease of KCNJ5 expression was identified in CYP11B2-positive cells compared with CYP11B2-negative cells in adenomas with *KCNJ5* mutations.

3. Summary

Aldosterone-producing adenomas are the surgically correctable form of primary aldosteronism [17]. Next generation sequencing targeted to aldosterone-producing adenomas with positive expression of CYP11B2 has unveiled the existence of somatic mutations and explained aldosterone overproduction [44-49]. However, pathogenic mechanisms contributing to the diverse adenoma sizes and the associated biochemical features remain largely unclear. In this thesis, we utilized steroid and transcriptome profiling of aldosterone-producing adenomas of distinctly different diameter (micro and macro aldosterone-producing adenomas) to identify circulating biomarkers and key modulators that regulate adrenal cell growth of aldosterone-producing adenomas, and performed functional characterization.

In paper I [96], we compared peripheral venous plasma steroid profiles of patients with micro, macro aldosterone-producing adenomas and bilateral adrenal hyperplasia measured by LC-MS/MS. Steroid profiling highlighted the steroids, including aldosterone, 18-oxocortisol, 18-hydroxycortisol, and dehydroepiandrosterone sulfate, with distinct concentrations among the 3 groups. Steroid profiling achieved a high predictive accuracy of the 3 groups while a low specificity for micro aldosterone-producing adenomas. The hypothetical diagnostic algorithm that integrated steroid profiling, CT and adrenal venous sampling limited to patients with conflicting steroid profiling and CT results would have improved the detection rate of micro aldosterone-producing adenomas. It would have also elevated the overall predictive accuracy of aldosterone-producing adenoma and bilateral adrenal hyperplasia to a comparable level achieved by adrenal venous sampling-based management. Thus, peripheral venous plasma steroid profiles are highly different between patients with micro and macro aldosterone-producing adenomas, and are potentially useful for the identification of patients with micro aldosterone-producing adenomas in whom adrenal venous sampling should be considered mandatory.

In paper II [97], the comparison of transcriptomes of aldosterone-producing adenomas of distinctly different sizes (diameter ≤ 10 mm versus ≥ 30 mm) by mRNA sequencing analysis highlighted a number of differentially expressed genes between these 2 groups of aldosterone-producing adenomas with different genotypes (no mutation detected versus *KCNJ5* mutations). Gene ontology enrichment analysis highlighted different patterns of differentially expressed gene sets in aldosterone-producing adenomas with different genotypes, indicating the distinct biology that underlies their development. Cell death was the most significantly enriched biological process in aldosterone-producing adenomas with no mutation detected. We validated the differential expression of 10 genes with a known function in cell death and proliferation in an expanded sample set. The gene *BEX1*, with an unknown function in the adrenal gland, was selected for functional characterization due to its differential expression in the aldosterone-producing adenomas with different diameter and genotypes. Stable *BEX1* expression in human adrenocortical cells did not alter cell cycle progression or sensitivity to apoptosis, but conferred protection from ferroptosis. The higher expression profile of *BEX1* in micro aldosterone-producing adenomas may indicate a high level of anti-ferroptotic mechanism in these adrenal tissues that produce notably high pathological levels of aldosterone. This postulation was supported by the higher *BEX1* expression in micro aldosterone-producing adenomas and aldosterone-producing micronodules compared with the paired adjacent cortex. These findings demonstrate that micro and macro aldosterone-producing adenomas display distinct transcriptome profiles that is helpful for the identification of potential modulators of the deregulated cell growth in aldosterone-producing adenomas. *BEX1* promotes cell survival of adrenal cells by mediating the inhibition of ferroptosis and indicate a pathogenic role for *BEX1* in aldosterone-producing adenomas.

In paper III [98], we aimed to investigate the functional role of *KCNJ5* mutations in aldosterone-producing adenomas. Therefore, we performed *in vitro* functional and immunohistochemical characterization of *KCNJ5*. The expression of *KCNJ5*-G151R, L168R and G151E in human adrenocortical cells caused apoptosis, whereas T158A had no such effect. Instead, compared with control cells, a low-level induction of T158A induced a significant increase in cell proliferation, but an increased level of induction ablated this difference. The use of our newly developed *KCNJ5* antibody demonstrated a lower expression of *KCNJ5* in aldosterone-producing adenomas carrying *KCNJ5* mutations compared with aldosterone-producing adenomas with other genotypes or aldosterone-producing micronodules. We also identified a decreased *KCNJ5* expression in cells expressing CYP11B2 compared with CYP11B2-negative cells in aldosterone-producing adenomas with *KCNJ5* mutations. Collectively, these findings indicate that *KCNJ5* mutations induce cell toxicity and their cell growth effects are likely to be determined by the expression level of the mutated *KCNJ5* channel.

In summary, this thesis has identified circulating steroid biomarkers for aldosterone-producing adenomas with different adenoma sizes and potential modulators (*BEX1* and *KCNJ5* mutations) that may contribute to such size differences of aldosterone-producing adenomas. It provides an alternative method for subtype differentiation of primary aldosteronism that could be especially helpful for clinical centers with limited access to the technically demanding procedure of adrenal venous sampling. It also deepens our understanding of the pathogenesis of aldosterone-producing adenomas that could be useful for future perspectives in the diagnosis and clinical management of primary aldosteronism.

4. Zusammenfassung

Aldosteron-produzierende Adenome sind die chirurgisch korrigierbare Form des primären Hyperaldosteronismus [17]. Next-Generation Sequencing von Aldosteron-produzierenden Adenomen mit positiver Expression von CYP11B2 enthüllte die Existenz somatischer Mutationen und erklärte die Überproduktion von Aldosteron [44-49]. Pathogene Mechanismen, die zu den verschiedenen Adenomgrößen und den damit verbundenen biochemischen Merkmalen beitragen, bleiben jedoch weitgehend unbekannt. In dieser Arbeit verwendeten wir Steroid- und Transkriptom-Profilung von Aldosteron-produzierenden Adenomen mit deutlich unterschiedlichem Durchmesser (Mikro- und Makro-Aldosteron-produzierende Adenome), um zirkulierende Biomarker und Schlüsselmodulatoren, die das Nebennierenzellwachstum von Aldosteron-produzierenden Adenomen regulieren, zu identifizieren. Nachfolgend wurde eine funktionelle Charakterisierung durchgeführt.

In Artikel I [96] verglichen wir mittels LC-MS/MS gemessene periphere venöse Plasma-Steroidprofile von Patienten mit Mikro- und Makro-Aldosteron-produzierenden Adenomen sowie bilateraler Nebennierenhyperplasie. Das Steroid-Profilung hob die Steroide, einschließlich Aldosteron, 18-Oxocortisol, 18-Hydroxycortisol und Dehydroepiandrosteronsulfat, mit unterschiedlichen Konzentrationen zwischen diesen 3 Gruppen hervor. Das Steroid-Profilung erreichte eine hohe Vorhersagegenauigkeit der 3 Gruppen, jedoch eine geringe Spezifität für Mikro-Aldosteron-produzierende Adenome. Der hypothetische Diagnosealgorithmus, welcher Steroid-Profilung, CT und Nebennierenvenenkatheteruntersuchung (adrenal vein sampling) integriert und sich auf Patienten mit widersprüchlichen Steroid-Profilung- und CT-Ergebnissen begrenzt, hätte die Erkennungsrate von Mikro-Aldosteron-produzierenden Adenomen verbessert. Er hätte ebenfalls die allgemeine Vorhersagegenauigkeit eines Aldosteron-produzierenden Adenoms und bilateraler Nebennierenhyperplasie auf ein durch die Nebennierenvenenkatheteruntersuchung basierendes Management vergleichbares Level erhöht. Dementsprechend unterscheiden sich peripher venösen Plasma-Steroidprofile stark zwischen Patienten mit Mikro- und Makro-Aldosteron-produzierenden Adenomen und sind möglicherweise nützlich für die Identifizierung von Patienten mit Mikro-Aldosteron-produzierenden Adenomen, bei denen eine Nebennierenvenenkatheteruntersuchung als obligatorisch angesehen werden sollte.

In Artikel II [97] hat der Vergleich der mittels mRNA-Sequenzierungsanalyse ermittelten Transkriptome von Aldosteron-produzierenden Adenomen mit deutlich unterschiedlichen Größen (Durchmesser ≤ 10 mm versus ≥ 30 mm) eine Reihe von differentiell exprimierten Genen zwischen diesen beiden Gruppen von Aldosteron-produzierenden Adenomen mit unterschiedlichen Genotypen hervorgehoben (keine Mutation versus *KCNJ5*-Mutation). Gene Ontology Enrichment Analyse zeigte unterschiedliche Muster differentiell exprimierter Gensätze in Aldosteron-produzierenden Adenomas mit den beiden verschiedenen Genotypgruppen auf, was auf die unterschiedliche Biologie hinweist, die ihrer Entwicklung zugrunde liegt. Der Zelltod war der am signifikantesten angereicherte biologische Prozess bei Aldosteron-produzierenden Adenomen, bei denen keine Mutation festgestellt wurde. In einem erweiterten Probensatz validierten wir die differentielle Expression von 10 Genen mit einer bekannten Funktion im Bezug auf Zelltod und Proliferation. Das Gen *BEX1*, welches eine unbekannte Funktion in der Nebenniere hat, wurde aufgrund seiner unterschiedlichen Expression in den Aldosteron-produzierenden Adenomen mit unterschiedlichem Durchmesser und Genotypen für die funktionelle Charakterisierung ausgewählt. Eine stabile *BEX1*-Expression in menschlichen Nebennierenrinenzellen veränderte weder die Zellzyklus-Progression noch die Empfindlichkeit gegenüber Apoptose, verlieh jedoch Schutz vor Ferroptose. Das höhere Expressionsprofil von *BEX1* in Mikro-Aldosteron-produzierenden Adenomen

kann auf ein hohes Maß an anti-ferroptotischen Mechanismus in diesen Nebennierengeweben hinweisen, welche bemerkenswert hohe pathologische Aldosteronspiegel produzieren. Diese Annahme wurde durch die höhere *BEX1*-Expression in Mikro-Aldosteron-produzierenden Adenomen und Aldosteron-produzierenden Mikronoduli im Vergleich zum gepaarten nebenliegenden Kortex gestützt. Diese Ergebnisse zeigen, dass Mikro- und Makro-Aldosteron-produzierende Adenome unterschiedliche Transkriptom-Profile aufweisen, was für die Identifizierung potenzieller Modulatoren des deregulierten Zellwachstums in Aldosteron-produzierenden Adenomen hilfreich ist. *BEX1* fördert das Überleben von Nebennierenzellen durch die Initiierung der Ferroptose-Hemmung und deutet auf eine pathogene Rolle von *BEX1* in Aldosteron-produzierenden Adenomen hin.

In Artikel III [98] untersuchten wir die funktionelle Rolle von *KCNJ5*-Mutationen in Aldosteron-produzierenden Adenomen. Dazu führten wir eine funktionelle *in vitro* sowie immunhistochemische Charakterisierung von *KCNJ5* durch. Die Expression von *KCNJ5*-G151R, L168R und G151E in menschlichen Nebennierenrindezellen verursachte Apoptose, während T158A keinen solchen Effekt hatte. Stattdessen induzierte eine Induktion von T158A auf niedrigem Niveau im Vergleich zu Kontrollzellen einen signifikanten Anstieg der Zellproliferation, jedoch beseitigte ein erhöhtes Maß an Induktion diesen Unterschied. Die Verwendung unseres neu entwickelten *KCNJ5*-Antikörpers zeigte eine geringere Expression von *KCNJ5* in Aldosteron-produzierenden Adenomen mit *KCNJ5*-Mutationen im Vergleich zu Aldosteron-produzierenden Adenomen mit anderen Genotypen oder Aldosteron-produzierenden Mikronoduli. Wir identifizierten in Aldosteron-produzierenden Adenomen mit *KCNJ5*-Mutationen auch eine verminderte *KCNJ5*-Expression in Zellen, welche *CYP11B2* exprimieren im Vergleich zu *CYP11B2*-negativen Zellen. Zusammengefasst zeigen diese Befunde, dass *KCNJ5*-Mutationen Zelltoxizität induzieren und ihre Zellwachstumseffekte wahrscheinlich durch das Expressionslevel des mutierten *KCNJ5* Kanals bestimmt werden.

Zusammenfassend hat diese Arbeit zirkulierende Steroid-Biomarker für Aldosteron-produzierende Adenome mit unterschiedlichen Adenomgrößen sowie potenzielle Modulatoren (*BEX1* und *KCNJ5*-Mutationen) identifiziert, die zu solchen Größenunterschieden von Aldosteron-produzierenden Adenomen beitragen können. Es bietet eine alternative Methode zur Subtypdifferenzierung des primären Hyperaldosteronismus, die insbesondere für klinische Zentren mit eingeschränktem Zugang zum technisch anspruchsvollen Verfahren der Nebennierenvenenkatheteruntersuchung hilfreich sein könnte. Es vertieft auch unser Verständnis der Pathogenese von Aldosteron-produzierenden Adenomen, welches für zukünftige Perspektiven bei der Diagnose und der klinischen Behandlung des primären Hyperaldosteronismus nützlich sein könnte.

5. Significance and perspectives

The findings of this thesis have contributed to a better characterization of clinical phenotypes of primary aldosteronism that is helpful for the subtype classification and selection of patients for targeted therapies. Future genomics, metabolomics, and proteomics profiling of biological samples from patients with primary aldosteronism may advance the diagnosis of primary aldosteronism through the use of omics-signatures to tailor treatments to individual patient characteristics.

This project has also enabled a better understanding of pathogenic mechanisms driving the formation and growth of adrenal cells in aldosterone-producing adenomas. For the first time, we have shown that ferroptosis, a form of regulated cell death related to cell metabolism and redox biology, might be involved in the pathogenesis of aldosterone-producing adenomas. Further characterization of ferroptosis in adrenal cells by transcriptome analysis and *ex vivo* experiments may advance our understanding of this novel pathogenic mechanism in aldosterone-producing adenoma.

6. Contribution to the publications

6.1 Contribution to paper I

For the paper I entitled “Classification of microadenomas in patients with primary aldosteronism by steroid profiling”, I have performed immunohistochemistry for CYP11B2 on formalin-fixed, paraffin-embedded adrenal tissues, real-time polymerase chain reaction using Taqman gene expression assays, statistical analyses of clinical characteristics and steroid concentrations, and constructed the diagnostic algorithm integrating steroid profiling, CT and adrenal venous sampling. In addition, I interpreted the results, and drafted the manuscript, artwork for figures and tables.

Dr. Jacopo Burrello, who shared first authorship of paper I, performed logistic regression analysis to identify steroids associated with aldosterone-producing adenomas and bilateral adrenal hyperplasia, random forest algorithm using peripheral venous steroid profiling, and constructed an online prediction tool for subtype classification. He also contributed to the interpretation of the results and artwork of figures and tables.

Due to the comparable contributions to paper I, Dr. Jacopo Burrello and I have shared first authorship.

6.2 Contribution to paper II

For the paper II entitled “*BEX1* is differentially expressed in aldosterone-producing adenomas and protects human adrenocortical cells from ferroptosis”, I performed RNA extraction, reverse transcription, and real-time polymerase chain reaction using Taqman gene expression assays. I generated the HAC15 empty vector control cell line and the HAC15 cell line with stable expression of *BEX1*-DDK that was confirmed by Western blotting and immunofluorescence for DDK-tag. I performed cell viability assays and flow cytometry to assess cell cycle and cell death. I also performed all statistical analyses of clinical data from patients, assays, flow cytometry, and partial bioinformatic analyses. I drafted the manuscript, artwork of figures and tables and took part in the revision of the manuscript.

6.3 Contribution to paper III

For the paper III entitled “Primary aldosteronism: *KCNJ5* mutations and adrenocortical cell growth”, I performed DNA sequencing for the confirmation of *KCNJ5* mutations in HAC15 stable cell lines with inducible *KCNJ5* expression, cell proliferation and apoptosis assays using the established stable cell lines, and immunohistochemistry and immunofluorescence on formalin-fixed, paraffin-embedded adrenal tissues or HAC15 cells. I also performed all statistical analyses of patient clinical data, assays and scores of immunostaining intensity. I drafted the manuscript, artworks of figures and tables, and took part in the revision of the manuscript.

6.4 Confirmation of co-authors

All co-authors have confirmed their contributions and gave their agreements to submission of the submitted publications. The publications included in this thesis are not the subject of another thesis. The signed lists of co-authors are submitted in a separate file.

7. Paper I

Title: Classification of microadenomas in patients with primary aldosteronism by steroid profiling

Authors: Yang Y*, Burrello J*, Burrello A, Eisenhofer G, Peitzsch M, Tetti M, Knösel T, Beuschlein F, Lenders JWM, Mulatero P, Reincke M, Williams TA

Journal: Journal of Steroid Biochemistry and Molecular Biology

Year: 2019

Volume: 189

Pages: 274-282

DOI: 10.1016/j.jsbmb.2019.01.008

*Authors contributed equally to the work



Contents lists available at ScienceDirect

Journal of Steroid Biochemistry and Molecular Biology

journal homepage: www.elsevier.com/locate/jsbmb

Classification of microadenomas in patients with primary aldosteronism by steroid profiling



Yuhong Yang^{a,1}, Jacopo Burrello^{b,1}, Alessio Burrello^c, Graeme Eisenhofer^{d,e}, Mirko Peitzsch^d, Martina Tetti^b, Thomas Knösel^f, Felix Beuschlein^{a,g}, Jacques W.M. Lenders^{e,h}, Paolo Mulatero^b, Martin Reincke^a, Tracy Ann Williams^{a,b,*}

^a Medizinische Klinik und Poliklinik IV, Klinikum der Universität, Ludwig-Maximilians-Universität München, Munich, Germany

^b Division of Internal Medicine and Hypertension, Department of Medical Sciences, University of Turin, Turin, Italy

^c Department of Electronics and Telecommunications, Polytechnic University of Turin, Turin, Italy

^d Institute of Clinical Chemistry and Laboratory Medicine, University Hospital Carl Gustav Carus, Technische Universität Dresden, Dresden, Germany

^e Department of Medicine III, University Hospital Carl Gustav Carus, Technische Universität Dresden, Dresden, Germany

^f Institute of Pathology, Ludwig-Maximilians-Universität München, Munich, Germany

^g Klinik für Endokrinologie, Diabetologie und Klinische Ernährung, Universitätsspital Zürich, Zürich, Switzerland

^h Department of Medicine, Radboud University Medical Center, Nijmegen, the Netherlands

ARTICLE INFO

Keywords:

Primary aldosteronism
Aldosterone-producing adenoma
Conn syndrome
Bilateral adrenal hyperplasia
Adrenal cortex
Steroid profiling

ABSTRACT

In primary aldosteronism (PA) the differentiation of unilateral aldosterone-producing adenomas (APA) from bilateral adrenal hyperplasia (BAH) is usually performed by adrenal venous sampling (AVS) and/or computed tomography (CT). CT alone often lacks the sensitivity to identify micro-APAs. Our objectives were to establish if steroid profiling could be useful for the identification of patients with micro-APAs and for the development of an online tool to differentiate micro-APAs, macro-APAs and BAH. The study included patients with PA (n = 197) from Munich (n = 124) and Torino (n = 73) and comprised 33 patients with micro-APAs, 95 with macro-APAs, and 69 with BAH. Subtype differentiation was by AVS, and micro- and macro-APAs were selected according to pathology reports. Steroid concentrations in peripheral venous plasma were measured by liquid chromatography-tandem mass spectrometry. An online tool using a random forest model was built for the classification of micro-APA, macro-APA and BAH. Micro-APA were classified with low specificity (33%) but macro-APA and BAH were correctly classified with high specificity (93%). Improved classification of micro-APAs was achieved using a diagnostic algorithm integrating steroid profiling, CT scanning and AVS procedures limited to patients with discordant steroid and CT results. This would have increased the correct classification of micro-APAs to 68% and improved the overall classification to 92%. Such an approach could be useful to select patients with CT-undetectable micro-APAs in whom AVS should be considered mandatory.

1. Introduction

Primary aldosteronism (PA) is the most frequent form of endocrine hypertension characterized by aldosterone overproduction relative to suppressed plasma renin [1–3]. Patients with PA have an increased risk of cardiovascular and cerebrovascular events and renal disease

progression relative to patients with primary hypertension including those with similar cardiovascular risk profiles [4–7]. This highlights the importance of early diagnosis and appropriate clinical management to minimize detrimental cardiovascular outcomes.

Unilateral PA is mainly caused by an aldosterone-producing adenoma (APA) and is potentially curable by laparoscopic unilateral

Abbreviations: 17-OH-progesterone, 17-hydroxyprogesterone; 18OH-cortisol, 18-hydroxycortisol; APA, aldosterone-producing adenoma; ARR, aldosterone-to-renin ratio; AVS, adrenal venous sampling; BAH, bilateral adrenal hyperplasia; CT, computed tomography; CYP11B1, 11 β -hydroxylase; CYP11B2, aldosterone synthase; CYP17A1, 17 α -hydroxylase; DHEA, dehydroepiandrosterone; DHEAS, dehydroepiandrosterone sulphate; HSD3B2, 3 β -hydroxysteroid dehydrogenase type 2; H&E, hematoxylin and eosin; LC-MS/MS, liquid chromatography-tandem mass spectrometry; Macro-APA, macro-aldosterone-producing adenoma; Micro-APA, micro-aldosterone-producing adenoma; MRA, mineralocorticoid receptor antagonist; OR, odds ratio; PA, primary aldosteronism

* Corresponding author at: Medizinische Klinik und Poliklinik IV, Klinikum der Universität München, LMU München, Ziemssenstr. 1, D-80336, München, Germany.

E-mail address: Tracy.Williams@med.uni-muenchen.de (T.A. Williams).

¹ These authors contributed equally to this work.

<https://doi.org/10.1016/j.jsbmb.2019.01.008>

Received 13 August 2018; Received in revised form 16 December 2018; Accepted 13 January 2019

Available online 14 January 2019

0960-0760/© 2019 Elsevier Ltd. All rights reserved.

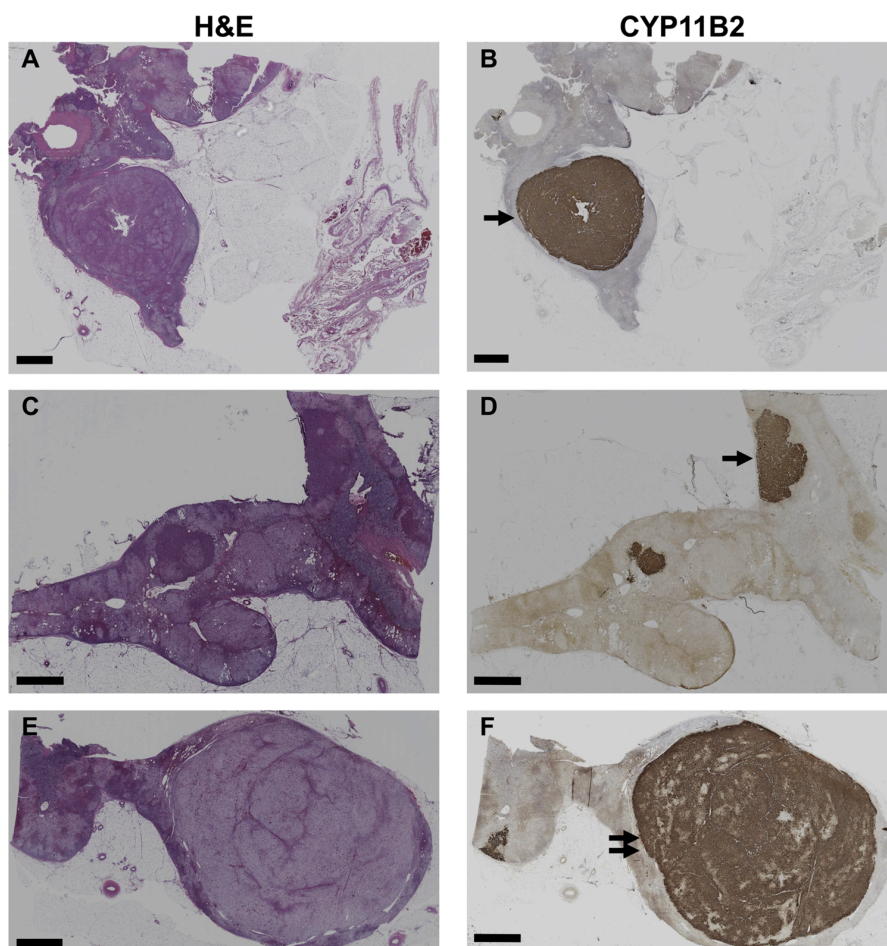


Fig. 1. CYP11B2 immunohistochemistry micro-APA and macro-APA.

The histopathology of resected adrenals from patients with a micro-APA (Panels A, B, C and D) or a macro-APA (Panels E and F) are shown with hematoxylin and eosin (H&E) staining (Panels A, C and E) and CYP11B2 immunostaining (Panels B, D and F). Micro-APAs in this study were classified as a single micro-APA (diameter < 10 mm, as indicated by a single arrow in panel B) or the largest CYP11B2 positive nodule (with diameter < 10 mm, as indicated by a single arrow in panel D) in an adrenal with more than one nodule with CYP11B2 immunostaining. An example of a macro-APA is indicated with a double arrow in panel F. Scale bar = 2 mm. CYP11B2, aldosterone synthase; H&E, hematoxylin and eosin.

adrenalectomy whereas bilateral PA (bilateral adrenal hyperplasia [BAH]) is usually treated with a mineralocorticoid receptor antagonist (MRA). These specific treatment options emphasize the central role of an accurate differentiation of APA from BAH in the diagnostic work up of PA which is usually performed by computed tomography (CT) and adrenal venous sampling (AVS) [8]. The sensitivity of CT imaging is often insufficient for the identification of APAs less than 10 mm in diameter, while AVS displays high sensitivity and specificity (95% and 100%, respectively) to distinguish unilateral from bilateral PA [9,10]. AVS is a technically-demanding and invasive procedure with non-standardized protocols and variable interpretation of results, and alternative approaches to reduce or even replace AVS for subtype differentiation in PA are currently sought [11–16].

Various definitions of size of micro-APAs have been used which usually consider the CT-undetectable feature [9,17–20]. Micro-APAs have been classified as < 10 mm in diameter, although in certain circumstances, ie, localization in an expanded adrenal limb, micro-APAs of 6 mm in diameter have been detected by CT [17]. CYP11B2 (aldosterone synthase) expression per tumour area by immunohistochemistry has been reported as higher in micro-APAs compared with macro-APAs together with a higher reported capacity for aldosterone production per tumour area [21]. CT-undetectable micro-APAs have a reported prevalence of 13%–30% in patients with APAs [9,17–20] and therefore comprise a significant proportion of patients with APAs with potentially distinctive adrenal steroid profiles and clinical outcomes.

In the present study, we determined the liquid chromatography-tandem mass spectrometry (LC-MS/MS)-based steroid profiles of

peripheral venous plasma samples from patients with micro-APAs (< 10 mm in diameter), macro-APAs (≥ 10 mm in diameter) and BAH. Our objectives were to establish if steroid profiling could be useful to select patients with micro-APAs in whom AVS should be considered mandatory and determine if a diagnostic algorithm that integrates steroid profiling could help rationalize the use of AVS procedures in patients with PA.

2. Subjects and methods

The subjects included in this study were 197 patients diagnosed with PA from two referral centers (124 patients from Medizinische Klinik IV, Klinikum der Ludwig-Maximilians-Universität München, Munich, Germany and 73 patients from Division of Internal Medicine and Hypertension, University of Turin, Turin, Italy). The study was approved by the appropriate institutional ethics committees and written informed consent was obtained from all patients.

2.1. Diagnosis and treatment

PA was diagnosed in both Munich and Torino in accordance with the Endocrine Society Clinical Guideline using the aldosterone-to-renin ratio (ARR) as a screening test, confirmatory testing by saline infusion testing and subtype differentiation by AVS. Detailed methods for the diagnosis of PA and AVS procedures are described elsewhere [10,22]. In all patients, AVS procedures were performed under basal conditions and successful catheterization was defined with a selectivity index

(adrenal vein to peripheral cortisol ratio) ≥ 2.0 . Unilateral PA was defined by a lateralization ratio (dominant to contralateral aldosterone-to-cortisol concentration ratio) ≥ 4.0 .

2.2. Classification of micro-APAs and macro-APAs and assessment of postoperative outcomes

Pathology reports were used for an assessment of the diameter of the largest nodule in resected adrenals for an initial classification of adenomas as micro-APAs or macro-APAs. Macro-APAs were defined by the largest nodule diameter ≥ 10 mm from pathology reports alone. Micro-APAs, from the initial assessment from pathology reports, were then analysed by CYP11B2 immunohistochemistry [23] and this group included either a single microadenoma with CYP11B2 immunostaining (diameter < 10 mm) or the largest nodule (with diameter < 10 mm) in an adrenal with more than 1 nodule with CYP11B2 immunostaining (Fig. 1). Cases of diffuse hyperplasia were excluded. Several adrenals showed aldosterone-producing cell clusters which are defined as tight clusters of cells with strong CYP11B2 immunostaining with *zona glomerulosa* morphology located beneath the capsule and extending into the *zona fasciculata* [24,25]. The follow-up data of clinical and biochemical parameters were obtained in the surgically treated patients at 6–12 months. Outcomes were defined as complete, partial and absent clinical and biochemical success based on blood pressure measurements and antihypertensive medication dosage for clinical outcomes or plasma potassium and hormonal (aldosterone and renin) measurements for biochemical outcomes [26].

2.3. Genotyping and gene expression analysis

Genomic DNA was extracted from frozen adrenal tissues and DNA fragments of *KCNJ5*, *ATP1A1*, *ATP2B3* and *CACNA1D* were amplified by PCR using the primers shown in Table A.1, Supplementary data and sequenced as described [27,28]. To our knowledge, PCR amplifications using these primers potentially identify all somatic APA mutations in the above genes described to date including the APA mutations described in *CACNA1D* listed in Prada et al. [29], with the exception of *CACNA1D* Glu412Asp, and the new *CACNA1D* mutation described recently by Nanba et al. [30].

Total RNA was extracted from adrenal tissues (tumours and adjacent cortex) and reverse transcribed as described previously [27]. Real-time PCR was performed in duplicate using TaqMan gene expression assays, and expression levels of *CYP11B2* were analyzed by $2^{-\Delta\Delta Ct}$ relative quantification using *GAPDH* as the endogenous reference gene. All samples were included in the gene expression analysis with available adenoma and corresponding adjacent cortical tissue (8 micro-APAs and 32 macro-APAs). *CYP11B2* gene expression analysis indicated an absence of *CYP11B2* upregulation in 1 of the 8 samples classified as micro-APAs (tumour-to-adjacent tissue *CYP11B2* expression ratio = 0.934; genotype determined as wild type) and in 1 of 32 samples classified as macro-APAs (tumour-to-adjacent tissue *CYP11B2* expression ratio = 0.926, genotype determined as wild type). This indicates the missed dissection of the *CYP11B2* positive nodule for the micro-APA and the dissection of a nonfunctional adenoma as the largest nodule for the sample classified as a macro-APA (Fig. A.1, Supplementary data).

2.4. Immunohistochemistry and immunohistochemical characterization

Immunohistochemistry was performed on formalin-fixed, paraffin-embedded tissue sections (3 μ m) with an anti-CYP11B2 antibody (dilution 1:200, mouse monoclonal anti-human antibody, clone 17B, from Dr Celso E. Gomez-Sanchez) [23] as described previously [31].

2.5. LC-MS/MS-based steroid profiling

Steroid profiling of peripheral venous plasma was done by LC-MS/MS as described in full elsewhere [32] for the simultaneous measurement of 15 steroids [aldosterone, 18-oxocortisol, 18-hydroxycortisol (18OH-cortisol), 21-deoxycortisol, corticosterone, 11-deoxycorticosterone, progesterone, cortisol, cortisone, 11-deoxycortisol, 17-hydroxyprogesterone (17-OH-progesterone), pregnenolone, androstenedione, dehydroepiandrosterone (DHEA), and dehydroepiandrosterone sulphate (DHEAS)].

2.6. Statistical analyses

Quantitative normally distributed variables are expressed as means with SDs and quantitative non-normally distributed variables are reported as medians and interquartiles. Categorical variables are presented as absolute numbers and percentages. Comparisons between two groups were assessed by a *t* test or a Mann-Whitney test; multiple comparisons were assessed by ANOVA followed by Bonferroni test for pairwise comparisons, or Kruskal-Wallis test with pairwise comparisons. Chi-square and Fisher's exact-tests were used to compare categorical data. A logistic regression analysis identified steroids associated with micro-APAs compared with macro-APAs and BAH with odds ratios (OR) for steroids calculated per ng/mL. An OR greater than 1 indicates an increased likelihood of micro-, macro-APAs or BAH, and an OR less than 1 indicates a decreased likelihood. IBM SPSS Statistics version 25.0 were used for statistical analyses. *P* values are given to three decimal places and are considered significant when *P* < 0.05 .

2.7. Predictive model

Random forest algorithms were performed using MATLAB R2017b and PYTHON 2.7 to assess how concentrations of steroids in peripheral venous plasma could be used to classify micro-, macro-APAs and BAH. The prediction model can be used via an online tool which requires operating system Windows version 64-bit or higher and is available at <https://github.com/ABurrello/Steroid-profiling-in-PA/archive/master.zip>.

3. Results

3.1. Patient characteristics, outcomes and immunohistochemical characterization

Demographic and clinical characteristics at study entry and post-operative follow-up of all patients are shown in Table A.2 (Supplementary data). There was an overall difference in this cohort in the sex distribution of micro- and macro-APAs and BAH (*P* < 0.001) with micro-APAs and BAH more prevalent in men than in women (micro-APAs: 78.8% vs 21.2%; BAH: 73.9% vs 26.1%). Patients with macro-APAs displayed the highest baseline concentrations of plasma aldosterone (*P* < 0.001) and the lowest serum potassium concentrations (*P* < 0.001) relative to the micro-APA or BAH group.

Micro-APAs displayed a lower prevalence of somatic *KCNJ5* mutations (3.2% vs 47.4%, *P* < 0.001) and a higher proportion of the wild-type genotype (80.7% vs 36.2%, *P* < 0.001) compared with macro-APAs.

Complete clinical and biochemical success were less frequent in the micro-APA than in the macro-APA group (12.1% vs 40.0%, *P* = 0.003, 84.8% vs 96.8%, *P* = 0.023, respectively) whereas absent biochemical success was more prevalent in the micro-APA group (9.1% vs 1.1%, *P* = 0.036). In total, 8 patients (5 with micro-APAs, 3 with macro-APAs) displayed partial or absent biochemical success. CYP11B2 immunohistochemistry of these 8 resected adrenals demonstrated the presence of a solitary functional macroadenoma in 3 samples. The remaining 5 adrenals comprised 1 with a solitary micro-APA and 4 which did not have a solitary APA but showed more than one nodule with

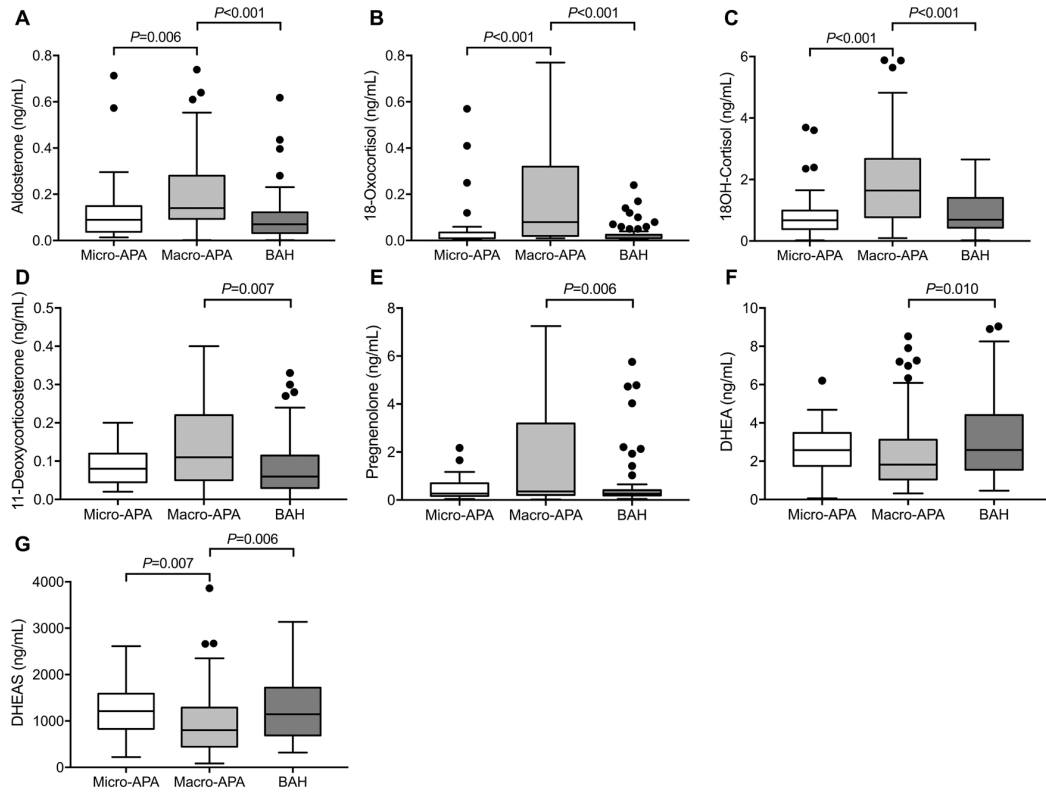


Fig. 2. Peripheral plasma steroid concentrations in patients with micro-APAs, macro-APAs and BAH.

The box and whisker plots (Panels A–G) represent peripheral plasma concentrations of the indicated steroids in patients with PA stratified for APA according to tumor diameter (micro-APAs ≤ 10 mm ($n = 33$) and macro-APAs > 10 mm ($n = 95$)) and BAH ($n = 69$). Only steroids with significant differences in concentrations between micro-APAs, macro-APAs and BAH are shown. Horizontal lines within boxes indicate the median, boxes and whiskers represent the 25th to 77th percentiles and the minimum and maximum values, respectively, after exclusion of outliers that are defined by 1.5 times the interquartile range and are indicated by filled circles. Concentrations are indicated in ng/mL which are converted to pmol/L by dividing by the molecular weight of each steroid: aldosterone, 360.44; 18-oxocortisol, 376.45; 18-hydroxycortisol, 378.46; 11-deoxycorticosterone, 330.46; pregnenolone, 316.48; DHEA, 288.42; DHEAS, 367.50. P values were calculated using Kruskal-Wallis tests followed by pairwise comparisons. 18OH-cortisol, 18-hydroxycortisol; APA, aldosterone-producing adenoma; BAH, bilateral adrenal hyperplasia; DHEA, dehydroepiandrosterone; DHEAS, dehydroepiandrosterone sulfate.

CYP11B2 immunostaining, with or without aldosterone-producing cell clusters [25], with the larger nodule considered the micro-APA.

3.2. LC-MS/MS-based steroid profiling

LC-MS/MS-based steroid profiling of peripheral venous plasma revealed some distinct differences between patients with micro-APAs, macro-APAs and BAH (Fig. 2 and Table A.3, Supplementary data). Patients with micro-APAs had lower peripheral plasma concentrations of aldosterone ($P = 0.006$), 18-oxocortisol ($P < 0.001$) and 18-hydroxycortisol ($P < 0.001$) compared with patients with macro-APAs. The concentrations of the androgen precursor DHEAS were higher in patients with micro-APAs versus those with macro-APAs ($P = 0.007$). There were no significant differences in single steroid concentrations between patients with micro-APAs and BAH (Table A.3, Supplementary data). Patients with macro-APAs displayed higher concentrations of aldosterone, 18-oxocortisol, 18-hydroxycortisol ($P < 0.001$) compared with patients with BAH (Fig. 2 and Table A.3, Supplementary data). Higher concentrations of 11-deoxycorticosterone and pregnenolone ($P = 0.001$ and $P = 0.006$, respectively) and lower concentrations of DHEA and DHEAS ($P = 0.010$ and $P = 0.006$, respectively) were measured in patients with macro-APAs relative to patients with BAH.

Potential associations of steroids with micro-APA, macro-APA and BAH were determined by logistic regression models adjusting each steroid separately for sex and age to avoid a reduction of the predictive

value of variables by collinearity (Table 1). Only steroids were entered into the model which displayed a significant difference between subtype in the univariate analysis (Fig. 2, Table A.3, Supplementary data). Age had no impact on diagnosis, whereas female sex was associated with an increased likelihood of a diagnosis of a macro-APA compared with a micro-APA and with BAH.

With the adjustment for sex and age, only lower concentrations of 18-hydroxycortisol were associated with an increased likelihood of a micro-APA (OR 0.484 per ng/mL, 95% CI 0.289–0.812, $P = 0.006$). Higher concentrations of 18-hydroxycortisol were associated with an increased likelihood of a macro-APA versus BAH (OR 2.241 per ng/mL, 95% CI 1.458–3.444, $P < 0.001$) (Table 1). Higher concentrations of aldosterone, pregnenolone and 11-deoxycorticosterone were also associated with macro-APAs versus BAH (Table 1). In contrast, lower concentrations of DHEA were associated with an increased likelihood of a diagnosis of a macro-APA (OR 0.786 per ng/mL, 95% CI 0.656–0.941, $P = 0.009$) (Table 1).

3.3. Random forest algorithm using steroid profiling

Random forest classification trees were used to build a prediction model for micro-APAs, macro-APAs or BAH using peripheral plasma steroid concentrations. The algorithm created 30 different classification trees to optimize the prediction model and the predictive performance of each steroid was estimated (Fig. 3A) and the first classification tree of

Table 1
Peripheral plasma steroids associated with subtype diagnosis in primary aldosteronism.

Steroids (per ng/mL)	OR (95% CI)	P value	OR (95% CI)	P value	OR (95% CI)	P value
	Micro-APA vs. BAH (n = 101*)		Micro-APA vs. Macro-APA (n = 127*)		Macro-APA vs. BAH (n = 162*)	
Age	0.992 (0.949–1.036)	0.713	0.969 (0.928–1.011)	0.148	1.021 (0.985–1.058)	0.253
Sex (ref: female)	0.674 (0.228–1.992)	0.476	0.209 (0.076–0.572)	0.002	3.015 (1.433–6.343)	0.004
Aldosterone	11.215 (0.682–184.508)	0.091	0.422 (0.045–3.969)	0.451	877.947 (23.235–33172.977)	< 0.001
Age	0.995 (0.953–1.038)	0.813	0.966 (0.925–1.009)	0.116	1.022 (0.989–1.056)	0.201
Sex (ref: female)	0.808 (0.286–2.284)	0.687	0.197 (0.072–0.541)	0.002	3.271 (1.596–6.702)	0.001
18-Oxocortisol	1.291 (0.598–2.787)	0.515	0.761 (0.342–1.692)	0.503	2.984 (0.911–9.774)	0.071
Age	0.993 (0.951–1.037)	0.753	0.964 (0.920–1.010)	0.122	1.019 (0.985–1.055)	0.279
Sex (ref: female)	0.772 (0.275–2.171)	0.624	0.253 (0.087–0.738)	0.012	2.651 (1.241–5.662)	0.012
18-Hydroxycortisol	0.925 (0.528–1.623)	0.787	0.484 (0.289–0.812)	0.006	2.241 (1.458–3.444)	< 0.001
Age	0.991 (0.949–1.035)	0.686	0.969 (0.928–1.011)	0.141	1.019 (0.986–1.054)	0.257
Sex (ref: female)	0.694 (0.236–2.040)	0.507	0.198 (0.073–0.542)	0.002	3.225 (1.562–6.658)	0.002
11-Deoxycorticosterone	8.194 (0.300–223.625)	0.212	0.807 (0.266–2.452)	0.705	137.637 (3.052–6207.424)	0.011
Age	0.994 (0.953–1.038)	0.790	0.961 (0.920–1.004)	0.077	1.024 (0.990–1.060)	0.165
Sex (ref: female)	0.794 (0.281–2.242)	0.664	0.198 (0.071–0.554)	0.002	3.363 (1.619–6.988)	0.001
Pregnenolone	1.062 (0.799–1.413)	0.677	0.743 (0.547–1.008)	0.057	1.486 (1.149–1.923)	0.003
Age	0.978 (0.933–1.025)	0.354	0.974 (0.930–1.021)	0.274	0.988 (0.950–1.027)	0.538
Sex (ref: female)	0.786 (0.276–2.238)	0.652	0.195 (0.071–0.532)	0.001	3.651 (1.768–7.540)	< 0.001
DHEA	0.845 (0.673–1.060)	0.146	1.068 (0.868–1.315)	0.534	0.786 (0.656–0.941)	0.009
Age	0.988 (0.941–1.038)	0.641	0.983 (0.937–1.031)	0.477	0.995 (0.956–1.035)	0.793
Sex (ref: female)	0.720 (0.242–2.142)	0.555	0.245 (0.086–0.699)	0.009	2.646 (1.249–5.607)	0.011
DHEAS	1.000 (0.999–1.001)	0.658	1.001 (1.000–1.001)	0.182	0.999 (0.998–0.999)	0.048

Logistic regression analysis to identify adrenal steroids associated with micro-APAs, macro-APAs and BAH. An odds ratio greater than 1 indicates an increased likelihood of micro-APAs compared with BAH or compared with macro-APAs or macro-APAs compared with BAH, and an odds ratio less than 1 indicates a decreased likelihood. APA, aldosterone-producing adenoma; BAH, bilateral adrenal hyperplasia; DHEA, dehydroepiandrosterone; DHEAS, dehydroepiandrosterone sulphate; OR, odds ratio. There were 33 patients in the micro-APA group; 94 in the macro-APA and 68 in the BAH groups. *1 patient from the BAH group was missing pregnenolone data and was not included and 1 patient from the macro-APA group had outlier steroid profiling data.

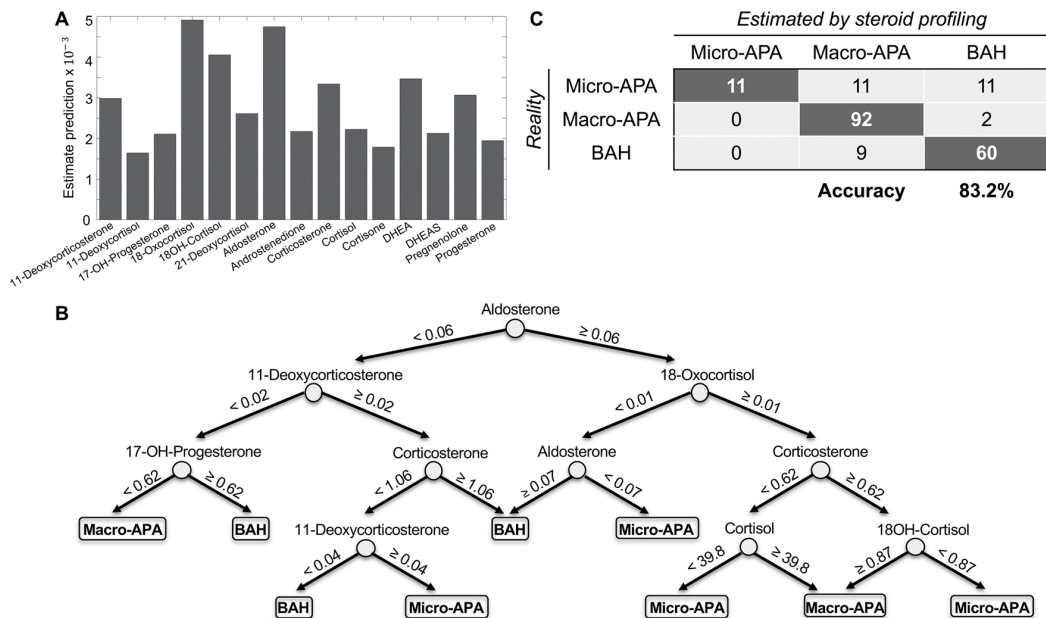


Fig. 3. Peripheral venous steroid profiling for the classification of micro-APAs, macro-APAs and BAH. The random forest algorithm constructed performance estimates for each steroid (Panel A), the first classification tree of the forest is shown for the prediction of micro-APAs, macro-APAs and BAH (Panel B), and a table with the estimated classification by steroid profiling and the actual classification by AVS (to differentiate BAH from APA) and pathology reports (to differentiate micro-APAs from macro-APAs) (Panel C). One patient had outlier steroid profiling results and was omitted. Numbers indicate steroid concentrations in ng/mL. To convert concentrations in ng/mL to pmol/L, concentrations should be divided by the molecular weight of each steroid. Molecular weights: 11-deoxycorticosterone, 330.46; 17-hydroxyprogesterone, 330.46; 18-hydroxycortisol, 330.46; 18-oxocortisol, 378.46; aldosterone, 360.44; corticosterone, 346.46; cortisol, 362.46. 17-OH-progesterone, 17-hydroxyprogesterone; 18OH-cortisol, 18-hydroxycortisol; APA, aldosterone-producing adenoma; BAH, bilateral adrenal hyperplasia; DHEA, dehydroepiandrosterone; DHEAS, dehydroepiandrosterone sulphate.

the forest is shown (Fig. 3B). AVS and pathology reports identified a total of 33 micro-APAs, 11 of the 33 micro-APA were correctly classified by the random forest model (Fig. 3C). The correct classification of macro-APAs was 96.8% (92 of 95, with 1 patient excluded as an

outlier), and 87.0% (60 of 69) of patients were correctly classified as BAH (Fig. 3C). The overall accuracy of steroid profiling for the classification of the 3 groups (micro-APAs, macro-APAs and BAH) was 83.2% (163/196), and the concordant diagnosis of APA and BAH between

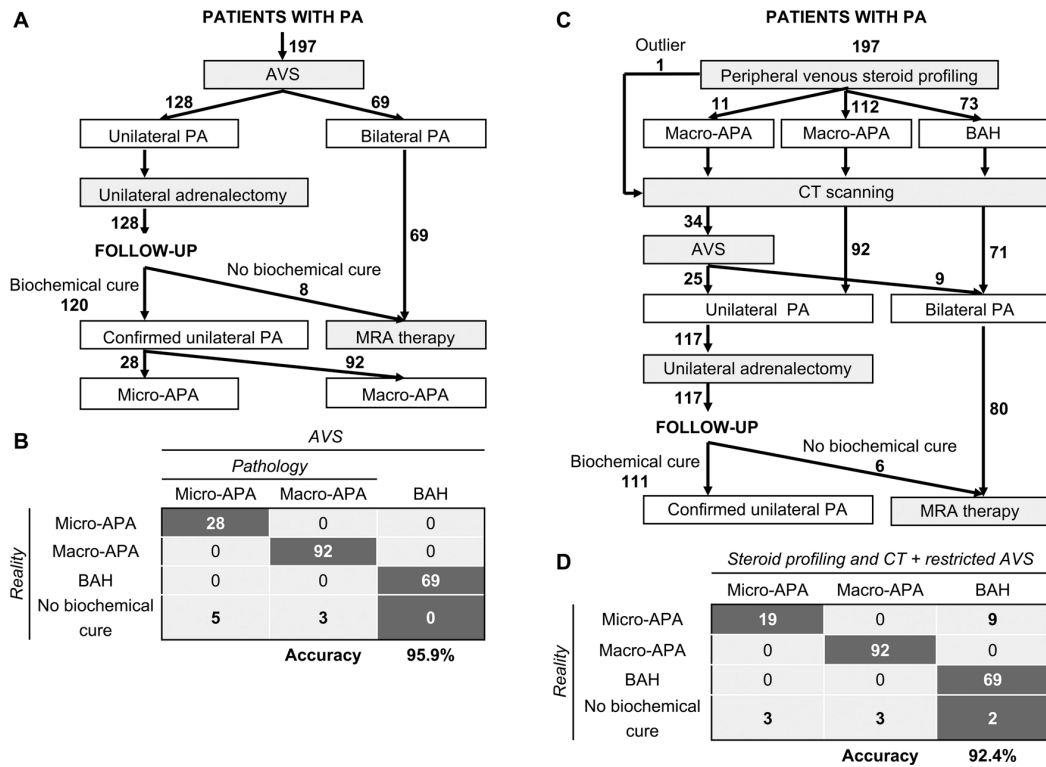


Fig. 4. Clinical management algorithms for patients with primary aldosteronism.

The AVS-based management of patients in this study is shown (Panel A), and results in the accurate differentiation of APA from BAH in at best 95.9% of patients (assuming a correct diagnosis of all patients with BAH) (Panel B). The diagnostic accuracy of APA is assessed here by the proportion of patients with biochemical cure (120 of 128 patients with complete biochemical success). No biochemical cure was observed in 6.3% (8 of 128 patients with absent or partial biochemical success). Therapeutic management based on peripheral venous steroid profiling and CT scanning with AVS in a restricted subset of patients (patients with discordant CT and steroid profiling results) would have reduced AVS procedures by at most 82.7% (34 of 197 patients addressed to AVS) and potentially 92.4% of patients would have had an accurate differentiation of APA from BAH (Panel C). The patient with outlier steroid profiling results would have been addressed to AVS. The number of patients with an absent or partial biochemical outcome would have been reduced to 6 (5.1%, 6 of 117) (Panel D). Numbers in bold indicate numbers of patients. APA, aldosterone-producing adenoma; AVS, adrenal venous sampling; CT, computed tomography; MRA, mineralocorticoid receptor antagonist; PA, primary aldosteronism.

steroid profiling and AVS was 88.8% (174/196) (Fig. 3C).

3.4. Diagnostic algorithm combining steroid profiling, CT and AVS

An AVS-based approach was used for the therapeutic management of the 197 patients in this study. Of these patients, 128 had laparoscopic unilateral adrenalectomy for resection of an APA and 69 were treated with MRAs for BAH (Fig. 4A). For the surgically-treated patients, 93.7% (120 of 128) displayed complete biochemical success after surgery. In patients with complete biochemical success, pathology reports indicated that the prevalence of micro-APAs was 23.3% (28 of 120 patients) and of macro-APAs 76.7% (92 of 120 patients). The remaining 6.3% (8 of 128 patients) displayed biochemical evidence of persistent hyperaldosteronism (partial or absent biochemical success). Assuming the patients with partial or absent biochemical success represent patients with a presurgical misdiagnosis of unilateral PA instead of bilateral PA, and the diagnosis of BAH with non-lateralized aldosterone secretion was accurate in all cases, the diagnostic accuracy of AVS-based management in the study cohort was 95.9% (189 of 197) (Fig. 4B).

We tested the performance of a diagnostic algorithm using peripheral venous steroid profiling and CT scanning in all patients and AVS limited to patients with discordant steroid profiling and CT scanning results (Fig. 4C). Applying this algorithm to the same cohort (n = 197 patients), peripheral venous steroid profiling would have predicted 11

patients with micro-APAs, 112 patients with macro-APAs and 73 patients with BAH. Of these patients, the 11 micro-APAs were correctly classified, 11 patients with micro-APAs were misclassified as macro-APAs, and 9 patients with BAH were incorrectly classified as macro-APAs. These 31 patients would be addressed to AVS for subtype differentiation because of potential discordant steroid profiling and CT scanning results.

An additional 2 of the 73 patients misclassified as BAH from steroid profiling instead of macro-APA would potentially be selected for AVS because of the detection of a unilateral adenoma at imaging. The patient with a macro-APA, classified as an outlier by steroid profiling, would also have been addressed to AVS. Therefore, a total of 34 patients would have AVS potentially resulting in, at the most, a theoretical reduction of AVS procedures by 82.7% (163 of 197 patients would bypass AVS assuming a normal CT morphology of the contralateral gland) with a comparable accuracy of diagnosis (92.4%) (Fig. 4D) to that of AVS-based management. The accuracy for the correct classification of micro-APAs could have reached 67.9% (19 of 28, 5 patients were excluded from the micro-APA group because they were not biochemically cured after adrenalectomy resulting in 28 patients with unilateral micro-APA), and the number of patients with incomplete biochemical cure after surgery (absent or partial biochemical success) would have decreased from 8 with the AVS algorithm (Fig. 4B) to 6 (5.1%) with the diagnostic algorithm incorporating steroid profiling (Fig. 4D). Eleven patients with micro-APAs would have been diagnosed

with BAH of which 9 were micro-APAs (from patients with complete biochemical success after surgery) and the remaining 2 patients (with absent or partial biochemical success) would have received the correct treatment with a MRA (Fig. 4D).

4. Discussion

We measured peripheral plasma steroid profiles by LC–MS/MS in a large series of patients with PA and determined the potential utility of integrating these measurements in therapeutic management. We focussed on using this approach to identify patients with micro-APAs which are often missed by CT in those centres that rely on CT for the differentiation of APA from BAH. The similar steroid profiles of patients with micro-APAs and BAH limits the application of a method based on steroid measurements alone but when considered in a diagnostic work up that includes interpretation of CT results and AVS (restricted to patients with discordant steroid profiles and CT data), the theoretical algorithm performed almost as well as AVS alone for the diagnosis of micro-APAs.

We also analysed the post-surgical clinical and biochemical outcomes of all patients with a unilateral APA ($n = 128$) included in the study in accordance with the PASO consensus, a standardized set of criteria to define outcomes of adrenalectomy for unilateral PA [26]. A smaller proportion of patients with micro-APAs achieved complete clinical and biochemical success than patients with macro-APAs but this is likely mainly due to the sex distribution difference between patients with micro-APAs (comprising a higher proportion of males and patients with a higher BMI) and with macro-APAs [26]. The sex distribution of our cohort may partially explain the difference between our findings and those of Omura et al., who reported an increase in the proportion of patients achieving clinical cure after surgical removal of micro-APAs ($n = 27$) compared with macro-APAs ($n = 42$) [18]. Although larger nodule size was associated with complete clinical success after adrenalectomy in a multicohort study [25] and APAs with *KCNJ5* mutations, which tend to be larger than other APAs [32,33], are also associated with favourable outcomes post-surgery [34].

Patients with absent or partial biochemical success after surgery were predominantly in the micro-APA group. CYP11B2 immunohistochemistry of the resected adrenals showed that they mostly comprised more than one micronodule with positive CYP11B2 immunostaining, in agreement with the suggestion that CYP11B2 immunohistochemistry of resected adrenals may be useful as an indicator of biochemical outcomes and highlight patients which require ongoing follow-up with biochemical as well as clinical re-assessment [31]. Despite the over-representation of micro-APAs in the group of patients who were not biochemically cured after adrenalectomy, this nonetheless comprised only 15% (5 of 33) of patients with micro-APAs indicating that it is worthwhile and potentially rewarding for patients to have further work up for the identification of micro-APAs.

The small area of the resected adrenal with CYP11B2 immunostaining in micro-APAs likely explains the decreased presurgical plasma aldosterone concentrations of the corresponding patients compared with those with macro-APAs as suggested by a previous report [21]. Patients with micro-APAs also had lower plasma concentrations of the hybrid steroids, 18-oxocortisol and 18-hydroxycortisol, relative to the macro-APA group but comparable to patients with BAH. This is feasibly explained by the larger size of APA carrying *KCNJ5* mutations [35,36] and the association of *KCNJ5*-mutated APAs with an increased production of 18-oxocortisol and 18-hydroxycortisol [11]. In line with this, we show that the micro-APA group displayed a lower prevalence of *KCNJ5* mutations compared with the macro-APA group. Further, a logistic regression model with adjustment of each steroid concentration for sex and age, showed an association of higher 18-hydroxycortisol concentrations (but not 18-oxocortisol) with an increased likelihood of a diagnosis of a macro-APA compared with micro-APA and with BAH. The association of female sex with macro-APAs and with increasing

plasma aldosterone concentrations is consistent with a meta-analysis report of patients with *KCNJ5*-mutated APAs displaying larger tumours and more pronounced hyperaldosteronism compared with patients with APAs without *KCNJ5* mutations [36].

Larger APAs may have increased glucocorticoid co-secretion [37,38] which would be expected to suppress pituitary ACTH production. ACTH is the main regulator of the synthesis of DHEA and DHEAS and therefore increased glucocorticoid co-secretion from macro-APAs may partly explain the lower concentrations of these steroids observed in patients with macro-APAs compared with patients with micro-APAs and BAH. Additional studies are required to address the role of APA size and genotype on glucocorticoid co-secretion with the inclusion of plasma ACTH measurements to establish their effects on the steroid profile.

In the PASO study, 6% of 699 patients did not display complete biochemical cure after adrenalectomy for APA and this group comprises cases of PA with bilateral asymmetrical aldosterone excess with a potential misdiagnosis of unilateral PA [26]. This compares favorably with CT based decision making for adrenalectomy, where 20% of patients with APA are not biochemically cured [39,40]. Using AVS results as the reference standard, the correct diagnosis of unilateral and bilateral PA by adrenal imaging (CT or magnetic resonance) was reported as 62.2% [41]. In another study on patients with unilateral APA (diagnosed by AVS) with follow-up data, 36% of patients who were biochemically cured after adrenalectomy would have been misdiagnosed on the basis of CT results [40]. Thus, neither CT nor AVS are completely reliable and strong interest focusses on approaches to improve the performance and accessibility of subtype differentiation in PA [12–17]. The potential utility of adrenal steroids in discriminating different subtypes of PA has been investigated in numerous studies with attention centering on the hybrid steroids 18-oxocortisol and 18-hydroxycortisol in urine or plasma [42]. Peripheral plasma 18-oxocortisol concentrations measured by LC–MS/MS can distinguish CT-detectable APA and BAH in patients from Japan [43]. However, in a European cohort, this method appears to be unreliable whereas a panel of 12 adrenal steroids in peripheral plasma differentiated APA from BAH with an accuracy of 80% [13]. The higher production of 18-oxocortisol in patients with *KCNJ5*-mutated APAs may explain the increased performance of 18-oxocortisol for differentiating APA from BAH in those cohorts with higher prevalences of *KCNJ5* mutations (as in Japan) compared with other populations (as in Europe) [13,43].

Genotype data in this study, as in most preceding studies, should be interpreted with caution because recent evidence shows that when sequencing is targeted to areas of the adenoma that are positive for CYP11B2 expression, somatic mutations are detected in almost 90% of APAs [30]. Therefore, the non-targeted sequencing approach used here is a limitation of the current study with an overrepresentation of the “wild-type” genotype notably in the micro-APA group because tissue dissection may have missed the micronodule. Further, the macro-APA group was not defined by CYP11B2 immunohistochemistry but by pathology reports of the largest nodule size (which would have been the nodule sampled for sequencing) and may comprise CYP11B2-negative nodules with a wild-type genotype [33]. In these cases, a secondary nodule (or multiple APCCs) responsible for the pathologic aldosterone production [34,44] would not have been sequenced. We showed by *CYP11B2* gene expression analysis of samples classified as adenomas compared with paired adjacent adrenal cortical tissue that the above occurred but in a minority of cases.

In the present study, patients with micro-APAs could not be predicted by steroid profiling alone. This was expected considering the high similarity we show of steroid profiles in patients with micro-APAs and BAH. To improve the reliability of identifying micro-APAs, we developed a hypothetical diagnostic algorithm integrating the additional consideration of CT imaging and using AVS only in patients with discordant steroid profiles and imaging data. The algorithm increased the probability of identifying micro-APAs whilst reducing the

proportion of AVS procedures by up to 82.7% but achieving a comparable accuracy of diagnosis with AVS-based management.

The strengths of our study are the large patient cohort with strict inclusion criteria for screening, diagnosis and subtype differentiation from 2 expert centres that use similar AVS protocols [10,22]. All patients had peripheral venous steroid measurements by LC–MS/MS and assessment of post-surgical clinical and biochemical outcomes in surgically-treated patients using the international PASO consensus. Further strengths are the development of an accessible online tool for the prediction of microAPA, macroAPA and BAH. Limitations of our study are the non-targeted genotyping approach and the potential inclusion of nonfunctional adenomas in the macro-APA group as discussed above and the relatively small number of patients with micro-APAs compared with macro-APAs and BAH. An additional limitation is the assumption of a correct detection of macro-APAs by CT scanning in the theoretical diagnostic algorithm.

5. Perspectives

Steroid profiling of peripheral venous plasma could potentially be used in combination with imaging data and AVS restricted to a small proportion of patients to identify patients in whom AVS should be considered mandatory. Such an approach may be useful in centres that rely on CT for subtype differentiation in PA because such approaches can lack the required sensitivity to detect micro-APAs.

Sources of funding

This work was supported by the European Research Council (ERC) under the European Union's Horizon 2020 research and innovation programme (grant agreement No [694913] to M. Reincke) and by the Deutsche Forschungsgemeinschaft (DFG, German Research Foundation) Projektnummer: 314061271 - TRR 205 to G. Eisenhofer, J.W.M. Lenders, M. Peitzsch, M. Reincke and T.A. Williams and grant RE 752/20-1 to M. Reincke; the Else Kröner-Fresenius Stiftung in support of the German Conns Registry-Else-Kröner Hyperaldosteronism Registry (2013_A182 and 2015_A171 to M. Reincke) and a grant from the Ministero dell'Istruzione, dell'Università e della Ricerca (MIUR, ex-60% 2015–2016 to T.A. Williams and 2016–2017 to P. Mulatero).

Acknowledgements

We gratefully acknowledge Nina Nirschl and Lisa Sturm for data management of the German Conn registry.

Appendix A. Supplementary data

Supplementary material related to this article can be found, in the online version, at doi:<https://doi.org/10.1016/j.jsbmb.2019.01.008>.

References

- [1] W.F. Young Jr, Primary aldosteronism: a common and curable form of hypertension, *Cardiol. Rev.* 7 (1999) 207–214.
- [2] M. Stowasser, Primary aldosteronism: rare bird or common cause of secondary hypertension? *Curr. Hypertens. Rep.* 3 (2001) 230–239.
- [3] P. Mulatero, M. Stowasser, K.C. Loh, C.E. Fardella, R.D. Gordon, L. Mosso, C.E. Gomez-Sanchez, F. Veglio, W.F. Young Jr, Increased diagnosis of primary aldosteronism, including surgically correctable forms, in centers from five continents, *J. Clin. Endocrinol. Metab.* 89 (2004) 1045–1050.
- [4] S. Savard, L. Amar, P.F. Plouin, O. Steichen, Cardiovascular complications associated with primary aldosteronism: a controlled cross-sectional study, *Hypertension* 62 (2013) 331–336.
- [5] P. Mulatero, S. Monticone, C. Bertello, A. Viola, D. Tizzani, A. Iannaccone, V. Crudo, J. Burrello, A. Milan, F. Rabbia, F. Veglio, Long-term cardio- and cerebrovascular events in patients with primary aldosteronism, *J. Clin. Endocrinol. Metab.* 98 (2013) 4826–4833.
- [6] S. Monticone, J. Burrello, D. Tizzani, C. Bertello, A. Viola, F. Buffolo, L. Gabetti, G. Mengozzi, T.A. Williams, F. Rabbia, F. Veglio, P. Mulatero, Prevalence and clinical manifestations of primary aldosteronism encountered in primary care practice, *J. Am. Coll. Cardiol.* 69 (2017) 1811–1820.
- [7] S. Monticone, F. D'Ascenzo, C. Moretti, T.A. Williams, F. Veglio, F. Gaita, P. Mulatero, Cardiovascular events and target organ damage in primary aldosteronism compared with essential hypertension: a systematic review and meta-analysis, *Lancet Diabetes Endocrinol.* 6 (2018) 41–50.
- [8] J.W. Funder, R.M. Carey, F. Mantero, M.H. Murad, M. Reincke, H. Shibata, M. Stowasser, W.F. Young Jr, The management of primary aldosteronism: case detection, diagnosis, and treatment: an endocrine society clinical practice guideline, *J. Clin. Endocrinol. Metab.* 101 (2016) 1889–1916.
- [9] W.F. Young, A.W. Stanson, G.B. Thompson, C.S. Grant, D.R. Farley, J.A. van Heerden, Role for adrenal venous sampling in primary aldosteronism, *Surgery* 136 (2004) 1227–1235.
- [10] T.A. Williams, M. Reincke, Management of endocrine disease: diagnosis and management of primary aldosteronism: the Endocrine Society guideline 2016 revisited, *Eur. J. Endocrinol.* 179 (2018) R19–R29.
- [11] T.A. Williams, M. Peitzsch, A.S. Dietz, T. Dekkers, M. Bidlingmaier, A. Rieder, M. Treitl, Y. Rhayem, F. Beuschlein, J.W. Lenders, J. Deinum, G. Eisenhofer, M. Reincke, Genotype-specific steroid profiles associated with aldosterone-producing adenomas, *Hypertension* 67 (2016) 139–145.
- [12] T. Abe, M. Naruse, W.F. Young Jr, N. Kobashi, Y. Doi, A. Izawa, K. Akama, Y. Okumura, M. Ikenaga, H. Kimura, H. Saji, K. Mukai, H. Matsumoto, A novel CYP11B2-specific imaging agent for detection of unilateral subtypes of primary aldosteronism, *J. Clin. Endocrinol. Metab.* 101 (2016) 1008–1015.
- [13] G. Eisenhofer, T. Dekkers, M. Peitzsch, A.S. Dietz, M. Bidlingmaier, M. Treitl, T.A. Williams, S.R. Bornstein, M. Haase, L.C. Rump, H.S. Willenberg, F. Beuschlein, J. Deinum, J.W. Lenders, M. Reincke, Mass spectrometry-based adrenal and peripheral venous steroid profiling for subtyping primary aldosteronism, *Clin. Chem.* 62 (2016) 514–524.
- [14] U.L. Scholl, L. Abriola, C. Zhang, E.N. Reimer, M. Plummer, B.I. Kazmierczak, J. Zhang, D. Hoyer, J.S. Merkel, W. Wang, R.P. Lifton, Macrolides selectively inhibit mutant KCNJ5 potassium channels that cause aldosterone-producing adenoma, *J. Clin. Invest.* 127 (2017) 2739–2750.
- [15] M. Naruse, H. Umakoshi, M. Tsuiki, M. Yokomoto, T. Tagami, A. Tanabe, A. Shimatsu, The latest developments of functional molecular imaging in the diagnosis of primary aldosteronism, *Horm. Metab. Res.* 49 (2017) 929–935.
- [16] B. Heinze, C.T. Fuss, P. Mulatero, F. Beuschlein, M. Reincke, M. Mustafa, A. Schirbel, T. Deutschbein, T.A. Williams, Y. Rhayem, M. Quinkler, N. Rayes, S. Monticone, V. Wild, C.E. Gomez-Sanchez, A.C. Reis, S. Petersenn, H.J. Wester, S. Kropf, M. Fassnacht, K. Lang, K. Herrmann, A.K. Buck, C. Bluemel, S. Hahner, Targeting CXCR4 (CXC chemokine receptor type 4) for molecular imaging of aldosterone-producing adenoma, *Hypertension* 71 (2018) 317–325.
- [17] W.F. Young Jr, A.W. Stanson, C.S. Grant, G.B. Thompson, J.A. van Heerden, Primary aldosteronism: adrenal venous sampling, *Surgery* 120 (1996) 913–919 discussion 919–920.
- [18] M. Omura, H. Sasano, J. Saito, K. Yamaguchi, Y. Kakuta, T. Nishikawa, Clinical characteristics of aldosterone-producing microadenoma, macroadenoma, and idiopathic hyperaldosteronism in 93 patients with primary aldosteronism, *Hypertens. Res.* 29 (2006) 883–889.
- [19] F. Satoh, T. Abe, M. Tanemoto, M. Nakamura, M. Abe, A. Uruno, R. Morimoto, A. Sato, K. Takase, S. Ishidoya, Y. Arai, T. Suzuki, H. Sasano, T. Ishibashi, S. Ito, Localization of aldosterone-producing adrenocortical adenomas: significance of adrenal venous sampling, *Hypertens. Res.* 30 (2007) 1083–1095.
- [20] S. Karashima, Y. Takeda, Y. Cheng, T. Yoneda, M. Demura, M. Kometani, M. Ohe, S. Mori, K. Yagi, M. Yamagishi, Clinical characteristics of primary hyperaldosteronism due to adrenal microadenoma, *Steroids* 76 (2011) 1363–1366.
- [21] Y. Ono, Y. Nakamura, T. Maekawa, S.J. Felizola, R. Morimoto, Y. Iwakura, M. Kudo, K. Seiji, K. Takase, Y. Arai, C.E. Gomez-Sanchez, S. Ito, H. Sasano, F. Satoh, Different expression of 11beta-hydroxylase and aldosterone synthase between aldosterone-producing microadenomas and macroadenomas, *Hypertension* 64 (2014) 438–444.
- [22] S. Monticone, A. Viola, D. Rossato, F. Veglio, M. Reincke, C. Gomez-Sanchez, P. Mulatero, Adrenal vein sampling in primary aldosteronism: towards a standardized protocol, *Lancet Diabetes Endocrinol.* 3 (2015) 296–303.
- [23] C.E. Gomez-Sanchez, X. Qi, C. Velarde-Miranda, M.W. Plonczynski, C.R. Parker, W. Rainey, F. Satoh, T. Maekawa, Y. Nakamura, H. Sasano, E.P. Gomez-Sanchez, Development of monoclonal antibodies against human CYP11B1 and CYP11B2, *Mol. Cell. Endocrinol.* 383 (2014) 111–117.
- [24] C.E. Gomez-Sanchez, M. Kuppasamy, M. Reincke, T.A. Williams, Disordered CYP11B2 expression in primary aldosteronism, *Horm. Metab. Res.* 49 (2017) 957–962.
- [25] K. Omata, S.A. Tomlins, W.E. Rainey, Aldosterone-producing cell clusters in normal and pathological states, *Horm. Metab. Res.* 49 (2017) 951–956.
- [26] T.A. Williams, J.W.M. Lenders, P. Mulatero, J. Burrello, M. Rottenkolber, C. Adolf, F. Satoh, L. Amar, M. Quinkler, J. Deinum, F. Beuschlein, K.K. Kitamoto, U. Pham, R. Morimoto, H. Umakoshi, A. Prejbisz, T. Kocjan, M. Naruse, M. Stowasser, T. Nishikawa, W.F. Young Jr, C.E. Gomez-Sanchez, J.W. Funder, M. Reincke, Outcomes after adrenalectomy for unilateral primary aldosteronism: an international consensus on outcome measures and analysis of remission rates in an international cohort, *Lancet Diabetes Endocrinol.* 5 (2017) 689–699.
- [27] T.A. Williams, S. Monticone, V.R. Schack, J. Stindl, J. Buffolo, F. Buffolo, L. Annaratone, I. Castellano, F. Beuschlein, M. Reincke, B. Lucatello, V. Ronconi, F. Fallo, G. Bernini, M. Maccario, G. Giachetti, F. Veglio, R. Warth, B. Vilsen, P. Mulatero, Somatic ATP1A1, ATP2B3, and KCNJ5 mutations in aldosterone-producing adenomas, *Hypertension* 63 (2014) 188–195.
- [28] F.L. Fernandes-Rosa, T.A. Williams, A. Rieder, O. Steichen, F. Beuschlein, S. Boulkroun, T.M. Strom, S. Monticone, L. Amar, T. Meatchi, F. Mantero,

- M.V. Cicala, M. Quinkler, F. Fallo, B. Allolio, G. Bernini, M. Maccario, G. Giacchetti, X. Jeunemaitre, P. Mulatero, M. Reincke, M.C. Zennaro, Genetic spectrum and clinical correlates of somatic mutations in aldosterone-producing adenoma, *Hypertension* 64 (2014) 354–361.
- [29] E.T.A. Prada, J. Burrello, M. Reincke, T.A. Williams, Old and new concepts in the molecular pathogenesis of primary aldosteronism, *Hypertension* 70 (2017) 875–881.
- [30] K. Nanba, K. Omata, T. Else, P.C.C. Beck, A.T. Nanba, A.F. Turcu, B.S. Miller, T.J. Giordano, S.A. Tomlins, W.E. Rainey, Targeted molecular characterization of aldosterone-producing adenomas in white americans, *J. Clin. Endocrinol. Metab.* 103 (2018) 3869–3876.
- [31] L.S. Meyer, X. Wang, E. Susnik, J. Burrello, A. Burrello, I. Castellano, G. Eisenhofer, F. Fallo, G.A. Kline, T. Knosel, T. Kocjan, J.W.M. Lenders, P. Mulatero, M. Naruse, T. Nishikawa, M. Peitzsch, L.C. Rump, F. Beuschlein, S. Hahner, C.E. Gomez-Sanchez, M. Reincke, T.A. Williams, Immunohistopathology and steroid profiles associated with biochemical outcomes after adrenalectomy for unilateral primary aldosteronism, *Hypertension* 72 (2018) 650–657.
- [32] M. Peitzsch, T. Dekkers, M. Haase, F.C. Sweep, I. Quack, G. Antoch, G. Siegert, J.W. Lenders, J. Deinum, H.S. Willenberg, G. Eisenhofer, An LC-MS/MS method for steroid profiling during adrenal venous sampling for investigation of primary aldosteronism, *J. Steroid Biochem. Mol. Biol.* 145 (2015) 75–84.
- [33] A.T. Nanba, K. Nanba, J.B. Byrd, J.J. Shields, T.J. Giordano, B.S. Miller, W.E. Rainey, R.J. Auchus, A.F. Turcu, Discordance between imaging and immunohistochemistry in unilateral primary aldosteronism, *Clin. Endocrinol. (Oxf.)* 87 (2017) 665–672.
- [34] T. Dekkers, M. ter Meer, J.W. Lenders, A.R. Hermus, L. Schultze Kool, J.F. Langenhuijsen, K. Nishimoto, T. Ogishima, K. Mukai, E.A. Azizan, B. Tops, J. Deinum, B. Kusters, Adrenal nodularity and somatic mutations in primary aldosteronism: one node is the culprit? *J. Clin. Endocrinol. Metab.* 99 (2014) E1341–1351.
- [35] S. Boulkroun, F. Beuschlein, G.P. Rossi, J.F. Golib-Dzib, E. Fischer, L. Amar, P. Mulatero, B. Samson-Couterie, S. Hahner, M. Quinkler, F. Fallo, C. Letizia, B. Allolio, G. Ceolotto, M.V. Cicala, K. Lang, H. Lefebvre, L. Lenzini, C. Maniero, S. Monticone, M. Perrocheau, C. Pilon, P.F. Plouin, N. Rayes, T.M. Seccia, F. Veglio, T.A. Williams, L. Zinnamosca, F. Mantero, A. Benecke, X. Jeunemaitre, M. Reincke, M.C. Zennaro, Prevalence, clinical, and molecular correlates of KCNJ5 mutations in primary aldosteronism, *Hypertension* 59 (2012) 592–598.
- [36] L. Lenzini, G. Rossitto, G. Maiolino, C. Letizia, J.W. Funder, G.P. Rossi, A meta-analysis of somatic KCNJ5 K(+) channel mutations in 1636 patients with an aldosterone-producing adenoma, *J. Clin. Endocrinol. Metab.* 100 (2015) E1089–E1095.
- [37] K. Inoue, Y. Yamazaki, Y. Tsurutani, S. Suematsu, C. Sugisawa, J. Saito, M. Omura, H. Sasano, T. Nishikawa, Evaluation of cortisol production in aldosterone-producing adenoma, *Horm. Metab. Res.* 49 (2017) 847–853.
- [38] W. Arlt, K. Lang, A.J. Sitch, A.S. Dietz, Y. Rhayem, I. Bancos, A. Feuchtinger, V. Chortis, L.C. Gilligan, P. Ludwig, A. Riester, E. Asbach, B.A. Hughes, D.M. O’Neil, M. Bidlingmaier, J.W. Tomlinson, Z.K. Hassan-Smith, D.A. Rees, C. Adolf, S. Hahner, M. Quinkler, T. Dekkers, J. Deinum, M. Biehl, B.G. Keevil, C.H.L. Shackleton, J.J. Deeks, A.K. Walch, F. Beuschlein, M. Reincke, Steroid metabolome analysis reveals prevalent glucocorticoid excess in primary aldosteronism, *JCI Insight* 2 (2017) pii: 93136.
- [39] T. Dekkers, A. Prejbisz, L.J.S. Kool, H. Groenewoud, M. Velema, W. Spiering, S. Kolodziejczyk-Kruk, M. Arntz, J. Kadziela, J.F. Langenhuijsen, M.N. Kerstens, A.H. van den Meiracker, B.J. van den Born, F. Sweep, A. Hermus, A. Januszewicz, A.F. Ligthart-Naber, P. Makai, G.J. van der Wilt, J.W.M. Lenders, J. Deinum, S. Investigators, Adrenal vein sampling versus CT scan to determine treatment in primary aldosteronism: an outcome-based randomised diagnostic trial, *Lancet Diabetes Endocrinol.* 4 (2016) 739–746.
- [40] T.A. Williams, J. Burrello, L.A. Sechi, C.E. Fardella, J. Matrozzova, C. Adolf, R. Baudrand, S. Bernardi, F. Beuschlein, C. Catena, M. Doumas, F. Fallo, G. Giacchetti, D.A. Heinrich, G. Saint-Hilary, P.M. Jansen, A. Januszewicz, T. Kocjan, T. Nishikawa, M. Quinkler, F. Satoh, H. Umakoshi, J. Widimsky Jr, S. Hahner, S. Douma, M. Stowasser, P. Mulatero, M. Reincke, Computed tomography and adrenal venous sampling in the diagnosis of unilateral primary aldosteronism, *Hypertension* 72 (2018) 641–649.
- [41] M.J. Kempers, J.W. Lenders, L. van Outheusden, G.J. van der Wilt, L.J. Schultze Kool, A.R. Hermus, J. Deinum, Systematic review: diagnostic procedures to differentiate unilateral from bilateral adrenal abnormality in primary aldosteronism, *Ann. Intern. Med.* 151 (2009) 329–337.
- [42] P. Mulatero, S.M. di Cella, S. Monticone, D. Schiavone, M. Manzo, G. Mengozzi, F. Rabbia, M. Terzolo, E.P. Gomez-Sanchez, C.E. Gomez-Sanchez, F. Veglio, 18-hydroxycorticosterone, 18-hydroxycortisol, and 18-oxocortisol in the diagnosis of primary aldosteronism and its subtypes, *J. Clin. Endocrinol. Metab.* 97 (2012) 881–889.
- [43] F. Satoh, R. Morimoto, Y. Ono, Y. Iwakura, K. Omata, M. Kudo, K. Takase, K. Seiji, H. Sasamoto, S. Honma, M. Okuyama, K. Yamashita, C.E. Gomez-Sanchez, W.E. Rainey, Y. Arai, H. Sasano, Y. Nakamura, S. Ito, Measurement of peripheral plasma 18-oxocortisol can discriminate unilateral adenoma from bilateral diseases in patients with primary aldosteronism, *Hypertension* 65 (2015) 1096–1102.
- [44] F.L. Fernandes-Rosa, I. Giscos-Douriez, L. Amar, C.E. Gomez-Sanchez, T. Meatchi, S. Boulkroun, M.C. Zennaro, Different somatic mutations in multinodular adrenals with aldosterone-producing adenoma, *Hypertension* 66 (2015) 1014–1022.

ONLINE ONLY SUPPLEMENT

Classification of microadenomas in patients with primary aldosteronism by steroid profiling

Yuhong Yang^{1*}, Jacopo Burrello^{2*}, Alessio Burrello³, Graeme Eisenhofer^{4,5}, Mirko Peitzsch⁴,
Martina Tetti², Thomas Knösel⁶, Felix Beuschlein^{1,7}, Jacques WM Lenders^{5,8}, Paolo Mulatero²,
Martin Reincke¹, Tracy Ann Williams^{1,2}

¹Medizinische Klinik und Poliklinik IV, Klinikum der Universität, Ludwig-Maximilians-Universität München, Munich, Germany

²Division of Internal Medicine and Hypertension, Department of Medical Sciences, University of Turin, Turin, Italy

³Department of Electronics and telecommunications, Polytechnic University of Turin, Turin, Italy

⁴Institute of Clinical Chemistry and Laboratory Medicine, University Hospital Carl Gustav Carus, Technische Universität Dresden, Dresden, Germany

⁵Department of Medicine III, University Hospital Carl Gustav Carus, Technische Universität Dresden, Dresden, Germany

⁶Institute of Pathology, Ludwig-Maximilians-Universität München, Munich, Germany

⁷Klinik für Endokrinologie, Diabetologie und Klinische Ernährung, Universitätsspital Zürich, Zürich, Switzerland

⁸Department of Medicine, Radboud University Medical Center, Nijmegen, The Netherlands

* These authors contributed equally to this work

Contents

Figure A.1 CYP11B2 gene expression analysis of APAs *versus* adjacent cortex

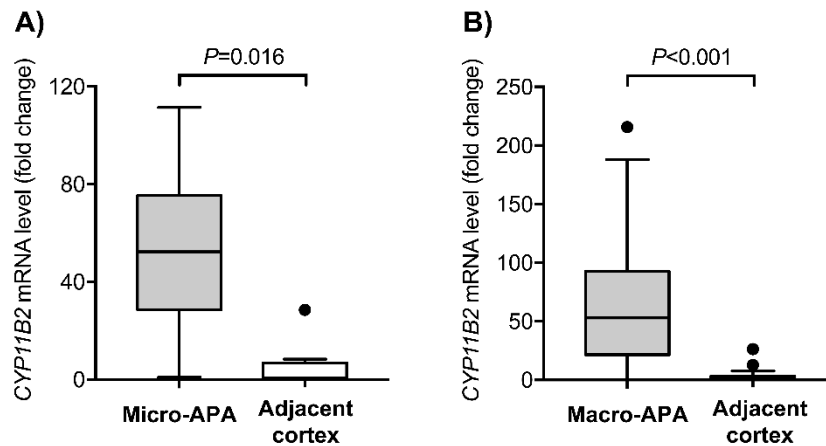
Table A.1 Gene mutation analysis of APAs

Table A.2 Demographic and clinical characteristics of patients with micro-APAs, macro-APAs and BAH

Table A.3 Peripheral plasma steroid concentrations in patients with micro-APAs, macro-APAs and BAH

References

Figure A.1 CYP11B2 gene expression analysis of APAs *versus* adjacent cortex



Real-time TaqMan qPCR was used to compare *CYP11B2* gene expression levels in samples classified as micro-APAs or macro-APAs compared with the respective paired adjacent cortical tissue (Adjacent cortex). Gene expression levels were calculated by the $2^{-\Delta\Delta Ct}$ quantification method using GAPDH as the endogenous reference gene. We included in the analysis all samples with available adenoma and corresponding adjacent cortical tissue. The samples comprised 8 micro-APAs (1 *KCNJ5* mutated, 7 wild type) and 32 macro-APAs (12 *KCNJ5* mutated, 6 with *ATP1A1* or *ATP2B3* mutations, 2 with *CACNA1D* mutations and 6 wild type). The box plots show fold-changes in gene expression (mRNA levels) of *CYP11B2* in the indicated tissue sample. Horizontal lines within boxes indicate the median, boxes and whiskers represent the 25th to 77th percentiles and the minimum and maximum values, respectively, after exclusion of outliers that are defined by 1.5 times the interquartile range and are indicated by filled circles. Levels of significance are indicated.

CYP11B2 gene expression analysis indicated an absence of *CYP11B2* gene upregulation in 1 of the 8 samples classified as micro-APAs (tumour-to-adjacent tissue *CYP11B2* expression ratio = 0.934; genotype determined as wild type) and in 1 of 32 samples classified as macro-APAs (tumour-to-adjacent tissue *CYP11B2* expression ratio = 0.926, genotype determined as wild type). This indicates the missed dissection of the *CYP11B2* positive nodule for the micro-APA and the dissection of a nonfunctional adenoma as the largest nodule for the sample classified as a macro-APA.

Table A.1 Gene mutation analysis of APAs

Gene Name	NCBI Reference	Target Exon	Primer sequence (5'-3')	Product size
<i>KCNJ5</i>	NM_000890	2	Forward: gcttcatttgggtgctcatt Reverse: gagatgactgcgttgttggga	313
<i>ATP1A1</i>	NM_000701	4	Forward: tatattgccttgaagtgtctgg Reverse: gaagtgggagacaaagacgg	334
<i>ATP1A1</i>	NM_000701	8	Forward: cgtggcttccttcaggttag Reverse: agagtgtaacattcgtgcaagc	386
<i>ATP2B3</i>	NM_021949	8	Forward: ttcttcctcttctctgtccc Reverse: ttcttaccctcagtttccgag	345
<i>CACNA1D</i>	NM_001128839	6	Forward: gtaaaggaggcatggttagg Reverse: tgctcagtaaagtgtctggt	375
<i>CACNA1D</i>	NM_001128839	8	Forward: ttgaattgccctgggtgtat Reverse: aatgtctggcaaccctctt	189
<i>CACNA1D</i>	NM_001128839	14	Forward: gtctgcatgggtgttctga Reverse: acgaagtgttctcggggaa	290
<i>CACNA1D</i>	NM_001128839	16	Forward: taaccttgggacggtcac Reverse: ccatgatccacaagcagc	367
<i>CACNA1D</i>	NM_001128839	23	Forward: cacgctaactgtgcaggga Reverse: tcagctctgccagaagag	279
<i>CACNA1D</i>	NM_001128839	27	Forward: ccaatctacaaccaccggt Reverse: gaccaaggacagaagccaa	198
<i>CACNA1D</i>	NM_001128839	32	Forward: acggttcttctcactgtcg Reverse: cttcagcagaggcatttggt	338

The forward and reverse primers used to amplify exons 2 of *KCNJ5* and the forward primers for the amplification of exons 8 and 27 of *CACNA1D* anneal within the respective exons (indicated in bold) and result in partial amplification of exons. For *KCNJ5*, a 323 bp 5' fragment and a 311 bp 3' fragment of exon 2 is not amplified and for *CACNA1D*, exon 8, a 19 bp fragment at the 5' end is not amplified and for exon 27, a 43 bp 5' fragment is not amplified. The *CACNA1D* primers detect all mutations described in Prada et al [1] except Glu412Asp mutation that is encoded by exon 9 [2] but includes the recently described Val259Gly mutation encoded by exon 6 by Nanba et al [3].

Table A.2 Demographic and clinical characteristics of patients with micro-APAs, macro-APAs and BAH

VARIABLE	N	Total (n=197)	Diagnosis			Overall P value	Pairwise Comparison (P value)		
			Micro-APA (n=33)	Macro-APA (n=95)	BAH (n=69)		Micro-APA vs. Macro-APA	Micro-APA vs. BAH	Macro-APA vs. BAH
Age (years)	197	51 [44-58]	52 [44-57]	52 [44-58]	49 [42-58]	0.647	NA	NA	NA
Sex (Female)	75	75 (38.1%)	7 (21.2%)	50 (52.7%)	18 (26.1%)	<0.001	0.002	0.592	0.001
BMI (kg/m ²)	196	28.0±4.4	29.3±3.8	27.1±4.6	28.5±4.2	0.027	0.046	1.000	0.174
BASELINE PARAMETERS									
Aldosterone (pmol/L)	197	722 [466-1235]	663 [516-1243]	968 [583-1462]	508 [369-790]	<0.001	0.158	0.086	<0.001
DRC (mU/L)	124	3.5 [2.0-9.6]	3.3 [2.0-9.5]	3.1 [2.0-10.0]	4.1 [2.5-9.7]	0.480	NA	NA	NA
PRA (pmol/L/min)	73	2.6 [1.6-5.1]	2.6 [2.6-6.4]	2.6 [1.3-3.8]	2.6 [1.4-6.4]	0.848	NA	NA	NA
ARR_DRC	124	119 [55-273]	166 [71-346]	169 [57-357]	93 [51-146]	0.026	1.000	0.097	0.051
ARR_PRA	73	377 [204-590]	366 [212-498]	416 [245-810]	238 [158-460]	0.100	NA	NA	NA
Lowest serum K ⁺ (mmol/L)	196	3.2 [2.8-3.6]	3.2 [2.8-3.3]	2.9 [2.5-3.2]	3.5 [3.3-3.9]	<0.001	0.318	<0.001	<0.001
Systolic BP (mmHg)	197	158 [144-175]	160 [148-175]	155 [144-180]	158 [141-170]	0.510	NA	NA	NA
Diastolic BP (mmHg)	197	98 [89-106]	100 [90-106]	98 [90-106]	98 [89-105]	0.878	NA	NA	NA
Antihypertensive medication (DDD)	194	3.3 [2.0-5.0]	3.0 [2.1-4.4]	3.5 [2.0-6.0]	3.0 [1.5-5.0]	0.107	NA	NA	NA
CLINICAL OUTCOME									
Complete	42	42 (32.8%)	4 (12.1%)	38 (40.0%)	NA	0.003	NA	NA	NA
Partial	67	67 (52.4%)	21 (63.6%)	46 (48.4%)	NA	0.132	NA	NA	NA
Absent	19	19 (14.8%)	8 (24.3%)	11 (11.6%)	NA	0.091	NA	NA	NA
BIOCHEMICAL OUTCOME									
Complete	120	120 (93.8%)	28 (84.8%)	92 (96.8%)	NA	0.023	NA	NA	NA
Partial	4	4 (3.1%)	2 (6.1%)	2 (2.1%)	NA	0.292	NA	NA	NA
Absent	4	4 (3.1%)	3 (9.1%)	1 (1.1%)	NA	0.036	NA	NA	NA

RESECTED ADRENAL***Size at pathology***

Largest nodule diameter (mm)	128	14 [9-18]	7 [5-9]	15 [12-20]	NA	<0.001	NA	NA	NA
<i>Genotype</i>	125	125	31	94	NA				
Wild-type*	59	59 (47.2%)	25 (80.7%)	34 (36.2%)	NA	<0.001	NA	NA	NA
<i>KCNJ5</i>	46	46 (36.8%)	1 (3.2%)	45 (47.9%)	NA	<0.001	NA	NA	NA
<i>CACNAID</i>	9	9 (7.2%)	4 (12.9%)	5 (5.3%)	NA	0.310	NA	NA	NA
<i>ATP1A1+ATP2B3</i>	11	11 (8.8%)	1 (3.2%)	10 (10.6%)	NA	0.369	NA	NA	NA

Quantitative normally distributed variables are expressed as means with SDs and quantitative non-normally distributed variables are reported as medians and interquartiles. Categorical variables are presented as absolute numbers and percentages. *P* values are calculated using Chi-square and Fisher's exact tests or ANOVA followed by Bonferroni tests or Kruskal-Wallis tests followed by pairwise comparisons as appropriate. APA, aldosterone-producing adenoma; ARR, aldosterone-to-renin ratio; BAH, bilateral adrenal hyperplasia; BMI, body mass index; BP, blood pressure; DDD, defined daily dose (defined daily dose is the assumed average maintenance dose per day for a drug used from its main indication in adults according to ATC/DDD Index 2018 https://www.whooc.no/atc_ddd_index/); DRC, direct renin concentration; K, potassium; N, number; NA, not applicable; PRA, plasma renin activity. *Wild-type indicates absence of mutations in *KCNJ5*, *CACNAID*, *ATP1A1* and *ATP2B3*.

Table A.3 Peripheral plasma steroid concentrations in patients with micro-APAs, macro-APAs and BAH

Steroids (ng/mL)	Micro-APA (n=33)	Macro-APA (n=95)	BAH (n=69)	Overall <i>P</i> value	Pairwise Comparison (<i>P</i> value)		
					Micro-APA vs. Macro-APA	Micro-APA vs. BAH	Macro-APA vs. BAH
Aldosterone	0.090 [0.038-0.149]	0.140 [0.094-0.280]	0.070 [0.033-0.123]	<0.001	0.006	1.000	<0.001
18-Oxocortisol	0.010 [0.010-0.035]	0.080 [0.020-0.320]	0.010 [0.010-0.025]	<0.001	<0.001	1.000	<0.001
18-OH-Cortisol	0.670 [0.385-0.995]	1.640 [0.770-2.670]	0.690 [0.430-1.405]	<0.001	<0.001	1.000	<0.001
21-Deoxycortisol	0.079 [0.035-0.090]	0.030 [0.010-0.091]	0.040 [0.018-0.091]	0.250	NA	NA	NA
Corticosterone	2.000 [0.600-4.500]	2.340 [1.200-4.480]	2.470 [1.160-5.500]	0.235	NA	NA	NA
11-Deoxycorticosterone	0.080 [0.045-0.120]	0.110 [0.050-0.220]	0.060 [0.030-0.115]	0.002	0.461	0.637	0.001
Progesterone	0.110 [0.060-0.180]	0.130 [0.090-0.220]	0.120 [0.080-0.215]	0.540	NA	NA	NA
Cortisol	115.00 [52.50-146.50]	117.00 [66.00-152.00]	112.00 [81.00-166.00]	0.370	NA	NA	NA
Cortisone	16.40 [11.95-21.45]	16.80 [12.10-19.70]	17.30 [13.55-21.60]	0.566	NA	NA	NA
11-Deoxycortisol	0.310 [0.130-0.540]	0.340 [0.200-0.700]	0.290 [0.185-0.665]	0.576	NA	NA	NA
17-OH-Progesterone	0.920 [0.375-1.290]	0.710 [0.400-1.140]	0.880 [0.500-1.295]	0.244	NA	NA	NA
Pregnenolone	0.270 [0.170-0.700]	0.360 [0.210-3.190]	0.255 [0.188-0.413]	0.005	0.119	1.000	0.006
Androstenedione	0.850 [0.590-1.160]	0.780 [0.500-1.330]	0.840 [0.590-1.235]	0.825	NA	NA	NA
DHEA	2.579 [1.751-3.481]	1.820 [1.047-3.120]	2.584 [1.551-4.411]	0.009	0.183	1.000	0.010
DHEAS	1210.0 [829.0-1588.0]	800.0 [444.0-1288.0]	1145.0 [689.5-1719.0]	0.001	0.007	1.000	0.006

Quantitative normally distributed variables are expressed as means with SDs and quantitative non-normally distributed variables are reported as medians and interquartiles. Categorical variables are presented as absolute numbers and percentages. *P* values are calculated using Kruskal-Wallis tests followed by pairwise comparisons as appropriate. To convert concentrations in ng/mL to pmol/L, concentrations should be divided by the molecular weight of each steroid. Molecular weights: 11-

deoxycorticosterone, 330.46; 17-hydroxyprogesterone, 330.46; 18-hydroxycortisol, 378.46; 18-oxocortisol, 376.45; aldosterone, 360.44; corticosterone, 346.46; cortisol, 362.46. 17-OH-progesterone, 17-hydroxyprogesterone; 18OH-cortisol, 18-hydroxycortisol; APA, aldosterone-producing adenoma; BAH, bilateral adrenal hyperplasia; DHEA, dehydroepiandrosterone; DHEAS, dehydroepiandrosterone sulphate; NA, not applicable.

0

References

- [1] E.T.A. Prada, J. Burrello, M. Reincke, T.A. Williams, Old and New Concepts in the Molecular Pathogenesis of Primary Aldosteronism, *Hypertension* 70 (2017) 875-881.
- [2] Y. Yamazaki, Y. Nakamura, K. Omata, K. Ise, Y. Tezuka, Y. Ono, R. Morimoto, Y. Nozawa, C.E. Gomez-Sanchez, S.A. Tomlins, W.E. Rainey, S. Ito, F. Satoh, H. Sasano, Histopathological Classification of Cross-Sectional Image-Negative Hyperaldosteronism, *J. Clin. Endocrinol. Metab.* 102 (2017) 1182-1192.
- [3] K. Nanba, K. Omata, T. Else, P.C.C. Beck, A.T. Nanba, A.F. Turcu, B.S. Miller, T.J. Giordano, S.A. Tomlins, W.E. Rainey, Targeted Molecular Characterization of Aldosterone-Producing Adenomas in White Americans, *J. Clin. Endocrinol. Metab.* 103 (2018) 3869-3876.

8. Paper II

Title: *BEX1* is differentially expressed in aldosterone-producing adenomas and protects human adrenocortical cells from ferroptosis

Authors: Yang Y, Tetti M, Vohra T, Adolf C, Seissler J, Hristov M, Belavgeni A, Bidlingmaier M, Linkermann A, Mulatero P, Beuschlein F, Reincke M, Williams TA

Journal: Hypertension

Year: 2021

Volume: 77

Pages: 1647-1658

DOI: 10.1161/HYPERTENSIONAHA.120.16774

PRIMARY ALDOSTERONISM

BEX1 Is Differentially Expressed in Aldosterone-Producing Adenomas and Protects Human Adrenocortical Cells From Ferroptosis

Yuhong Yang¹, Martina Tetti, Twinkle Vohra¹, Christian Adolf, Jochen Seissler, Michael Hristov, Alexia Belavgeni¹, Martin Bidlingmaier, Andreas Linkermann¹, Paolo Mulatero¹, Felix Beuschlein¹, Martin Reincke¹, Tracy Ann Williams¹

ABSTRACT: Aldosterone-producing adenomas (APAs) are a major cause of primary aldosteronism. Somatic mutations in ion channels and transporters drive the aldosterone overproduction in the majority of APAs with mutations in the KCNJ5 G protein-coupled potassium channel predominating in most reported populations. Our objective was to gain insight into biological mechanisms of APA tumorigenesis by comparing transcriptomes of APAs of distinct sizes by mRNA sequencing analysis (9 APAs with adenoma diameter ≥ 30 mm versus 12 APAs ≤ 10 mm). Genes with significantly altered expression levels between these 2 groups were identified in APAs with no mutation detected (348 genes) and with a *KCNJ5* mutation (155 genes). We validated the differential expression of 10 genes with a known function related to cell death and proliferation in an expanded sample set of 71 APAs by real-time quantitative polymerase chain reaction (58 macro-APAs, diameter ≥ 10 mm; 13 micro-APAs, diameter < 10 mm). We focused on *BEX1* that was upregulated in micro-APAs relative to macro-APAs (2.76-fold, $P < 0.001$) and compared with paired adrenal cortex (3.85-fold, $P < 0.05$), and showed a linear negative correlation with APA diameter in the no mutation detected group ($r = -0.501$, $P = 0.007$). Compared with control cells, stable expression of *BEX1* in human adrenocortical cells did not alter cell cycle progression or sensitivity to apoptosis but conferred protection from ferroptosis ($P < 0.01$), a form of regulated cell death, measured by flow cytometry. Taken together, these findings demonstrate that *BEX1* promotes cell survival in adrenal cells by mediating the inhibition of ferroptosis and suggest a function for *BEX1* in the pathogenesis of APAs. (*Hypertension*. 2021;77:1647–1658. DOI: 10.1161/HYPERTENSIONAHA.120.16774.)

• **Data Supplement**

Key Words: adenoma ■ aldosterone ■ cell death ■ flow cytometry ■ mutation

Primary aldosteronism (PA) is the most frequent surgically correctable cause of hypertension. The unilateral forms of the disease are mainly caused by an aldosterone-producing adenoma (APA) and are specifically treated and potentially cured by adrenalectomy.^{1,2} The surgically removed adrenals have been used to demonstrate the presence of somatic mutations in APAs in genes encoding ion channels (*KCNJ5*,³ *CACNA1D*,^{4,5} *CACNA1H*,⁶ *CLCN2*)⁷ and transporters (*ATP1A1*,^{5,8} *ATP2B3*).⁹ These mutations disturb ion homeostasis and activate Ca^{2+} signaling resulting in increased expression of *CYP11B2* (encoding aldosterone synthase)

and constitutive aldosterone production.^{6,9} The use of targeted next-generation sequence analysis guided by CYP11B2-immunohistochemistry of paraffin-embedded adrenals has greatly increased the detection of somatic mutations in APAs to achieve a combined prevalence of over 90%.^{10–12}

The role of the above mutations in cell death and proliferation is less clear. Activating somatic mutations in *CTNNB1*, encoding β -catenin, have been identified in APAs.¹³ The prevalence of *CTNNB1* mutations in APAs is lower than in other adrenocortical tumors,¹⁴ but the proportion of APAs with constitutive Wnt/ β -catenin

Correspondence to: Tracy Ann Williams, Medizinische Klinik und Poliklinik IV, Klinikum der Universität München, LMU München, Ziemssenstr 1, D-80336 München, Germany. Email tracy.williams@med.uni-muenchen.de

The Data Supplement is available with this article at <https://www.ahajournals.org/doi/suppl/10.1161/HYPERTENSIONAHA.120.16774>.

For Sources of Funding and Disclosures, see page 1656.

© 2021 American Heart Association, Inc.

Hypertension is available at www.ahajournals.org/journal/hyp

Novelty and Significance

What Is New?

- Transcriptome profiles of aldosterone-producing adenomas with highly diverse diameters are distinctly different.
- Gene ontology enrichment analysis identifies over-representation of cell death in a subset of aldosterone-producing adenomas.
- The *BEX1* (brain expressed X-linked 1) gene is upregulated in micro- compared with macro-aldosterone-producing adenomas and with paired adjacent adrenal cortex.
- In human adrenocortical cells in vitro, BEX1 confers protection from ferroptosis—a form of nonapoptotic regulated cell death.

What Is Relevant?

- mRNA-seq analysis of aldosterone-producing adenomas of diverse sizes identifies a multitude of genes involved in cell growth mechanisms.
- BEX1 may promote cell survival in small aldosterone-producing adenomas by mediating the inhibition of ferroptosis.

Summary

BEX1 suppresses ferroptosis in human adrenocortical cells and may play a role in the pathogenesis of aldosterone-producing adenomas.

Nonstandard Abbreviations and Acronyms

APA	aldosterone-producing adenoma
HAC15	human adrenocortical cell
NMD	no mutation detected
NRF2	nuclear factor erythroid 2–related factor 2
PA	primary aldosteronism

signaling is high¹⁵ implicating other factors in the activation of this pathway. Different *KCNJ5* mutations have diverse effects on adrenocortical cell growth¹⁶ depending on the level of Na⁺ conductance that determines the degree of cell toxicity.^{3,17}

We hypothesized that transcriptome profiling of APAs of distinctly different diameter may highlight genes that function in cell death and proliferation. We used mRNA sequencing (mRNA-seq) to compare the transcriptomes of small and large APAs from patients with PA with a similar known duration of hypertension. Our objective was to identify novel genes and biological mechanisms involved in the deregulated cell growth of adrenal cells and translate these findings to a potential role in APA pathogenesis.

MATERIALS AND METHODS

The authors declare that all supporting data are available within the article and its [Data Supplement](#). mRNA-seq data have been made publicly available and can be accessed at https://github.com/MedIVLMUMunich/MacroMicroAPA_RNAseq.

Patient Samples

The study comprised 71 APAs surgically removed from patients diagnosed with unilateral PA at 2 referral centers (39 from the Medizinische Klinik IV, Klinikum der

Ludwig-Maximilians-Universität München, Munich, Germany and 32 from the Hypertension unit, Department of Medical Sciences, University of Torino, Turin, Italy). For 17 APAs, the corresponding adjacent cortex was also available. PA was diagnosed according to current guidelines^{1,18} including adrenal venous sampling for subtype differentiation of unilateral from bilateral PA.¹⁹ All patients included in the study displayed complete biochemical success after surgery according to the PASO criteria confirming the diagnosis of unilateral PA.²⁰ The study also included 20 cortisol-producing adenomas and 8 incidentalomas diagnosed at the Munich center. Adenoma diameters were determined from the largest nodule at pathology. Research protocols were approved by local ethics committees, and all participants provided written informed consent.

Sanger Sequencing of Genomic DNA

KCNJ5 and hot spot regions of *ATP1A1*, *ATP2B3*, and *CACNA1D* were sequenced by Sanger sequencing of PCR-amplified genomic DNA extracted from fresh frozen nodules resected from patients with APA as described previously,²¹ *CTNNA1* was sequenced using primers shown in Table S1 in the [Data Supplement](#)). The histopathology of all formalin-fixed paraffin-embedded adrenals was evaluated using a specific CYP11B2 monoclonal antibody²² to confirm the presence of an APA or an aldosterone-producing nodule in the resected gland.²³

Next-Generation Sequencing and Bioinformatics Analysis

mRNA-seq transcriptome profiling was performed of 21 APAs comprising 9 large macro-APAs with adenoma diameter ≥ 30 mm (5 with a *KCNJ5* mutation and 4 with no mutation detected [NMD]) and 12 micro-APAs with adenoma diameter ≤ 10 mm (6 with a *KCNJ5* mutation and 6 with NMD). mRNA-seq was performed by QIAGEN Genomics (Hilden, Germany). Heatmap and unsupervised hierarchical clustering and volcano plots were performed using R or the ClustVis web tool (<https://biit.cs.ut.ee/clustvis/>).²⁴

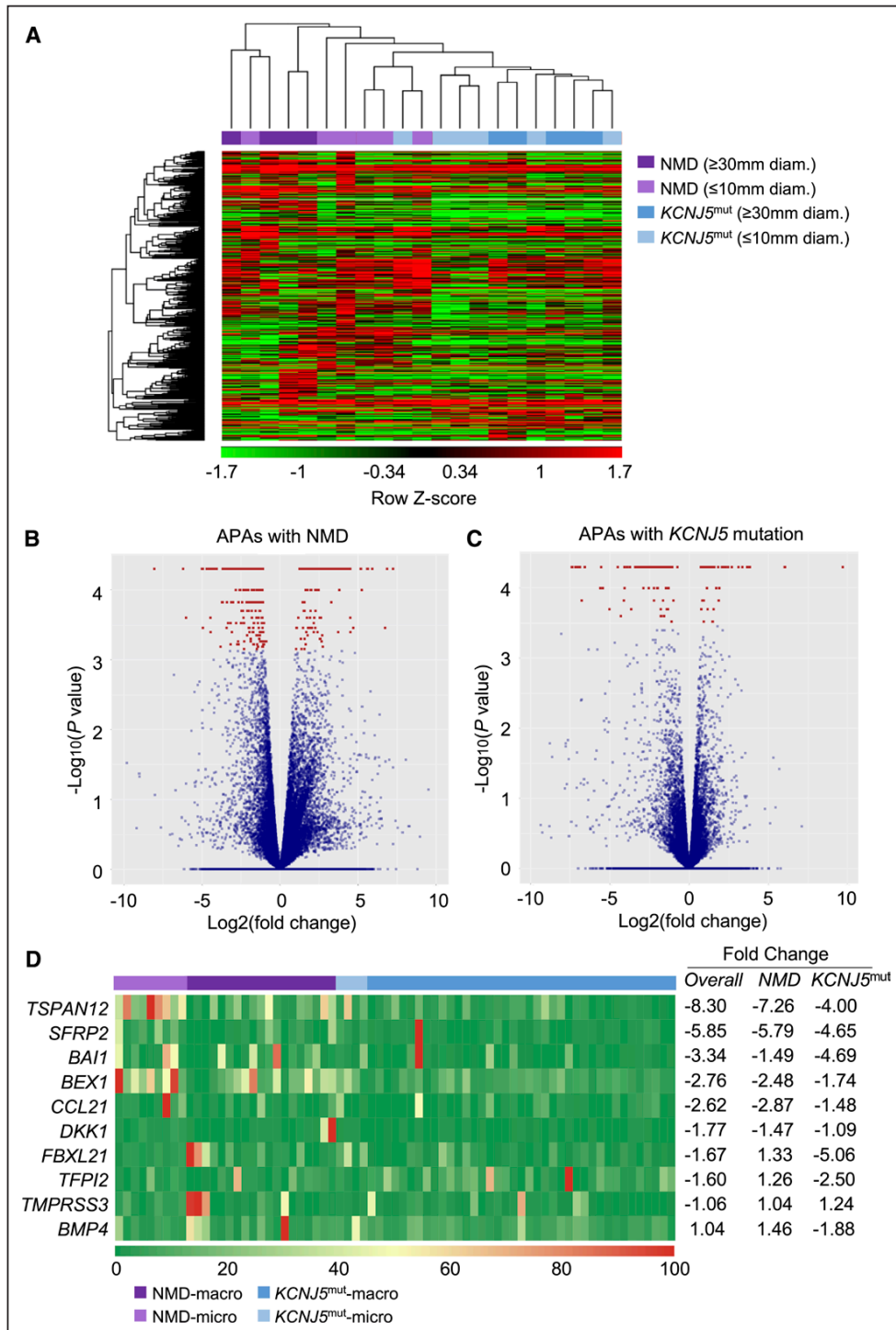


Figure 1. Distinct transcriptome profiles in aldosterone-producing adenomas (APAs) with different genotypes and adenoma diameters.

The heat map shows unsupervised hierarchical clustering of 500 genes with the largest coefficient of variation based on normalized (fragments per kilobase of transcript [FPKM], per million mapped reads) identified by mRNA-seq (A). Row Z-score indicates the difference in expression level of a gene in SD units from the mean expression level in all samples. Volcano plots by mRNA-seq analysis highlight genes in red that were differentially expressed in APAs with NMD (B) or with a *KCNJ5* mutation (C). Differential expression was defined as an adjusted $P < 0.05$ using the Benjamini-Hochberg False Discovery Rate method. Red dots in the region of $\text{Log}_2(\text{fold change}) < 0$ represent downregulated (Continued)

Cell Lines and Culture Conditions

Human adrenocortical (HAC15) cells²⁵ (a kind gift from Professor William E. Rainey, University of Michigan, Ann Arbor) were used to establish stable cell lines as described previously.¹⁶

Flow Cytometry

Vibrant DyeCycle Violet stain was used for cell cycle analysis. Propidium iodide was used to quantify proportions of propidium iodide-positive dead cells following ferroptosis induction (with 4 $\mu\text{mol/L}$ [1S, 3R]-RSL3 [RSL3]) in the presence or absence of ferroptosis inhibitor (10 $\mu\text{mol/L}$ liproxstatin-1). Cell populations were detected on a FACSCalibur (BD Biosciences) or a BD Accuri C6 flow cytometer with FL2 detector (BD Biosciences). Data were analyzed with FLOWJo version 10.4. All experiments were performed in triplicate, with a minimum of 7000 (cell cycle experiments) or 15 000 (ferroptosis experiments) single cells analyzed per sample.

Statistical Analysis

Statistical analyses were performed using IBM SPSS version 25.0 and GraphPad Prism version 8.2.1. Data were analyzed using the Kolmogorov-Smirnov test and Shapiro-Wilk test to determine distributions. Statistical significance was assessed by a *t* test (paired where appropriate) or a Mann-Whitney *U* test (Wilcoxon rank matched pairs test if needed) or a Bonferroni post-test after 2-way ANOVA. Chi-square and Fisher exact tests were used to compare categorical variables. Univariate correlations were assessed using Pearson correlations. $P < 0.05$ were considered statistically significant.

RESULTS

mRNA-Seq Transcriptome Analysis of APAs

Tumor samples used for mRNA-seq analysis (21 APAs) displayed a median nodule diameter of 34.0 mm (32.5–37.5) and 7.5 mm (6.3–10.0) ($P < 0.001$), in each group (APAs ≥ 30 mm versus APAs ≤ 10 mm diameter). There were no significant differences between the 2 groups in known duration of hypertension (Table S2).

Unsupervised hierarchical clustering of 500 genes with the largest coefficient of variation classified 4 gene clusters categorized by genotype and adenoma diameter (Figure 1A). Differential expression analysis identified 348 and 155 significantly altered genes in the NMD and *KCNJ5* subgroups, respectively (Figure 1B and 1C). Specifically, there were 119 upregulated and 229 downregulated DEGs in APAs with NMD, and 54 upregulated and

101 downregulated DEGs in the *KCNJ5* subgroup. The top 20 upregulated and downregulated genes in APAs (diameter ≥ 30 mm versus ≤ 10 mm) with NMD and with *KCNJ5* mutations are shown in Tables S3 and S4, respectively. The complete list of DEGs can be downloaded for: the total dataset: https://github.com/MedIVLMUMunich/MacroMicroAPA_RNAseq/raw/main/Total_DEGs.xlsx; and stratified by APAs with NMD: https://github.com/MedIVLMUMunich/MacroMicroAPA_RNAseq/raw/main/NMD_DEGs.xlsx; and with a *KCNJ5* mutation: https://github.com/MedIVLMUMunich/MacroMicroAPA_RNAseq/raw/main/KCNJ5_DEGs.xlsx.

Gene Ontology Enrichment Analysis

DEGs were annotated to Gene Ontology terms of biological processes that identified different patterns of gene set enrichment between macro- and micro-APAs according to genotype (APAs with NMD and with a *KCNJ5* mutation). Cell death was the most significantly enriched biological process in APAs with NMD ($P = 6.4 \times 10^{-8}$; Figure S1A). Other enriched Gene Ontology terms in this group were related to axon guidance, angiogenesis, cell migration, the cellular response to zinc ions or Wnt signaling (Figure S1A). APAs with *KCNJ5* mutations showed enrichment of genes related to cholesterol biosynthesis, the cell cycle and cell division. Other enriched terms in this group were associated with RNA processing, signal transduction, and organization of cellular components (Figure S1B).

DEGs Involved in Cell Death and Proliferation

Unsupervised hierarchical clustering of the top 40 DEGs associated with cell death and proliferation identified by the mRNA-seq analysis categorized gene clusters according to adenoma diameter in the NMD and *KCNJ5* subgroups (Figure S2). In the mRNA-seq analysis, no ferroptosis suppressor was differentially expressed in APAs with *KCNJ5* mutations. Conversely, 2 DEGs *MT1G* (metallothionein 1G) and *CAV1* (caveolin 1), encoding ferroptosis inhibitor proteins, were identified in the NMD subgroup (\log_2 [APA ≥ 30 mm/ ≤ 10 mm] = 3.10, adjusted $P = 0.0068$; \log_2 [APA ≥ 30 mm/ ≤ 10 mm] = -1.87, adjusted $P = 0.0415$; Figure S3).

The expression levels of a subset of DEGs (identified by mRNA-seq analysis) with a reported role in cell death and proliferation were determined in an expanded sample set of APAs ($n = 71$; median diameter 15.0 mm

Figure 1 Continued. genes in APAs ≥ 30 mm diameter compared with ≤ 10 mm diameter; red dots in the region of \log_2 (fold change) > 0 represents upregulated genes in the NMD and *KCNJ5*^{mut} subgroups as indicated. The second heatmap shows the mRNA expression levels of 10 genes, determined by real-time qPCR, of an expanded cohort of 71 APAs. The 10 genes selected for study were all DEGs of interest identified from the mRNA-seq analysis with a previously described role in cell death and proliferation (D). Genes studied are shown on the left of the figure, sample identity is color-coded at the top of the figure, and fold changes in gene expression (real-time qPCR quantification) are shown on the right, in the overall group (NMD+*KCNJ5*^{mut}) and stratified for APAs with NMD or *KCNJ5* mutations (*KCNJ5*^{mut}). The color-coded matrix shows the relative quantification (RQ) values of genes for each sample ($2^{-\Delta\Delta C_t}$) compared with the median micro-APA gene expression level of each gene. RQ values were then transformed to a 0 to 100 grading scale with the smallest RQ value set as 0 and largest value as 100. Macro-APAs are defined as ≥ 10 mm; micro-APAs as < 10 mm diameter. *KCNJ5* indicates gene encoding potassium inwardly rectifying channel subfamily J member 5; *KCNJ5*^{mut}, APAs with *KCNJ5* mutations; and NMD, APAs with no mutation detected.

[11.0–21.0]; Table 1). APAs in this sample set were stratified into macro- and micro-APAs according to a cutoff diameter of 10 mm (macro-APAs [diameter ≥10 mm], n=58, median diameter, 16.0 mm [14.0–22.8]; micro-APAs [diameter <10 mm], n=13, median diameter, 7.0 mm [6.5–8.0], $P<0.001$). The macro-APA group comprised a higher proportion of women (63.8% and 30.8% in the macro- and micro-APA groups, respectively, $P=0.029$) and APAs with a *KCNJ5* mutation (67.2% in macro-APAs versus 30.8% in micro-APAs, $P=0.015$). The micro-APAs included a higher proportion of APAs with NMD (69.2% versus 32.8%; Table 1).

Figure 1D shows the relative expression levels in macro- versus micro-APAs of 10 genes with a known role in cell death and proliferation. These genes included those with a role in β -catenin signaling (mRNA levels in macro- versus micro-APAs: *TSPAN12*, -8.30 -fold, $P<0.0001$; *SFRP2*, -5.85 -fold, $P<0.001$; *DKK1*,

-1.77 -fold, $P<0.01$). *TSPAN12*, *BEX1*, *FBXL21*, and *TMPRSS3* gene expression levels were weakly correlated with adenoma diameter in the combined group of APAs (APAs with NMD+APAs with *KCNJ5* mutations), stronger correlations were observed in APAs with NMD (Table 2). In the NMD group, *FBXL21* and *TMPRSS3* gene expression was strongly positively correlated with adenoma diameter (*FBXL21*: $r=0.761$, $P<0.001$; *TMPRSS3*: $r=0.727$, $P<0.001$), a moderate negative correlation of *TSPAN12* and *BEX1* gene expression with adenoma diameter was observed (*TSPAN12*: $r=-0.572$, $P=0.001$; *BEX1*: $r=-0.501$, $P=0.007$; Table 2).

BEX1 Gene Expression Is Increased in Micro-APAs and Aldosterone-Producing Micronodules

In the expanded cohort of APAs (n=71), *BEX1* gene expression was 2.76-fold higher in micro-APAs relative

Table 1. Clinical and Biochemical Parameters of Patients With APA Stratified by Adenoma Diameter

Variables	Total cohort (n=71)	Macro-APA (n=58)	Micro-APA (n=13)	P value
Age at surgery, y (n=71)	48.2±11.5	48.2±11.4	48.1±12.4	0.978
Sex (ref. women; n=71)	41 (57.7%)	37 (63.8%)	4 (30.8%)	0.029
BMI, kg/m ² (n=66)	26.2 (22.7–30.1)	26.0 (22.4–30.0)	26.4 (23.4–31.5)	0.502
Systolic BP, mmHg (n=68)	150 (140–166)	149 (140–161)	160 (150–174)	0.029
Diastolic BP, mmHg (n=68)	94 (85–101)	92 (85–100)	100 (88–108)	0.217
Duration HTN, mo (n=69)	97 (29–171)	99 (24–174)	97 (51–207)	0.586
Anti-HTN meds (DDD; n=66)	3.0 (1.5–4.8)	3.0 (1.1–4.5)	3.7 (2.6–4.9)	0.179
PAC, pmol/L (n=69)	838 (590–1419)	859 (586–1404)	805 (571–1523)	0.939
DRC, mU/L (n=36)	3.4 (2.0–7.6)	3.3 (2.0–8.2)	4.5 (2.4–6.5)	0.903
ARR_DRC (n=36)	197 (92–356)	218 (92–371)	160 (89–283)	0.480
PRA, pmol/L per min (n=32)	2.6 (2.3–6.4)	2.6 (2.6–5.1)	6.4 (1.3–8.3)	0.564
ARR_PRA (n=32)	352 (142–596)	377 (150–609)	225 (111–841)	0.458
Lowest serum K ⁺ , mmol/L (n=70)	3.0±0.6	2.9±0.6	3.2±0.4	0.145
Nodule diameter, mm (n=71)	15.0 (11.0–21.0)	16.0 (14.0–22.8)	7.0 (6.5–8.0)	<0.001
APAs_KCNJ5 mutation (n=43)	43 (60.6%)	39 (67.2%)	4 (30.8%)	0.015
APAs_NMD (n=28)	28 (39.4%)	19 (32.8%)	9 (69.2%)	0.015
Clinical outcome (n=63)				0.115
Complete success	27 (42.9%)	25 (47.2%)	2 (20.0%)	
Partial success	28 (44.4%)	23 (43.4%)	5 (50.0%)	
Absent success	8 (12.7%)	5 (9.4%)	3 (30.0%)	
Biochemical outcome (n=61)				NA
Complete success	61 (100.0%)	50 (100.0%)	11 (100.0%)	
Partial success	0 (0.0%)	0 (0.0%)	0 (0.0%)	
Absent success	0 (0.0%)	0 (0.0%)	0 (0.0%)	

All variables refer to baseline data. Nodule diameter refers to the diameter of the largest adrenal nodule at pathology. Macro-APAs were defined by diameter of the largest nodule ≥10 mm; micro-APAs were defined by diameter of the largest nodule <10 mm. Quantitative normally distributed variables are expressed as means±SD and quantitative non-normally distributed variables are reported as medians (IQR). Categorical variables are presented as absolute numbers and percentages. P values were calculated using χ^2 and Fisher exact tests or t test or Mann-Whitney U test as appropriate. P values of <0.05 were considered significant. The defined daily dose is the assumed average maintenance dose per day for a drug used for its main indication in adults according to ATC/DDD Index 2019 https://www.whocc.no/atc_ddd_index/. APA indicates aldosterone-producing adenoma; ARR, aldosterone-to-renin ratio; BMI, body mass index; BP, blood pressure; DDD, defined daily dose; DRC, direct renin concentration; HTN, hypertension; IQR, interquartile range; K⁺, potassium ions; *KCNJ5*, gene encoding potassium inwardly rectifying channel subfamily J member 5; meds, medications; n, number; NA, not applicable; NMD, no mutation detected; PAC, plasma aldosterone concentration; PRA, plasma renin activity; and ref, reference.

Table 2. Correlation of Gene Expression Levels With APA Diameter According to Genotype

Gene	Protein	Overall		NMD		KCNJ5 ^{mut}	
		r	P value	R	P value	r	P value
TSPAN12	Tetraspanin 12	−0.388	0.001	−0.572	0.001	−0.148	0.344
SFRP2	Secreted frizzled-related protein 2	−0.038	0.760	−0.397	0.036	0.129	0.433
BAI1	Brain-specific angiogenesis inhibitor 1	−0.105	0.411	−0.210	0.293	0.068	0.689
BEX1	Brain expressed X-linked 1	−0.376	0.001	−0.501	0.007	−0.241	0.119
CCL21	Chemokine, C-C motif, ligand 21	−0.152	0.207	−0.249	0.201	−0.037	0.813
DKK1	Dickkopf-related protein 1	−0.139	0.249	−0.169	0.390	−0.175	0.269
FBXL21	F-box and leucine-rich repeat protein 21	0.361	0.005	0.761	<0.001	−0.251	0.159
TFPI2	Tissue factor pathway inhibitor 2	0.039	0.748	0.017	0.932	0.008	0.959
TMPRSS3	Transmembrane serine protease 3	0.443	0.001	0.727	<0.001	0.317	0.083
BMP4	Bone morphogenetic protein 4	0.111	0.358	0.389	0.041	−0.124	0.427

Values indicate Pearson correlation coefficients (r) and respective P value in the overall group (NMD+KCNJ5^{mut}) of APAs or stratified for APAs with NMD or KCNJ5 mutations. Gene expression levels of 71 APAs (28 with NMD and 43 with KCNJ5 mutations) were determined by real-time quantitative polymerase chain reaction as described in the online supplemental methods section. APA indicates aldosterone-producing adenoma; KCNJ5, gene encoding potassium inwardly rectifying channel subfamily J member 5; KCNJ5^{mut}, KCNJ5 gene mutations; and NMD, no mutation detected.

to macro-APAs ($P<0.001$), and 2.31-fold upregulated in APAs with NMD compared with APAs with a KCNJ5 mutation ($P<0.0001$; Figure 2A and 2B). The linear negative correlation of BEX1 gene expression with adenoma diameter in the NMD subgroup is shown in Figure 2C. Micro-APAs (n=5) displayed a 3.85-fold increase in BEX1 expression compared with their paired adjacent cortex ($P<0.05$); whereas this difference was not observed for adrenals with macro-APAs (n=12; Figure 2D). An analysis of BEX1 mRNA levels in other adrenal tumors showed no apparent differences in BEX1 gene expression according to tumor diameter in cortisol-producing adenomas (n=20) and in incidentalomas (n=8) (Figure 2E and 2F).

Analysis of publicly available transcriptome data²⁶ demonstrated significantly higher BEX1 gene expression levels in aldosterone-producing micronodules (APMs, n=4), compared with paired zona fasciculata (zF, n=4; 8.75-fold, $P<0.0001$) and zona reticularis (n=4; 2.30-fold, $P<0.05$). In this small sample set, BEX1 expression was higher, but did not reach statistical significance, in APMs versus paired adjacent zona glomerulosa (zG, n=4; 1.87-fold, $P=0.0501$). Conversely, BEX1 gene expression was significantly increased in zG relative to paired zF (4.69-fold, $P<0.001$; Figure S4).

Role of BEX1 in Inhibition of Cell Death by Ferroptosis

We generated a stable human adrenocortical HAC15 cell line expressing BEX1 with a C-terminal DYKDDDDK tag (BEX1-DDK) (Figure 3A). Immunofluorescence staining demonstrated the localization of BEX1-DDK in the nucleus and cytoplasm (Figure 3B). The proportion of cells in the G0/G1, S, and G2/M phases of the cell cycle was indistinguishable between HAC15 control and BEX1-DDK cells (Figure 3C and 3D). The effect

of 2 μ M staurosporine—an inducer of apoptosis—was highly similar in the BEX1-DDK cell line and HAC15 control cells in a cell viability assay (Figure 3E). In contrast, treatment with 4 μ M RSL3 (a ferroptosis inducer) caused notably less cell death in the HAC15 BEX15-DDK cell line compared with HAC15 control cells (Figure 4A and 4B). The protective effect of BEX1 against RSL3-induced cell death was confirmed by flow cytometry measurements using (propidium iodide) fluorescence staining of dead cells (Figure 4A, 4B, and 4D). Specificity of RSL3-induced cell death was demonstrated by ablation of this response in the presence of 10 μ M liproxstatin-1 (liproxstatin-1, a ferroptosis inhibitor; Figure 4C and 4D).

DISCUSSION

We identified genes with significantly altered expression levels between APAs of distinct sizes with a focus on genes with a potential role in cell death and proliferation. We selected BEX1, encoding brain expressed X-linked 1,²⁷ for further study because the function of this gene in the adrenal cortex is unknown and differential expression levels of BEX1 in different subsets of APAs have been previously reported.⁵ Using in vitro functional analyses employing flow cytometry of human adrenocortical cell lines with stable overexpression of BEX1, we demonstrated a novel role for BEX1 as a suppressor of cell death by ferroptosis.

BEX1 transcripts are abundantly expressed in brain. In peripheral tissues, the highest gene expression levels are observed in the adrenal and testis.^{27,28} Previous studies have reported a role for BEX1 in the regeneration of neurons,²⁹ skeletal muscle,³⁰ and liver,³¹ associated with its function in cell cycle regulation²⁹ and apoptosis.³¹ In addition, BEX1 has been identified as a part of a ribonucleoprotein processing complex that promotes

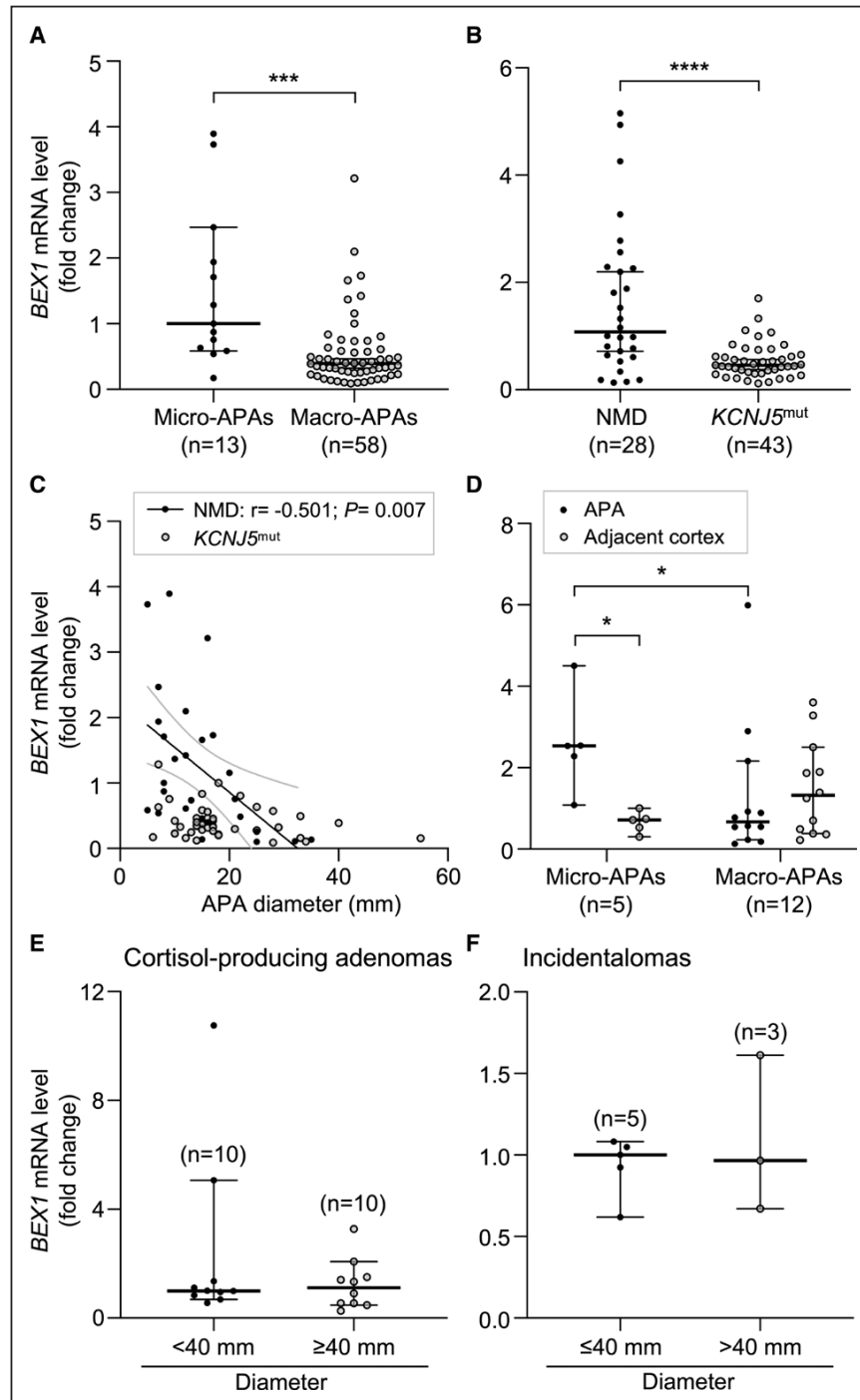


Figure 2. BEX1 gene expression in adrenal tumors.

Real-time qPCR analysis of *BEX1* gene expression in micro and macro-aldosterone-producing adenomas (APAs; **A**) and in APAs with APAs with no mutation detected (NMD) and with a *KCNJ5*-mutation (**B**). A linear negative correlation of *BEX1* gene expression was observed with APA diameter in APAs with NMD (**C**). *BEX1* gene expression was higher in micro-APAs compared with their paired adjacent cortex but not in macro-APAs relative to paired adjacent adrenal cortex (**D**). There were no apparent differences in *BEX1* gene expression according to adenoma size in cortisol-producing adenomas (**E**) and incidentalomas (**F**). Statistical analyses were performed on $2^{-\Delta\Delta Ct}$ values using a Mann-Whitney *U* test, Pearson correlation analysis or a Wilcoxon matched-pairs signed rank test. * $P < 0.05$, *** $P < 0.001$, **** $P < 0.0001$. Each point represents a single sample. Horizontal lines indicate the median, whiskers represent 95% CIs. *KCNJ5* indicates gene encoding potassium inwardly rectifying channel subfamily J member 5; *KCNJ5*^{mut}, APAs with *KCNJ5* mutations; and n, number.

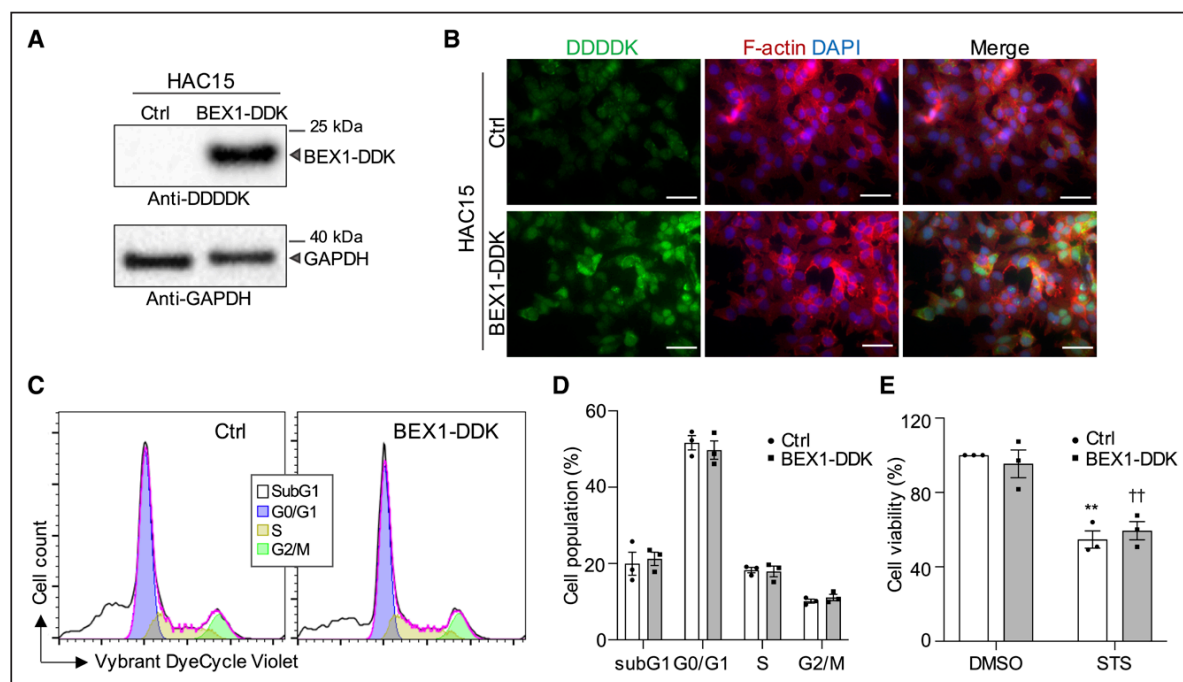


Figure 3. BEX1 has no effect on cell cycle progression and apoptosis in adrenocortical cells.

Western blot analysis of human adrenocortical cell (HAC15) cells selected for stable expression of empty vector (HAC15 Ctrl) or BEX1 with a C-terminal DYKDDDDK tag (BEX1-DDK) (A). Anti-DDDDK immunofluorescence staining of BEX1-DDK expressed in HAC15 cells compared with HAC15 Ctrl cells with F-actin and DAPI stain highlighting the cytoplasm and nucleus, respectively (B). HAC15 cell cycle analysis of Ctrl and BEX1-DDK cells, measured by flow cytometry with Vybrant DyeCycle violet DNA staining in a representative experiment (C) and from 3 independent experiments (D). Cell viability of HAC15 Ctrl and BEX1-DDK cells after 6 h treatment with vehicle (0.02% DMSO) or 2 $\mu\text{mol/L}$ STS (staurosporine, inducer of apoptosis). Data are normalized to the HAC15 Ctrl cell line treated with 0.02% DMSO vehicle and data are shown from 3 independent experiments (E). In E, **difference ($P < 0.01$) from HAC15 Ctrl cells treated with vehicle, ††difference ($P < 0.01$) from HAC15 BEX1-DDK cells treated with vehicle. BEX1-DDK, HAC15 cells with stable expression of BEX1 with a C-terminal DYKDDDDK tag; Ctrl, HAC15 cells with stable expression of empty vector. DAPI indicates 4', 6-diamidino-2-phenylindole, dihydrochloride; DDK, DDDDK tag; DMSO, dimethyl sulfoxide; F-actin, filamentous actin; and STS, staurosporine.

translocation and maturation of mRNAs encoding proinflammatory genes in the heart.³²

Ferroptosis is an iron-dependent form of regulated cell death, morphologically and biochemically distinct from apoptosis, characterized by the accumulation of redox-active iron, lipid hydroperoxides, and oxidized polyunsaturated fatty acid-containing phospholipids.^{33–35} Adrenocortical cells are especially sensitive to ferroptosis,^{36,37} an observation likely related to the vulnerability of steroidogenic tissues to redox imbalance caused by electron leakage by cytochrome P450 enzymes and reactive oxygen species generation.^{38–41}

Herein, we report an inverse correlation of *BEX1* gene expression with APA diameter and an upregulation of *BEX1* transcription in micro-APAs, but not macro-APAs, compared with paired adjacent adrenal cortex. The differential expression levels of *BEX1* in different adrenal tissue samples may reflect different levels of steroidogenesis and production of reactive oxygen species. In this context, *BEX1*-mediated protection from ferroptosis may involve a response to increased steroidogenesis and oxidative stress thereby providing a growth advantage for

zona glomerulosa cells with aldosterone overproduction over adjacent cells. Thus, these findings may translate to a role for *BEX1* in APA pathogenesis via promoting cell survival and facilitating adenoma formation. In support of this concept, analysis of publicly available transcriptome data²⁶ revealed relatively high *BEX1* gene expression in APMs (the revised nomenclature for aldosterone-producing cell clusters),²³ a potential origin of APAs,^{42,43} compared with paired adrenocortical zones.

Like APMs, micro-APAs display strong CYP11B2 (aldosterone synthase) immunostaining.^{23,26,44} In micro-APAs, CYP11B2 immunoreactivity per tumor area is more intense than in macro-APAs⁴⁴ and the intensity of CYP11B2 immunostaining is inversely correlated with APA diameter.^{44,45} The higher CYP11B2 expression associated with micro-APAs is likely required for sufficient aldosterone production to cause clinically overt PA from small adenomas.⁴⁴ In support of this, in the present study, the baseline median plasma aldosterone concentration of the micro-APA group was similar to that of the macro-APA group, indicating the microadenomas could sustain high levels of steroidogenesis despite their smaller size.

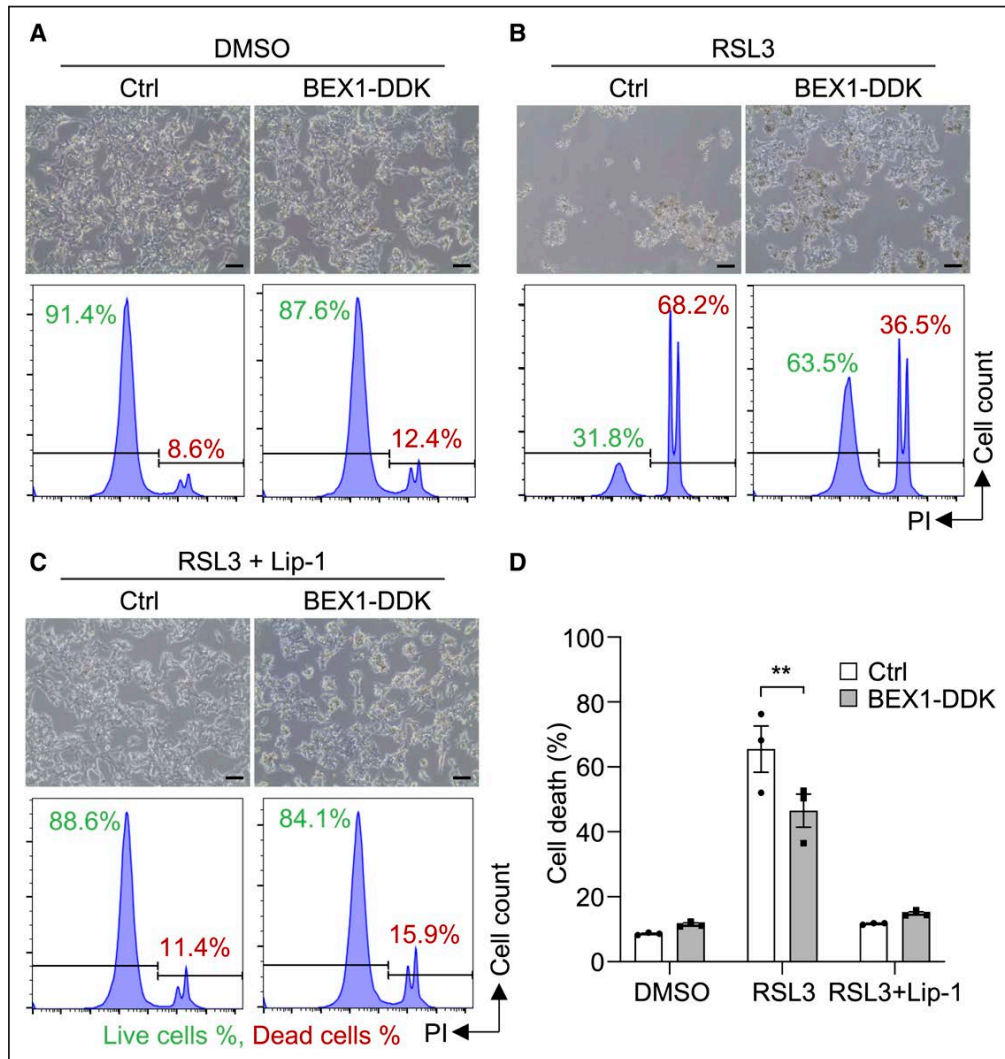


Figure 4. BEX1 inhibits cell death by ferroptosis in adrenocortical cells.

Human adrenocortical cell (HAC15) BEX1-DDK cells are less susceptible to cell death caused by the ferroptosis inducer RSL3 [(1*S*, 3*R*)-RSL3] compared with the HAC15 Ctrl cell line (A and B, upper). Analysis of cell death by flow cytometry with propidium iodide (PI) of HAC15 Ctrl and BEX1-DDK cells after treatment with vehicle (0.004% DMSO), 4 μmol/L RSL3 or 4 μmol/L RSL3+10 μmol/L Lip-1 for 24 h. The proportion (%) of PI-negative cells (alive, in green) or positive cells (dead, in red) measured by flow cytometry is indicated within each chromatogram in a representative experiment (A–C, lower) and from 3 independent experiments (D). Bars represent means of 3 independent experiments, error bars indicate SEM. *P* values were calculated by 2-way ANOVA with a Bonferroni post-test. In D, **difference (*P*<0.01) between HAC15 BEX1-DDK cells and HAC15 Ctrl cells treated with RSL3. BEX1-DDK, HAC15 cells with stable expression of BEX1 with a C-terminal DYKDDDDK tag; Ctrl, HAC15 cells with stable expression of empty vector; DDK, DDDDK tag. DMSO indicates dimethyl sulfoxide; Lip-1, liproxstatin-1; and RSL3, (1*S*,3*R*)-RSL-3.

If CYP11B2 immunoreactivity is taken as a surrogate of pathological steroidogenesis associated with an APA, decreased CYP11B2 immunoreactivity per tumor area with increasing APA diameter may suggest a reduced ability to elicit an oxidative stress response.^{39,41,46} Thus, there would be a decreased requirement for anti-ferroptotic mechanisms and *BEX1* gene expression. The protection from a cell death mechanism in tumors of a small size may seem paradoxical, but we have previously reported that APAs with NMD (unlike in APAs with

a *KCNJ5* mutation) display a decreased proliferation index with increasing adenoma diameter¹⁶ indicating a progressive activation of antiproliferation mechanisms. Taken together, mechanisms that control different forms of cell death and proliferation likely initiate and self-regulate tumor growth to restrict the size of a subset of APAs.

In a microarray analysis of 8 APAs with *KCNJ5* mutations compared with 5 APAs with *CACNA1D* or *ATP1A1* mutations, Azizan et al⁵ identified *BEX1* as a differentially expressed gene with significantly increased expression in

adenomas with *CACNA1D* or *ATP1A1* mutations. Because these tumors tend to be small, with diameters <10 mm,⁵ our findings of increased *BEX1* transcription in micro-APAs are in agreement with the report of Azizan et al.⁵ However, it is unclear if the high *BEX1* expression and modulation of ferroptosis in the NMD group we detected is related to APAs of small diameter in general or to a specific aldosterone-driver mutation or mutations, which we were unable to detect by our sequencing approach. In a later study,⁴⁷ and of high relevance to the present work, the same group of researchers, identified a role for oxidative stress in APA pathogenesis by the analysis of the transcriptomes of APAs with their paired zona glomerulosa.⁴⁷ The study demonstrated that the top canonical biological pathway associated with the differentially expressed genes (APA versus paired zona glomerulosa) was the NRF2 (nuclear factor erythroid 2-related factor 2)-mediated oxidative stress response,⁴⁷ which is a critical cellular mechanism to maintain intracellular redox homeostasis and limit oxidative damage.⁴⁸

A strength of our study is the transcriptome analysis using sample stratification by adenoma diameter and genotype to specifically identify genes that function in cell death and proliferation. An additional strength is the validation of gene expression levels in a large sample cohort from 2 expert referral centers using standardized diagnostic procedures.⁴⁹ Furthermore, all APAs used in the study were resected from patients with complete biochemical success after surgery highlighting the appropriate diagnosis of unilateral PA.² Finally, we performed a functional characterization of the *BEX1* gene to identify a novel role in adrenocortical cells which is relevant to APA pathogenesis. The sequencing approach we used is a study limitation as it was not targeted to CYP11B2-positive lesions and therefore the NMD group potentially contained aldosterone-driver mutations.¹⁰⁻¹²

In conclusion, the *BEX1* gene is differentially expressed in APAs according to nodule diameter and protects human adrenocortical cells in vitro from a form of regulated cell death called ferroptosis.

PERSPECTIVES

Ferroptosis, a form of cell death associated with cell metabolism and redox biology, may function in the pathogenesis of APAs. Future studies are required to clarify this function and elucidate the potential role of *BEX1*. We are currently planning further transcriptomics studies using our stable *BEX1* adrenocortical cell lines and flow cytometry analyses of single cell suspensions, isolated from APA and paired adjacent cortex tissue samples, treated with ferroptosis inducers and inhibitors to gain a better understanding of the role of *BEX1* and of ferroptosis in adrenocortical cells.

ARTICLE INFORMATION

Received December 1, 2020; accepted February 11, 2021.

Affiliations

Medizinische Klinik und Poliklinik IV, Klinikum der Universität München, LMU München, Germany (Y.Y., T.V., C.A., M.B., F.B., M.R., T.A.W.). Division of Internal Medicine and Hypertension, Department of Medical Sciences, University of Turin, Italy (M.T., P.M., T.A.W.). Medizinische Klinik und Poliklinik IV, Diabetes Zentrum, Klinikum der Universität München, LMU München, Germany (J.S.). Institut für Prophylaxe und Epidemiologie der Kreislaufkrankheiten (IPEK), Klinikum der Universität München, Germany (M.H.). Division of Nephrology, University Hospital Carl Gustav Carus, Technische Universität Dresden, Germany (A.B., A.L.). Klinik für Endokrinologie, Diabetologie und Klinische Ernährung, Universitätsspital Zürich, Switzerland (F.B.).

Acknowledgments

The excellent support of Elisabeth Christine Obster from the German Conn registry is gratefully acknowledged and the expert technical assistance of Isabella-Sabrina Kinker and Petra Rank.

Sources of Funding

This work was financed by the Deutsche Forschungsgemeinschaft (DFG) project number 444776998 to T.A. Williams (WI 5359/2-1) and M. Reincke (RE 752/31-1) and project number 314061271-TRR 205/project B15 to T.A. Williams (within the CRC/Transregio 205/1 "The Adrenal: Central Relay in Health and Disease"). The CRC/Transregio 205/1 also supports the work of C. Adolf, F. Beuschlein, and M. Reincke. This study was also supported by the European Research Council under the European Union Horizon 2020 research and innovation program (grant agreement No. 694913 to M. Reincke) and the Else Kröner-Fresenius Stiftung in support of the German Conn's Registry-Else-Kröner Hyperaldosteronism Registry (2013_A182, 2015_A171 and 2019_A104 to M. Reincke). Y. Yang is in receipt of a PhD fellowship from the China Scholarship Council.

Disclosures

None.

REFERENCES

- Funder JW, Carey RM, Mantero F, Murad MH, Reincke M, Shibata H, Stowasser M, Young WF Jr. The management of primary aldosteronism: case detection, diagnosis, and treatment: an endocrine society clinical practice guideline. *J Clin Endocrinol Metab*. 2016;101:1889–1916. doi: 10.1210/jc.2015-4061
- Williams TA, Lenders JWM, Mulatero P, Burrello J, Rottenkolber M, Adolf C, Satoh F, Amar L, Quinkler M, Deinum J, et al. Outcomes after adrenalectomy for unilateral primary aldosteronism: an international consensus on outcome measures and analysis of remission rates in an international cohort. *Lancet Diabetes Endocrinol*. 2017;5:689–699. doi: 10.1016/S2213-8587(17)30135-3
- Choi M, Scholl UI, Yue P, Björklund P, Zhao B, Nelson-Williams C, Ji W, Cho Y, Patel A, Men CJ, et al. K+ channel mutations in adrenal aldosterone-producing adenomas and hereditary hypertension. *Science*. 2011;331:768–772. doi: 10.1126/science.1198785
- Scholl UI, Goh G, Stöltzing G, de Oliveira RC, Choi M, Overton JD, Fonseca AL, Korah R, Starker LF, Kunstman JW, et al. Somatic and germline *CACNA1D* calcium channel mutations in aldosterone-producing adenomas and primary aldosteronism. *Nat Genet*. 2013;45:1050–1054. doi: 10.1038/ng.2695
- Azizan EA, Poulsen H, Tuluc P, Zhou J, Clausen MV, Lieb A, Maniero C, Garg S, Bochukova EG, Zhao W, et al. Somatic mutations in *ATP1A1* and *CACNA1D* underlie a common subtype of adrenal hypertension. *Nat Genet*. 2013;45:1055–1060. doi: 10.1038/ng.2716
- Namba K, Blinder AR, Rege J, Hattangady NG, Else T, Liu CJ, Tomlins SA, Vats P, Kumar-Sinha C, Giordano TJ, et al. Somatic *CACNA1H* mutation as a cause of aldosterone-producing adenoma. *Hypertension*. 2020;75:645–649. doi: 10.1161/HYPERTENSIONAHA.119.14349
- Dutta RK, Arnesen T, Heie A, Walz M, Alesina P, Söderkvist P, Gimm O. A somatic mutation in *CLCN2* identified in a sporadic aldosterone-producing adenoma. *Eur J Endocrinol*. 2019;181:K37–K41. doi: 10.1530/EJE-19-0377
- Beuschlein F, Boulkroun S, Osswald A, Wieland T, Nielsen HN, Lichtenauer UD, Penton D, Schack VR, Amar L, Fischer E, et al. Somatic mutations in *ATP1A1* and *ATP2B3* lead to aldosterone-producing adenomas and secondary hypertension. *Nat Genet*. 2013;45:440–444. doi: 10.1038/ng.2550
- Okii K, Plonczynski MW, Luis Lam M, Gomez-Sanchez EP, Gomez-Sanchez CE. Potassium channel mutant *KCNJ5 T158A* expression in HAC-15 cells

- increases aldosterone synthesis. *Endocrinology*. 2012;153:1774–1782. doi: 10.1210/en.2011-1733
10. Nanba K, Omata K, Else T, Beck PCC, Nanba AT, Turcu AF, Miller BS, Giordano TJ, Tomlins SA, Rainey WE. Targeted molecular characterization of aldosterone-producing adenomas in White Americans. *J Clin Endocrinol Metab*. 2018;103:3869–3876. doi: 10.1210/clinem/2018-01004
 11. De Sousa K, Boulkroun S, Baron S, Nanba K, Wack M, Rainey WE, Rocha A, Giscos-Douriez I, Meatchi T, Amar L, et al. Genetic, cellular, and molecular heterogeneity in adrenals with aldosterone-producing adenoma. *Hypertension*. 2020;75:1034–1044. doi: 10.1161/HYPERTENSIONAHA.119.14177
 12. Nanba K, Yamazaki Y, Bick N, Onodera K, Tezuka Y, Omata K, Ono Y, Blinder AR, Tomlins SA, Rainey WE, Satoh F, Sasano H. Prevalence of somatic mutations in aldosterone-producing adenomas in Japanese patients. *J Clin Endocrinol Metab*. 2020;105:dagg595. doi: 10.1210/clinem/dgaa595
 13. Åkerström T, Maharjan R, Sven Willenberg H, Cupisti K, Ip J, Moser A, Stålberg P, Robinson B, Alexander Iwen K, Dralle H, et al. Activating mutations in CTNNB1 in aldosterone producing adenomas. *Sci Rep*. 2016;6:19546. doi: 10.1038/srep19546
 14. Tissier F, Cavard C, Groussin L, Perlemoine K, Fumey G, Hagneré AM, René-Corail F, Jullian E, Gicquel C, Bertagna X, et al. Mutations of beta-catenin in adrenocortical tumors: activation of the Wnt signaling pathway is a frequent event in both benign and malignant adrenocortical tumors. *Cancer Res*. 2005;65:7622–7627. doi: 10.1158/0008-5472.CAN-05-0593
 15. Berthon A, Drelon C, Ragazzon B, Boulkroun S, Tissier F, Amar L, Samson-Couterie B, Zennaro MC, Plouin PF, Skah S, et al. WNT/β-catenin signalling is activated in aldosterone-producing adenomas and controls aldosterone production. *Hum Mol Genet*. 2014;23:889–905. doi: 10.1093/hmg/ddt484
 16. Yang Y, Gomez-Sanchez CE, Jaquin D, Aristizabal Prada ET, Meyer LS, Knösel T, Schneider H, Beuschlein F, Reincke M, Williams TA. Primary aldosteronism: KCNJ5 mutations and adrenocortical cell growth. *Hypertension*. 2019;74:809–816. doi: 10.1161/HYPERTENSIONAHA.119.13476
 17. Scholl UI, Nelson-Williams C, Yue P, Grekin R, Wyatt RJ, Dillon MJ, Couch R, Hammer LK, Harley FL, Farhi A, et al. Hypertension with or without adrenal hyperplasia due to different inherited mutations in the potassium channel KCNJ5. *Proc Natl Acad Sci USA*. 2012;109:2533–2538. doi: 10.1073/pnas.1121407109
 18. Mulatero P, Monticone S, Deinum J, Amar L, Prejbisz A, Zennaro MC, Beuschlein F, Rossi GP, Nishikawa T, Morganti A, et al. Genetics, prevalence, screening and confirmation of primary aldosteronism: a position statement and consensus of the working group on endocrine hypertension of the European society of hypertension. *J Hypertens*. 2020;38:1919–1928. doi: 10.1097/HJH.0000000000002510
 19. Mulatero P, Sechi LA, Williams TA, Lenders JWM, Reincke M, Satoh F, Januszewicz A, Naruse M, Doumas M, Veglio F, et al. Subtype diagnosis, treatment, complications and outcomes of primary aldosteronism and future direction of research: a position statement and consensus of the Working Group on Endocrine Hypertension of the European Society of Hypertension. *J Hypertens*. 2020;38:1929–1936. doi: 10.1097/HJH.0000000000002520
 20. Yang Y, Reincke M, Williams TA. Treatment of unilateral PA by adrenalectomy: potential reasons for incomplete biochemical cure. *Exp Clin Endocrinol Diabetes*. 2019;127:100–108. doi: 10.1055/a-0662-6081
 21. Yang Y, Burrello J, Burrello A, Eisenhofer G, Peitzsch M, Tetti M, Knösel T, Beuschlein F, Lenders JWM, Mulatero P, et al. Classification of microadenomas in patients with primary aldosteronism by steroid profiling. *J Steroid Biochem Mol Biol*. 2019;189:274–282. doi: 10.1016/j.jsbmb.2019.01.008
 22. Gomez-Sanchez CE, Qi X, Velarde-Miranda C, Plonczynski MW, Parker CR, Rainey W, Satoh F, Maekawa T, Nakamura Y, Sasano H, et al. Development of monoclonal antibodies against human CYP11B1 and CYP11B2. *Mol Cell Endocrinol*. 2014;383:111–117. doi: 10.1016/j.mce.2013.11.022
 23. Williams TA, Gomez-Sanchez CE, Rainey WE, Giordano TJ, Lam AK, Marker A, Mete O, Yamazaki Y, Zerbini MCN, Beuschlein F, et al. International histopathology consensus for unilateral primary aldosteronism. *J Clin Endocrinol Metab*. 2021;106:42–54. doi: 10.1210/clinem/dgaa484
 24. Metsalu T, Vilo J. ClustVis: a web tool for visualizing clustering of multivariate data using principal component analysis and heatmap. *Nucleic Acids Res*. 2015;43(W1):W566–W570. doi: 10.1093/nar/gkv468
 25. Parmar J, Key RE, Rainey WE. Development of an adrenocorticotropin-responsive human adrenocortical carcinoma cell line. *J Clin Endocrinol Metab*. 2008;93:4542–4546. doi: 10.1210/jc.2008-0903
 26. Nishimoto K, Tomlins SA, Kuick R, Cani AK, Giordano TJ, Hovelson DH, Liu CJ, Sanjanwala AR, Edwards MA, Gomez-Sanchez CE, et al. Aldosterone-stimulating somatic gene mutations are common in normal adrenal glands. *Proc Natl Acad Sci USA*. 2015;112:E4591–E4599. doi: 10.1073/pnas.1505529112
 27. Yang QS, Xia F, Gu SH, Yuan HL, Chen JZ, Yang QS, Ying K, Xie Y, Mao YM. Cloning and expression pattern of a spermatogenesis-related gene, BEX1, mapped to chromosome Xq22. *Biochem Genet*. 2002;40:1–12. doi: 10.1023/a:1014565320998
 28. Fagerberg L, Hallström BM, Oksvold P, Kampf C, Djureinovic D, Odeberg J, Habuka M, Tahmasebpoor S, Danielsson A, Edlund K, et al. Analysis of the human tissue-specific expression by genome-wide integration of transcriptomics and antibody-based proteomics. *Mol Cell Proteomics*. 2014;13:397–406. doi: 10.1074/mcp.M113.035600
 29. Vilar M, Murillo-Carretero M, Mira H, Magnusson K, Besset V, Ibáñez CF. Bex1, a novel interactor of the p75 neurotrophin receptor, links neurotrophin signaling to the cell cycle. *EMBO J*. 2006;25:1219–1230. doi: 10.1038/sj.emboj.7601017
 30. Jiang C, Wang JH, Yue F, Kuang S. The brain expressed x-linked gene 1 (Bex1) regulates myoblast fusion. *Dev Biol*. 2016;409:16–25. doi: 10.1016/j.ydbio.2015.11.007
 31. Gu Y, Wei W, Cheng Y, Wan B, Ding X, Wang H, Zhang Y, Jin M. A pivotal role of BEX1 in liver progenitor cell expansion in mice. *Stem Cell Res Ther*. 2018;9:164. doi: 10.1186/s13287-018-0905-2
 32. Accornero F, Schips TG, Petrosino JM, Gu SQ, Kanisicak O, van Berlo JH, Molkentin JD. BEX1 is an RNA-dependent mediator of cardiomyopathy. *Nat Commun*. 2017;8:1875. doi: 10.1038/s41467-017-02005-1
 33. Dixon SJ, Lemberg KM, Lamprecht MR, Skouta R, Zaitsev EM, Gleason CE, Patel DN, Bauer AJ, Cantley AM, Yang WS, et al. Ferroptosis: an iron-dependent form of nonapoptotic cell death. *Cell*. 2012;149:1060–1072. doi: 10.1016/j.cell.2012.03.042
 34. Stockwell BR, Friedmann Angeli JP, Bayir H, Bush AI, Conrad M, Dixon SJ, Fulda S, Gascón S, Hatzios SK, Kagan VE, et al. Ferroptosis: a regulated cell death nexus linking metabolism, redox biology, and disease. *Cell*. 2017;171:273–285. doi: 10.1016/j.cell.2017.09.021
 35. Dixon SJ, Stockwell BR. The hallmarks of ferroptosis. *Annu Rev Cancer Biol*. 2019;3:35–54. doi: 10.1146/annurev-cancerbio-030518-055844
 36. Belavgeni A, Bornstein SR, von Mässenhausen A, Tonnus W, Stumpf J, Meyer C, Othmar E, Latk M, Kanczkowski W, Kroiss M, et al. Exquisite sensitivity of adrenocortical carcinomas to induction of ferroptosis. *Proc Natl Acad Sci USA*. 2019;116:22269–22274. doi: 10.1073/pnas.1912700116
 37. Weigand I, Schreiner J, Röhrig F, Sun N, Landwehr LS, Urlaub H, Kendl S, Kiseljak-Vassiliades K, Wierman ME, Angeli JPF, et al. Active steroid hormone synthesis renders adrenocortical cells highly susceptible to type II ferroptosis induction. *Cell Death Dis*. 2020;11:192. doi: 10.1038/s41419-020-2385-4
 38. Rapoport R, Sklan D, Hanukoglu I. Electron leakage from the adrenal cortex mitochondrial P450_{scc} and P450_{c11} systems: NADPH and steroid dependence. *Arch Biochem Biophys*. 1995;317:412–416. doi: 10.1006/abbi.1995.1182
 39. Prasad R, Kowalczyk JC, Meimaridou E, Storr HL, Metherell LA. Oxidative stress and adrenocortical insufficiency. *J Endocrinol*. 2014;221:R63–R73. doi: 10.1530/JOE-13-0346
 40. Lim JB, Barker KA, Eller KA, Jiang L, Molina V, Saifee JF, Sikes HD. Insights into electron leakage in the reaction cycle of cytochrome P450 BM3 revealed by kinetic modeling and mutagenesis. *Protein Sci*. 2015;24:1874–1883. doi: 10.1002/pro.2793
 41. Zou Y, Li H, Graham ET, Deik AA, Eaton JK, Wang W, Sandoval-Gomez G, Clish CB, Doench JG, Schreiber SL. Cytochrome P450 oxidoreductase contributes to phospholipid peroxidation in ferroptosis. *Nat Chem Biol*. 2020;16:302–309. doi: 10.1038/s41589-020-0472-6
 42. Nishimoto K, Seki T, Kurihara I, Yokota K, Omura M, Nishikawa T, Shibata H, Kosaka T, Oya M, Suematsu M, et al. Case report: nodule development from subcapsular aldosterone-producing cell clusters causes hyperaldosteronism. *J Clin Endocrinol Metab*. 2016;101:6–9. doi: 10.1210/jc.2015-3285
 43. Sun N, Meyer LS, Feuchtinger A, Kunzke T, Knösel T, Reincke M, Walch A, Williams TA. Mass spectrometry imaging establishes 2 distinct metabolic phenotypes of aldosterone-producing cell clusters in primary aldosteronism. *Hypertension*. 2020;75:634–644. doi: 10.1161/HYPERTENSIONAHA.119.14041
 44. Ono Y, Nakamura Y, Maekawa T, Felizola SJ, Morimoto R, Iwakura Y, Kudo M, Seiji K, Takase K, Arai Y, et al. Different expression of 11β-hydroxylase and aldosterone synthase between aldosterone-producing microadenomas

- and macroadenomas. *Hypertension*. 2014;64:438–444. doi: 10.1161/HYPERTENSIONAHA.113.02944
45. Monticone S, Castellano I, Versace K, Lucatello B, Veglio F, Gomez-Sanchez CE, Williams TA, Mulatero P. Immunohistochemical, genetic and clinical characterization of sporadic aldosterone-producing adenomas. *Mol Cell Endocrinol*. 2015;411:146–154. doi: 10.1016/j.mce.2015.04.022
46. Shimada K, Hayano M, Pagano NC, Stockwell BR. Cell-line selectivity improves the predictive power of pharmacogenomic analyses and helps identify NADPH as biomarker for ferroptosis sensitivity. *Cell Chem Biol*. 2016;23:225–235. doi: 10.1016/j.chembiol.2015.11.016
47. Zhou J, Lam B, Neogi SG, Yeo GS, Azizan EA, Brown MJ. Transcriptome pathway analysis of pathological and physiological aldosterone-producing human tissues. *Hypertension*. 2016;68:1424–1431. doi: 10.1161/HYPERTENSIONAHA.116.08033
48. Ma Q. Role of Nrf2 in oxidative stress and toxicity. *Annu Rev Pharmacol Toxicol*. 2013;53:401–426. doi: 10.1146/annurev-pharmtox-011112-140320
49. Williams TA, Reincke M. Management of endocrine disease: diagnosis and management of primary aldosteronism: the endocrine society guideline 2016 revisited. *Eur J Endocrinol*. 2018;179:R19–R29. doi: 10.1530/EJE-17-0990

Online-only supplement

***BEX1* is differentially expressed in aldosterone-producing adenomas and protects human adrenocortical cells from ferroptosis**

Yuhong Yang¹, Martina Tetti², Twinkle Vohra¹, Christian Adolf¹, Jochen Seissler³, Michael Hristov⁴, Alexia Belavgeni⁵, Martin Bidlingmaier¹, Andreas Linkermann⁵, Paolo Mulatero², Felix Beuschlein^{1,6}, Martin Reincke¹, Tracy Ann Williams^{1,2}

¹Medizinische Klinik und Poliklinik IV, Klinikum der Universität München, LMU München, München, Germany

²Division of Internal Medicine and Hypertension, Department of Medical Sciences, University of Turin, Turin, Italy

³Medizinische Klinik und Poliklinik IV, Diabetes Zentrum, Klinikum der Universität München, LMU München, München, Germany

⁴Institut für Prophylaxe und Epidemiologie der Kreislaufkrankheiten (IPEK), Klinikum der Universität München, München, Germany

⁵Division of Nephrology, University Hospital Carl Gustav Carus, Technische Universität Dresden, Dresden, Germany

⁶Klinik für Endokrinologie, Diabetologie und Klinische Ernährung, Universitätsspital Zürich, Zürich, Switzerland

Corresponding author: Tracy Ann Williams, Medizinische Klinik und Poliklinik IV, Klinikum der Universität München, LMU München, Ziemssenstr. 1, D-80336 München, Germany

Tel: +49 89 4400 52941

Fax: +49 89 4400 54428

Email: Tracy.Williams@med.uni-muenchen.de; tracyann.williams@unito.it

Running title: *BEX1* expression in aldosterone-producing adenomas

Online-only supplementary content

Expanded methods		Page 2-4
References		Page 5
Table S1	Primer pairs used for detection of <i>CTNNB1</i> mutations	Page 6
Table S2	APA samples used for mRNA-seq analysis: clinical and biochemical parameters of corresponding patients stratified by adenoma diameter	Page 7
Table S3	Top differentially expressed genes in APAs with NMD	Page 8
Table S4	Top differentially expressed genes in APAs with <i>KCNJ5</i> mutations	Page 9
Figure S1	Top 10 overrepresented GO terms of biological process enriched in the comparisons between macro- and micro-APAs stratified by genotypes	Page 10
Figure S2	Distinct expression of genes with a reported role in cell death and proliferation in APAs with different genotypes and adenoma diameter	Page 11
Figure S3	Expression of reported ferroptosis suppressors in APAs with different genotypes and adenoma diameter	Page 12
Figure S4	<i>BEX1</i> is differentially expressed in APMs and adrenocortical zones	Page 13

Expanded methods

The authors declare that all supporting data are available within the article and its online supplementary files. mRNA sequencing (mRNA-seq) data have been made publicly available and can be accessed at https://github.com/MedIVLMUMunich/MacroMicroAPA_RNAseq

Next generation sequencing and bioinformatics analysis

Total RNA was isolated from dissected nodules of fresh frozen adrenal tissues using a Maxwell 16 LEV simplyRNA Tissue Kit (Promega) according to the manufacturer's instructions. mRNA-seq transcriptome profiling was performed by QIAGEN Genomics (Hilden, Germany). A mRNA seq library was prepared by Illumina TruSeq Stranded mRNA Library Prep Kit (Illumina Inc.) and sequenced using NextSeq 500 technology (Illumina Inc.), producing an average of 44.0 million reads per run. The quality of the raw sequencing was evaluated using FastQC version 0.11.4, the vast majority of data displayed a quality score >30. TopHat 2.1.0 was used to align sequencing reads to the reference human genome GRCh37, and aligned sequences were assembled into transcripts by Cufflinks 2.2.1 and annotated according to Ensembl Release 75 data. Heatmap and unsupervised hierarchical clustering and volcano plots were performed using R or the ClustVis web tool (<https://biit.cs.ut.ee/clustvis/>),¹ based on normalized fragments per kilobase of transcript per million mapped fragments of genes. Differentially expressed genes (DEGs) were identified by Cuffdiff 2.2.1, and visualized by volcano plots using R. An adjusted *P* value <0.05 using Benjamini-Hochberg False Discovery Rate method was set as the cut-off for significant differential expression. Differentially expressed transcripts were imported into R (package: topGO) for Gene Ontology (GO) enrichment analysis (biological process) using the elim method in Kolmogorov-Smirnov test. The top 10 significantly overrepresented GO terms were listed according to *P* values determined by comparing the estimated number of transcripts associated with specific GO terms compared with the reference background. DEGs associated with cell death and proliferation were identified from Entrez Gene (<https://www.ncbi.nlm.nih.gov/gene/>) and GeneCards (<https://www.genecards.org/>) databases. Ferroptosis suppressors were identified from FerrDb database (<http://www.zhounan.org/ferrdb/>).

Reverse transcription and quantitative real-time PCR

First-strand cDNAs were synthesized from total RNA (500 ng) using GoScript™ reverse transcriptase mix, oligo (dT) (Promega). TaqMan gene expression assays (Applied Biosystems) were used for quantification of genes of interest and *GAPDH* (Hs02786624_g1) with iTaq Universal probes supermix (Bio-Rad) on a QuantStudio 5 Real-Time PCR instrument (Applied Biosystems). TaqMan gene expression assays were used for *BAI1* (Hs00181777_m1), *BEX1* (Hs00218464_m1), *BMP4* (Hs03676628_s1), *CCL21* (Hs00171076_m1); *DKK1* (Hs00183740_m1), *FBXL21* (Hs00362638_m1), *SFRP2* (Hs00293258_m1), *TFPI2* (Hs04334126_m1), *TMPRSS3* (Hs00917537_m1), *TSPAN12* (Hs01113125_m1) and *GAPDH* was used as a reference gene. Gene expression levels were calculated using the $2^{-\Delta\Delta Ct}$ relative quantification method.

Cell lines and culture conditions

Human adrenocortical (HAC15) cells² (a kind gift from Professor William E. Rainey, University of Michigan, Ann Arbor) were cultured at 37°C and 5% CO₂ in DMEM (Dulbecco's Modified Eagle's Medium) F-12 Ham (1:1, Sigma-Aldrich) supplemented with 10% HyClone Cosmic Calf serum (GE Healthcare Life Sciences), 1% L-glutamine, 1x insulin-transferrin-selenium-sodium pyruvate (ITS), 1% antibiotic-antimycotic, and 0.01% Gentamycin. DMEM-F12 Ham supplemented with 0.1% HyClone Cosmic Calf serum (referred to as starvation medium) was used under some experimental conditions.

Generation of HAC15 cell lines stably expressing BEX1

A cDNA encoding BEX1 with a C-terminal DYKDDDDK tag was prepared by CloneEZ Seamless cloning in a pcDNA3.1⁺/C-(K)-DYK plasmid (GenScript). HAC15 cells (3x10⁶) were re-suspended in 100 mL nucleofector solution R (Lonza) containing 3 µg pcDNA3.1-*BEX1*-DYK. The plasmid was nucleofected (Lonza Amaxa Nucleofector, program X-005) and after 48 hours, selection was initiated with 1 mg/mL geneticin (G418 sulfate) in the presence of 10 µmol/L verapamil to inhibit P glycoprotein and prevent decreased sensitivity to the antibiotic.³

Western blotting

Cells were briefly washed with DPBS (Dulbecco's phosphate-buffered saline, Gibco) and lysed with RIPA (radioimmunoprecipitation assay buffer, Thermo Scientific) containing a cocktail of protease inhibitors (Sigma-Aldrich). Cell lysates were collected, and protein concentrations were determined using a bicinchoninic acid protein assay kit (BCA kit, Thermo Scientific). Protein samples were denatured in loading dye at 95°C for 10 minutes, separated by 10% SDS (sodium dodecyl sulfate)-polyacrylamide gel electrophoresis, and transferred to nitrocellulose membranes using a Mini Trans-Blot Cell system (Bio-Rad). Membranes were blocked with 10% blotting-grade blocker (Bio-Rad) in 0.1% TBST (Tween-20-Tris-Buffered Saline) and incubated with a rabbit polyclonal anti-DDDDK antibody (dilution: 1:2500, Abcam, ab1162) and an anti-GAPDH mouse monoclonal antibody (dilution: 1:5000, Sigma-Aldrich, MAB374). Membranes were washed with 0.1% TBST before incubating with horseradish peroxidase-conjugated anti-rabbit and anti-mouse secondary antibodies. Images were acquired on ChemiDoc XRS⁺ System (Bio-Rad) according to the manufacturer's instructions.

Immunofluorescence

Cells were seeded into 4-well Nunc chamber slides (1x10⁵ cells/well) and incubated for 24h, before changing to starvation medium and incubation for a further 24 h. Cells were fixed in 4% paraformaldehyde (Microcos GmbH), blocked with 1% BSA (bovine serum albumin, Sigma-Aldrich) and 0.3% Triton X-100 (Carl Roth) in 0.1% TBST. Immunofluorescence staining of BEX1-DDDDK was performed using a rabbit anti-DDDDK polyclonal antibody (dilution: 1:2000, Abcam, ab1162) and an anti-rabbit Alexa Fluor 488 secondary antibody (1:1000, Invitrogen). DyLight 594 Phalloidin (Cell Signaling) was used for staining of cytoskeleton actin filaments before mounting cells in antifade medium with DAPI (4',6-diamidino-2-phenylindole, Vector Laboratories).

Cell viability assay

Cells were plated in starvation medium into 96-well plates (2.5×10^4 cells) and incubated for 24 hours before treatment with vehicle alone (dimethyl sulfoxide, DMSO, 0.02%) or staurosporine (STS, 2 μ M, an apoptosis inducer, Tocris) for 6 hours. Cell viability was measured by quantification of metabolically active cells using a water-soluble tetrazolium salt-1 assay (WST-1, Roche). After incubation with WST-1 at 37°C for 3 hours, absorbance at 450 nm and 690 nm were determined on a FLUOstar Omega plate reader (BMG LABTECH).

Flow cytometry

For cell cycle experiments, 1×10^6 cells were incubated with Vibrant DyeCycle Violet (Invitrogen, 5 μ M) at 37°C for 30 min before analysis of fluorescence using excitation and emission maxima of 369/437 nm on a FACSCalibur instrument (BD Biosciences). For ferroptosis experiments, cells were seeded into 12-well plates (5×10^5 cells/well) and incubated for 24 hours. Cells were then further incubated for 24 hours in starvation medium before treatment for 24 hours with either (i) vehicle alone (0.004% DMSO); (ii) an inducer of ferroptosis (4 μ M RSL3 ([1S,3R]-RSL3); or (iii) an inducer of ferroptosis in the presence of a ferroptosis inhibitor (4 μ M RSL3 + 10 μ M Lip-1 [liproxstatin-1]. Cells were pre-incubated with lip-1 for 1 hour before RSL3 addition. Propidium iodide (PI, 1 μ g/mL, Invitrogen) was used for fluorescent staining of double stranded nucleic acids of dying or dead cells, and the percentage of PI-positive dead cells was determined using BD Accuri C6 (BD Biosciences) and an FL2 detector. The obtained data were analyzed with FLOWJo version 10.4. All experiments were carried out in triplicate, and a minimum of 7000 (cell cycle experiments) or 15000 (ferroptosis experiments) single cells were analyzed per sample.

Statistical analysis

Statistical analyses were performed using IBM SPSS version 25.0 and GraphPad Prism version 8.2.1. Data were analyzed using the Kolmogorov-Smirnov test and Shapiro-Wilk test to determine sample distributions. Statistical significance was assessed by a t-test (paired where appropriate) or a Mann-Whitney test (Wilcoxon rank matched pairs test if needed) or a Bonferroni's post-test after two-way ANOVA. Chi-square and Fisher's exact tests were used to compare categorical variables. Univariate correlations were assessed using Pearson correlations. *P* values <0.05 were considered statistically significant.

References

1. Metsalu T, Vilo J. Clustvis: a web tool for visualizing clustering of multivariate data using principal component analysis and heatmap. *Nucleic Acids Res.* 2015;43:W566-570. doi: 10.1093/nar/gkv468
2. Parmar J, Key RE, Rainey WE. Development of an adrenocorticotropin-responsive human adrenocortical carcinoma cell line. *J Clin Endocrinol Metab.* 2008;93:4542-4546. doi: 10.1210/jc.2008-0903
3. Yang Y, Gomez-Sanchez CE, Jaquin D, Aristizabal Prada ET, Meyer LS, Knösel T, Schneider H, Beuschlein F, Reincke M, Williams TA. Primary aldosteronism: KCNJ5 mutations and adrenocortical cell growth. *Hypertension.* 2019;74:809-816. doi: 10.1161/HYPERTENSIONAHA.119.13476
4. Nishimoto K, Tomlins SA, Kuick R, Cani AK, Giordano TJ, Hovelson DH, Liu CJ, Sanjanwala AR, Edwards MA, Gomez-Sanchez CE, Nanba K, Rainey WE. Aldosterone-stimulating somatic gene mutations are common in normal adrenal glands. *Proc Natl Acad Sci U S A.* 2015;112:E4591-4599. doi: 10.1073/pnas.1505529112

Gene	Type	Exon amplified	Transcript	Product size (bp)	Primer sequence (5' -> 3')
<i>CTNNB1</i>	PCR amplification primers	3	NM_001904.4	500	Forward: atcactgagctaaccctggc Reverse: actctcttttcttcaccacaaca
<i>CTNNB1</i>	Sequencing primers	3	NM_001904.4	323	Forward: aacattccaatctactaatgctaa Reverse: tcaaaactgcattctgactttca

Table S1. Primer pairs used for detection of *CTNNB1* mutations.

Variable	Total (n=21)	APAs ≥30mm (n=9)	APAs ≤10 mm (n=12)	P value
APAs with a <i>KCNJ5</i> mutation (n=11)	11 (52.4%)	5 (55.6%)	6 (50.0%)	1.000
APAs with NMD (n=10)	10 (47.6%)	4 (44.4%)	6 (50.0%)	1.000
Adrenal nodule (diam. mm; n=21)	10.0 [7.0-33.5]	34.0 [32.5-37.5]	7.5 [6.3-10.0]	< 0.001
Age at surgery (years; n=21)	46.5 ± 14.0	47.2 ± 14.9	46.0 ± 14.0	0.849
Sex (ref. Women; n=21)	11 (52.4%)	7 (77.8%)	4 (33.3%)	0.080
BMI (kg/m ² ; n=21)	26.2 ± 4.0	26.0 ± 4.0	26.4 ± 4.2	0.841
Systolic BP (mmHg; n=21)	155.4 ± 23.5	141.4 ± 9.6	165.8 ± 25.7	0.014
Diastolic BP (mmHg; n=21)	97.5 ± 12.1	95.1 ± 8.8	99.2 ± 14.1	0.453
Duration HTN (months; n=21)	92 [22-147]	69 [10-147]	100 [42-181]	0.508
Anti-HTN medication (DDD; n=9)	2.2 [1.1-3.2]	2.0 [1.0-3.2]	2.6 [1.6-3.5]	0.193
PAC (pmol/L; n=21)	1087 [631-1608]	1409 [795-2358]	996 [567-1508]	0.219
DRC (mU/L; n=10)	4.8 [2.0-7.1]	3.0 [1.8-8.4]	6.1 [2.9-6.7]	0.762
ARR_DRC (n=10)	161 [69-970]	552 [106-1344]	108 [48-275]	0.257
PRA (pmol/L/min; n=11)	2.6 [1.3-3.8]	2.6 [2.6-2.6]	2.3 [1.3-5.8]	0.776
ARR_PRA (n=11)	425 [310-983]	558 [377-983]	422 [205-1101]	0.776
Lowest serum K ⁺ (mmol/L; n=21)	3.1 ± 0.5	3.0 ± 0.6	3.1 ± 0.5	0.955

Table S2. APA samples used for mRNA-seq analysis: clinical and biochemical parameters of corresponding patients stratified by adenoma diameter

Resected adrenals from APAs were stratified by size of largest adrenal nodule at pathology of diameter ≥30 mm or ≤10 mm. All variables refer to baseline data. Quantitative normally distributed variables are expressed as means ± SD and quantitative non-normally distributed variables are reported as medians [IQR]. Categorical variables are presented as absolute numbers and percentages. *P* values were calculated using Chi-square and Fisher's exact tests or t test or Mann-Whitney tests as appropriate. APAs, aldosterone-producing adenomas; ARR, aldosterone-to-renin ratio; BMI, body mass index; BP, blood pressure; DDD, defined daily dose; diam., diameter; DRC, direct renin concentration; HTN, hypertension; K⁺, potassium ions; *KCNJ5*, gene encoding potassium inwardly rectifying channel subfamily J member 5; n, number; NMD, no mutation detected; PAC, plasma aldosterone concentration; PRA, plasma renin activity; ref., reference. The defined daily dose is the assumed average maintenance dose per day for a drug used for its main indication in adults according to ATC/DDD Index 2019 https://www.whocc.no/atc_ddd_index/

1) Top 20 upregulated genes in APAs with NMD (diameter ≥30 mm versus ≤10 mm)				
Gene	APAs ≥30 mm (FPKM)	APAs ≤10 mm (FPKM)	Log2_FC	Adjusted P value
<i>CGA</i>	46.0915	0.30656	7.23219	0.00682005
<i>C7orf43</i>	878.479	7.5155	6.86899	0.00682005
<i>GOLGA8M</i>	105.764	1.75808	5.91071	0.00682005
<i>SCGB1D2</i>	34.5128	0.693574	5.63694	0.00682005
<i>SPAG8</i>	126.477	2.61867	5.5939	0.00682005
<i>C1orf116</i>	2.18026	0.0842935	4.69294	0.0293539
<i>DNAJC5G</i>	8.35141	0.36617	4.51143	0.0320323
<i>ERP27</i>	42.5836	1.87697	4.50382	0.00682005
<i>TMPRSS3</i>	9.13878	0.448475	4.3489	0.00682005
<i>PTPRVP</i>	7.78396	0.413622	4.23412	0.00682005
<i>FBXL21</i>	9.29727	0.503102	4.20788	0.00682005
<i>AGXT</i>	2.83662	0.169847	4.06186	0.00682005
<i>HPD</i>	23.1012	1.44722	3.99661	0.00682005
<i>C2orf66</i>	10.671	0.69661	3.9372	0.00682005
<i>TRIM54</i>	17.9605	1.28591	3.80397	0.0117654
<i>TFPI2</i>	299.5	21.5381	3.79759	0.00682005
<i>KLC3</i>	1.1688	0.0875703	3.73844	0.0320323
<i>ICAM5</i>	1.07351	0.0825358	3.70118	0.00682005
<i>BMP4</i>	82.6717	6.43767	3.68278	0.00682005
<i>SLC30A3</i>	7.22548	0.587504	3.62042	0.00682005
2) Top 20 downregulated genes in APAs with NMD (diameter ≥30 mm versus ≤10 mm)				
Gene	APAs ≥30 mm (FPKM)	APAs ≤10 mm (FPKM)	Log2_FC	Adjusted P value
<i>TRBC2</i>	6.09704	1625.97	-8.05897	0.00682005
<i>RELN</i>	0.159952	11.8197	-6.20741	0.00682005
<i>SFRP2</i>	0.0963944	6.31274	-6.03317	0.0234198
<i>SPP1</i>	1.44412	44.9871	-4.96125	0.00682005
<i>COL25A1</i>	0.149522	4.61247	-4.94711	0.00682005
<i>ACVR1C</i>	0.0181787	0.475814	-4.71007	0.00682005
<i>LRR4C</i>	0.0751931	1.7918	-4.57467	0.00682005
<i>ENPP6</i>	0.0696874	1.57815	-4.50119	0.00682005
<i>SEL1L2</i>	0.0296904	0.671518	-4.49936	0.00682005
<i>MYRIP</i>	0.288528	6.33858	-4.45738	0.00682005
<i>KIAA1549L</i>	0.255241	5.60146	-4.45587	0.0234198
<i>TMEM132E</i>	0.144143	3.15007	-4.44981	0.0320323
<i>ALDH1A2</i>	0.902063	19.572	-4.43942	0.00682005
<i>WSCD2</i>	0.0346711	0.734741	-4.40543	0.00682005
<i>LAMP5</i>	0.297174	5.98316	-4.33153	0.00682005
<i>GPR133</i>	0.270912	5.33807	-4.30042	0.00682005
<i>PRKCQ</i>	0.173295	3.15566	-4.18664	0.00682005
<i>PLD5</i>	0.673111	11.3903	-4.08082	0.00682005
<i>TNNC1</i>	0.755305	12.477	-4.04607	0.00682005
<i>SOWAHA</i>	0.115113	1.52727	-3.72983	0.015646

Table S3. Top differentially expressed genes in APAs with NMD.

Expression levels identified by mRNA-seq are shown in FPKM (fragments per kilobase of transcript, per million mapped reads), differences in expression levels are given as log₂(fold change) (log₂_FC). The *P* value indicates level of statistical significance adjusted by the Benjamini-Hochberg False Discovery Rate method. APA, aldosterone-producing adenoma; FC, fold change; FPKM, fragments per kilobase of transcript, per million mapped reads; NMD, no mutation detected.

1) Top 20 upregulated genes in APAs with <i>KCNJ5</i> mutations (diameter ≥30 mm versus ≤10 mm)				
Gene	APAs ≥30 mm (FPKM)	APAs ≤10 mm (FPKM)	Log2_FC	Adjusted P value
<i>TRBC2</i>	2219.49	2.67241	9.69787	0.0103294
<i>AP001631.1</i>	8.35274	0.126997	6.03938	0.0103294
<i>MTUS2</i>	0.939324	0.06536	3.84514	0.0103294
<i>HCG9</i>	7.81512	0.584249	3.74161	0.0103294
<i>NTS</i>	25.9523	2.03214	3.67479	0.0103294
<i>SORCS3</i>	1.29507	0.126052	3.36094	0.0103294
<i>LPAR3</i>	1.92719	0.224175	3.1038	0.0103294
<i>FIGF</i>	5.90777	0.911699	2.69599	0.0103294
<i>IFI6</i>	225.838	40.8295	2.46761	0.0103294
<i>NOP56</i>	305.452	62.077	2.29881	0.0103294
<i>FUT1</i>	8.52805	1.90724	2.16073	0.0103294
<i>IGFN1</i>	0.81539	0.183746	2.14978	0.0103294
<i>CHRD1</i>	4.8011	1.10373	2.12098	0.0103294
<i>ISG15</i>	18.5925	4.34589	2.09699	0.0103294
<i>IFI27</i>	382.74	91.0709	2.0713	0.0103294
<i>CHST6</i>	3.52854	0.938261	1.91101	0.0182566
<i>PCDHB11</i>	1.33752	0.365664	1.87097	0.0257858
<i>TBX18</i>	8.3294	2.32673	1.83991	0.0103294
<i>IFI44</i>	76.6797	21.5377	1.83198	0.0103294
<i>OAS3</i>	7.47185	2.50074	1.57911	0.0103294
2) Top 20 downregulated genes in APAs with <i>KCNJ5</i> mutations (diameter ≥30 mm versus ≤10 mm)				
Gene	APAs ≥30 mm (FPKM)	APAs ≤10 mm (FPKM)	Log2_FC	Adjusted P value
<i>IGHA1</i>	2.51271	419.213	-7.38229	0.0103294
<i>AL132709.3</i>	0.2671	38.4787	-7.17053	0.0103294
<i>CALY</i>	0.00806987	1.0536	-7.02857	0.0103294
<i>IGKC</i>	3.30497	387.45	-6.87323	0.0103294
<i>MIR378H</i>	0.385754	42.0259	-6.76745	0.0257858
<i>IGLC1</i>	0.472613	45.1143	-6.57678	0.0103294
<i>IGLC2</i>	0.354545	17.2933	-5.6081	0.0182566
<i>SCG2</i>	0.239948	11.2124	-5.54623	0.0103294
<i>IGKV4-1</i>	0.234699	10.1855	-5.43956	0.0182566
<i>IGJ</i>	0.467998	10.612	-4.50305	0.0103294
<i>DBH</i>	0.331607	6.49978	-4.29284	0.0387352
<i>PAX8-AS1</i>	1.5599	26.5979	-4.09179	0.0103294
<i>CHRNA3</i>	0.105649	1.75949	-4.05781	0.0182566
<i>RASGEF1A</i>	0.134348	2.02587	-3.9145	0.0103294
<i>BAI1</i>	0.239394	3.5321	-3.88307	0.0103294
<i>CCL21</i>	0.621017	8.18441	-3.72017	0.0103294
<i>MZB1</i>	0.200344	2.53853	-3.66344	0.0318257
<i>GRM7</i>	0.053964	0.569929	-3.40071	0.0103294
<i>SCG5</i>	0.321675	3.2733	-3.34707	0.0103294
<i>RIMBP2</i>	0.064735	0.648018	-3.32342	0.0103294

Table S4. Top differentially expressed genes in APAs with *KCNJ5* mutations.

Expression levels identified by mRNA-seq are shown in FPKM (fragments per kilobase of transcript, per million mapped reads), differences in expression levels are given as log₂(fold change) (log₂_FC). The *P* value indicates level of statistical significance adjusted by Benjamini-Hochberg False Discovery Rate method. APA, aldosterone-producing adenoma; FC, fold change; FPKM, fragments per kilobase of transcript, per million mapped reads; *KCNJ5*, gene encoding potassium inwardly rectifying channel subfamily J member 5.

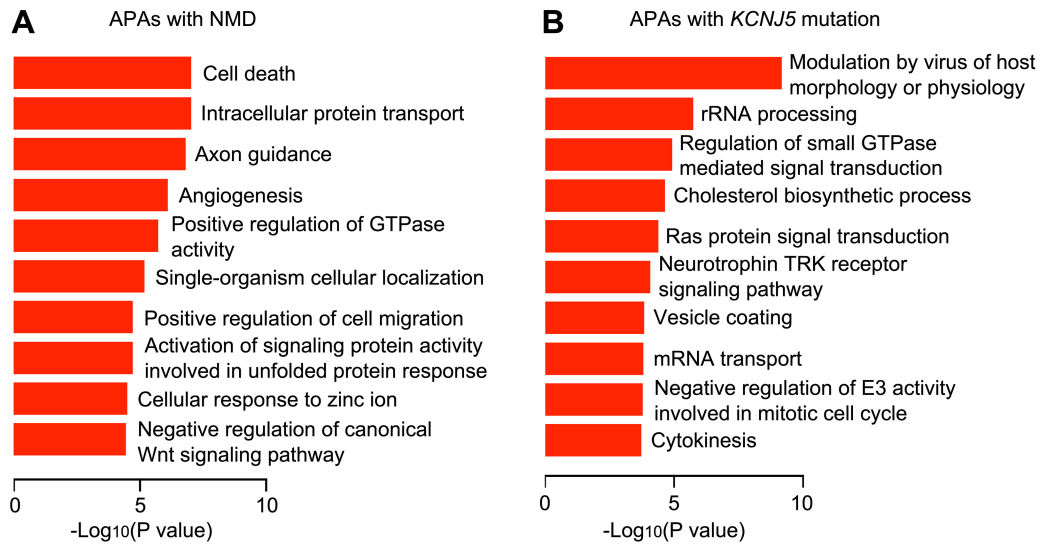


Figure S1. Top 10 overrepresented GO terms of biological process enriched in the comparisons between macro- and micro-APAs stratified by genotypes.

P values were determined using the elim method with the Kolmogorov-Smirnov test. Overrepresented GO terms are defined when the number of DEGs annotated to a specific GO term is higher than the estimated number of genes annotated to the background reference. E3, ubiquitin-protein ligase; *KCNJ5*, gene encoding potassium inwardly rectifying channel subfamily J member 5; NMD, no mutation detected.

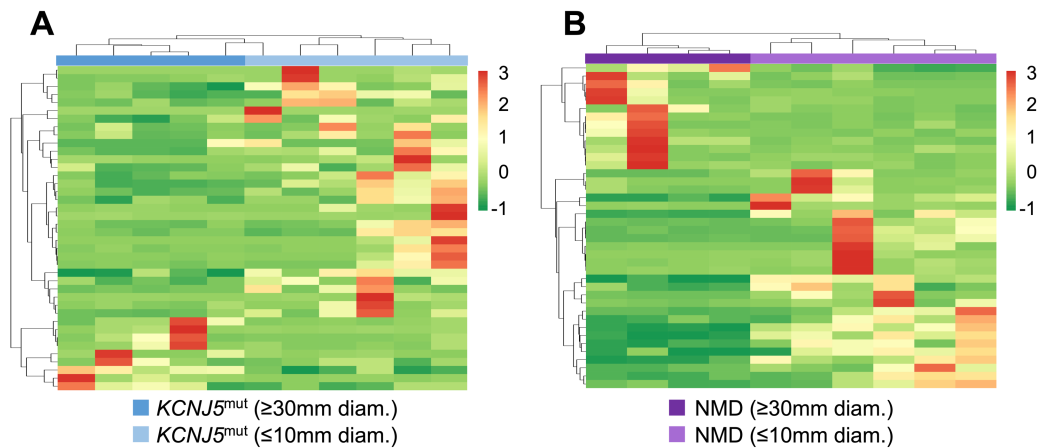


Figure S2. Distinct expression of genes with a reported role in cell death and proliferation in APAs with different genotypes and adenoma diameter.

The heat maps show unsupervised hierarchical clustering of top 40 DEGs associated with cell death and proliferation based on normalized FPKM (fragments per kilobase of transcript, per million mapped reads) identified by RNA-seq in *KCNJ5* (A) and NMD subgroup (B). The color-coded bar on the right of the figure indicates the difference in expression level of a gene in standard deviation units from the mean expression level in all samples. Gene function were obtained from Entrez Gene (<https://www.ncbi.nlm.nih.gov/gene/>) and GeneCards (<https://www.genecards.org/>) databases. diam., diameter; *KCNJ5*, gene encoding potassium inwardly rectifying channel subfamily J member 5; *KCNJ5*^{mut}, APAs with *KCNJ5* mutations; NMD, APAs with no mutation detected.

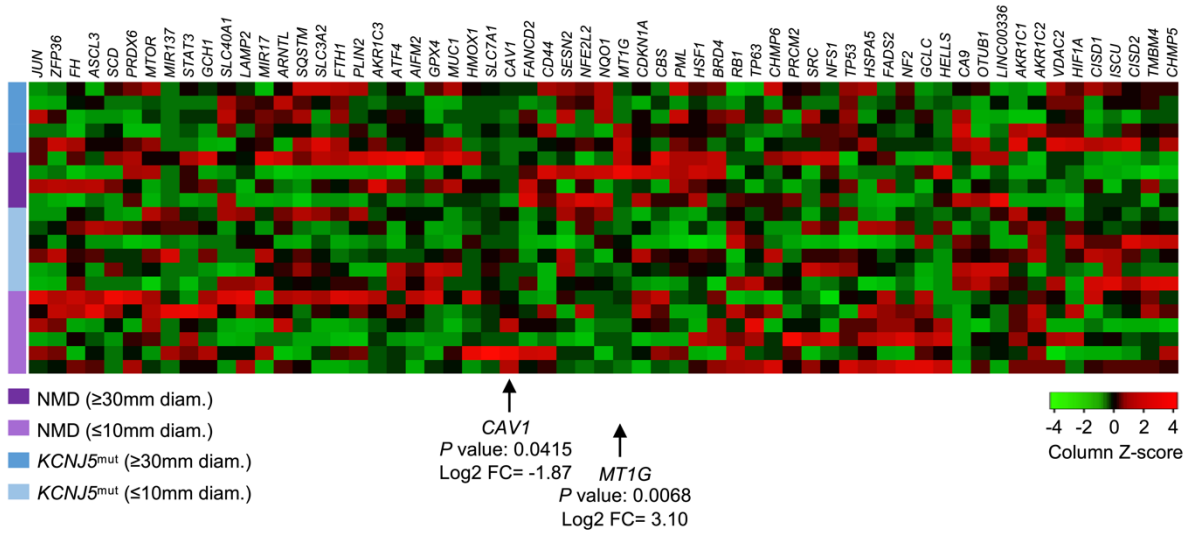


Figure S3. Expression of reported ferroptosis suppressors in APAs with different genotypes and adenoma diameter.

The heat map shows the transcription levels of 61 ferroptosis suppressors annotated in FerrDb database (<http://www.zhounan.org/ferrdb/>) based on normalized FPKM (fragments per kilobase of transcript, per million mapped reads) identified by mRNA-seq. Column Z-score indicates the difference in expression level of a gene in standard deviation units from the mean expression level in all samples. The genes (*CAV1* and *MT1G*) indicated by arrows were differentially expressed in APAs with NMD according to adenoma diameter. *P* values were adjusted using Benjamini-Hochberg False Discovery Rate method. diam., diameter; *KCNJ5*, gene encoding potassium inwardly rectifying channel subfamily J member 5; *KCNJ5*^{mut}, APAs with *KCNJ5* mutations; Log₂ FC, log₂(APA ≥ 30 mm/ ≤ 10 mm); NMD, APAs with no mutation detected.

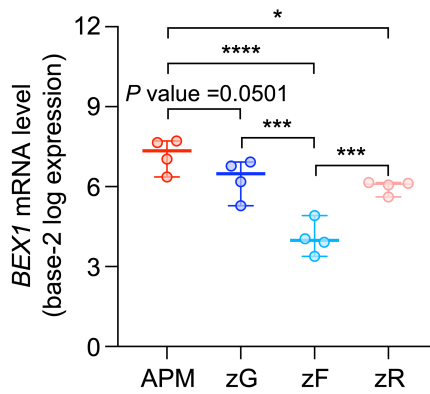


Figure S4. *BEX1* is differentially expressed in APMs and adrenocortical zones.

Data were derived from a microarray study that compared the transcriptomes of APMs and adrenocortical zones acquired from 4 adrenal glands by laser capture microdissection.⁴ Statistical analyses were performed on log₂-transformed values using two-way ANOVA models. * $P < 0.05$, *** $P < 0.001$, **** $P < 0.0001$. Each circle represents a single sample. Horizontal lines indicate the median, whiskers represent 95% confidential intervals. APM, aldosterone-producing micronodule; zF, zona fasciculata; zG, zona glomerulosa; zR, zona reticularis.

9. Paper III

Title: Primary aldosteronism: *KCNJ5* mutations and adrenocortical cell growth

Authors: Yang Y, Gomez-Sanchez CE, Jaquin D, Prada ETA, Meyer LS, Knösel T, Schneider H, Beuschlein F, Reincke M, Williams TA

Journal: Hypertension

Year: 2019

Volume: 74

Pages: 809-816

DOI: 10.1161/HYPERTENSIONAHA.119.13476

Primary Aldosteronism KCNJ5 Mutations and Adrenocortical Cell Growth

Yuhong Yang, Celso E. Gomez-Sanchez, Diana Jaquin, Elke Tatjana Aristizabal Prada, Lucie S. Meyer, Thomas Knösel, Holger Schneider, Felix Beuschlein, Martin Reincke, Tracy Ann Williams

Abstract—Aldosterone-producing adenomas with somatic mutations in the KCNJ5 G-protein-coupled inwardly rectifying potassium channel are a cause of primary aldosteronism. These mutations drive aldosterone excess, but their role in cell growth is undefined. Our objective was to determine the role of KCNJ5 mutations in adrenal cell proliferation and apoptosis. The Ki67 proliferative index was positively correlated with adenoma diameter in aldosterone-producing adenomas with a KCNJ5 mutation ($r=0.435$, $P=0.007$), a negative correlation was noted in adenomas with no mutation detected ($r=-0.548$, $P=0.023$). Human adrenocortical cell lines were established with stable expression of cumate-inducible wild-type or mutated KCNJ5. Increased cell proliferation was induced by low-level induction of KCNJ5-T158A expression compared with control cells ($P=0.009$), but increased induction ablated this difference. KCNJ5-G151R displayed no apparent proliferative effect, but KCNJ5-G151E and L168R mutations each resulted in decreased cell proliferation (difference $P<0.0001$ from control cells, both comparisons). Under conditions tested, T158A had no effect on apoptosis, but apoptosis increased with expression of G151R ($P<0.0001$), G151E ($P=0.008$), and L168R ($P<0.0001$). We generated a specific KCNJ5 monoclonal antibody which was used in immunohistochemistry to demonstrate strong KCNJ5 expression in adenomas without a *KCNJ5* mutation and in the zona glomerulosa adjacent to adenomas irrespective of genotype as well as in aldosterone-producing cell clusters. Double immunofluorescence staining for KCNJ5 and CYP11B2 (aldosterone synthase) showed markedly decreased KCNJ5 immunostaining in CYP11B2-positive cells compared with CYP11B2-negative cells in aldosterone-producing adenomas with a KCNJ5 mutation. Together, these findings support the concept that cell growth effects of KCNJ5 mutations are determined by the expression level of the mutated channel. (*Hypertension*. 2019;74:00-00. DOI: 10.1161/HYPERTENSIONAHA.119.13476.) • [Online Data Supplement](#)

Key Words: adenoma ■ adrenal cortex ■ aldosterone ■ apoptosis ■ cell proliferation ■ potassium channel

Unilateral primary aldosteronism (PA) is the most prevalent surgically-correctable form of hypertension. The constitutive production of aldosterone mainly originates from a unilateral aldosterone-producing adenoma (APA) and less often from unilateral hyperplasia (30% and 2% of cases of PA, respectively).¹ Major breakthroughs in understanding the pathophysiology of sporadic APAs have been made since the identification by Choi et al² of somatic mutations in the *KCNJ5* gene (causing KCNJ5-G151R or KCNJ5-L168R missense mutations) in a high proportion of these tumors.²⁻⁴ KCNJ5 is an inwardly rectifying potassium channel (also called GIRK4, [G protein-coupled inwardly rectifying potassium channel]) and the described mutations cause sodium ion conductance due to the loss of selectivity for potassium ions by the channel pore. In adrenocortical cells, the consequent membrane depolarization triggers opening of voltage-gated calcium

channels and calcium ion influx ultimately activates aldosterone production.²⁻⁵

The identification of additional APA somatic mutations in the CACNA1D (Cav1.3 calcium channel) and in the Na⁺/K⁺-ATPase and Ca²⁺-ATPase ion transporters (ATP1A1 and ATP2B3, respectively) highlighted the importance of intracellular ion homeostasis and calcium signaling in aldosterone production^{6,7} and, together with somatic mutations in CTNNB1 (β-catenin), these mutations can be detected in almost 90% of APAs.⁸ In most populations, a predominance of KCNJ5 mutations in APAs over other genotypes is reported^{3,4,9-11} with a global prevalence of 43%.¹²

A role for KCNJ5 mutations in adrenal cell growth has not been defined. When initially described, KCNJ5 mutations were proposed to result in both constitutive aldosterone production and cell proliferation² due to the established role of

Received May 31, 2019; first decision June 19, 2019; revision accepted July 29, 2019.

From the Medizinische Klinik und Poliklinik IV, Klinikum der Universität München, LMU München, Germany (Y.Y., D.J., E.T.A.P., L.S.M., H.S., F.B., M.R., T.A.W.); Endocrine Division, G.V. (Sonny) Montgomery VA Medical Center, University of Mississippi Medical Center, Jackson (C.E.G.-S.); Institute of Pathology, Ludwig-Maximilians-Universität München, Germany (T.K.); Klinik für Endokrinologie, Diabetologie und Klinische Ernährung, Universitätsspital Zürich, Switzerland (F.B.); Division of Internal Medicine and Hypertension, Department of Medical Sciences, University of Turin, Italy (T.A.W.).

The online-only Data Supplement is available with this article at <https://www.ahajournals.org/doi/suppl/10.1161/HYPERTENSIONAHA.119.13476>.

Correspondence to Tracy Ann Williams, Medizinische Klinik und Poliklinik IV, Klinikum der Universität München, LMU München, Ziemssenstr 1, D-80336 München, Germany. Email tracy.williams@med.uni-muenchen.de

© 2019 American Heart Association, Inc.

Hypertension is available at <https://www.ahajournals.org/journal/hyp>

DOI: 10.1161/HYPERTENSIONAHA.119.13476

calcium signaling in both processes.^{13,14} A function in driving aldosterone excess has been demonstrated by expression of mutated forms of *KCNJ5* in human adrenocortical cells in vitro⁵ but a decrease in cell proliferation resulted from expression of *KCNJ5*-T158A.⁵ This mutation (*KCNJ5*-T158A) has been identified in both sporadic APAs and a familial form of PA (called familial hyperaldosteronism type III)^{2,15} and the absence of an effect on cell proliferation in vitro is seemingly paradoxical to the massive cortical hyperplasia observed in a patient carrying the germline variant.^{2,16}

Aldosterone-producing cell clusters (APCC) are a histopathologic feature often found beneath the adrenal capsule under normal and pathological conditions.¹⁷ APCCs comprise tight nests of predominantly zona glomerulosa cells with intense immunohistochemistry staining for CYP11B2 (aldosterone synthase). A notable proportion of APCCs carry mutations in *CACNA1D*, *ATP1A1*, and *ATP2B3*, but *KCNJ5* mutations are curiously absent.^{17,18} Our objective was to establish the effects of *KCNJ5* mutations on cell growth in human adrenocortical cells by specifically addressing their roles in cell proliferation and apoptosis.

Methods

The data that support the findings of this study are available from the corresponding author on reasonable request.

Patient Samples

The study included 72 surgically resected adrenals from patients diagnosed with unilateral PA according to the Endocrine Society Guideline.¹⁹ Patients were screened for PA using the plasma aldosterone-to-direct renin concentration ratio, and diagnosis was confirmed by the intravenous saline load test according to local criteria.²⁰ Adenoma size was assessed from the diameter of the largest nodule at pathology, and CYP11B2 immunohistochemistry was done on all adrenals, and any without a well-circumscribed CYP11B2-positive adenoma were excluded. All participants gave written informed consent, and the protocol was approved by the local ethics committee.

DNA Sequencing

Genomic DNA was extracted from dissected nodules from fresh frozen adrenal tissues, and DNA fragments were amplified using primers flanking mutation hot spot regions in *KCNJ5*, *ATP1A1*, *ATP2B3*, and *CACNA1D* before DNA sequencing as described elsewhere.²¹

Production of HAC15 Stable Cell Lines With Inducible *KCNJ5* Expression

cDNAs encoding mutated and wild-type forms of *KCNJ5* were prepared by Gateway cloning (ThermoFisher Scientific) in cumate-inducible PiggyBac vectors (System Biosciences, Palo Alto, CA). Stable cell lines were established by cotransfection of human adrenocortical cells (HAC15 cells, a kind gift from Professor William E. Rainey, University of Michigan, Ann Arbor) with the PiggyBac vector (carrying the human *KCNJ5* cDNA) and the Super PiggyBac transposase according to the manufacturer's instructions (System Biosciences, Palo Alto, CA). Transfected cells were selected with puromycin (4 µg/mL) in the presence of verapamil (10 µmol/L) to inhibit the P glycoprotein.²² The macrolide antibiotic roxithromycin (20 µmol/L) was also included to inhibit any potential effects on cell growth of mutant *KCNJ5* channels²³ in the absence of the cumate inducer. Total RNA was extracted from stable cell lines after induction with cumate (10 µg/mL) for 72 hours, reverse transcribed and the *KCNJ5* gene was sequenced to confirm the mutated or wild-type *KCNJ5* genotype of all cell lines.²¹

Cell Proliferation and Apoptosis Assays

HAC15 cells (2.5×10⁴ cells/well) stably transfected with wild-type or mutated forms of *KCNJ5* (*T158A*, *G151R*, *G151E*, or *L168R*) or empty vector were plated in 96-well plates, and transcription was induced with 1 µg/mL or 10 µg/mL cumate in the absence of roxithromycin for 24 hours. Cell proliferation was determined with a WST-1 (water-soluble tetrazolium salt-1) assay (Roche), and apoptosis was quantified by an Annexin V apoptosis assay (Promega).

Generation of Monoclonal Antibodies Against Human *KCNJ5*

A peptide corresponding to the N-terminal portion of human *KCNJ5* (acetyl-36-ATDRTRLLAEGKKP-49-C) with the addition of a cysteine at the C-terminal end was synthesized by LifeTein LLC (Hillsborough, NJ) and conjugated to 5 mg of Imject™ Blue Carrier Protein (ThermoFisher Scientific) using Succinimidyl-6-(iodoacetyl) aminocaproate (Molecular Biosciences [Boulder], CO). Four Swiss Webster Female mice were immunized initially with 10 µg of immunogen with Complete Freund's Adjuvant (Millipore-Sigma) followed by immunization using incomplete Freund's adjuvant every 2 weeks. After 2 months of biweekly immunizations, the mice received the immunogen in saline intraperitoneally, and 3 days later were euthanized using isoflurane anesthesia, blood was withdrawn and spleens removed under aseptic conditions. Spleen cells were then obtained and frozen in liquid nitrogen using DMEM media containing 20% newborn calf serum, 5% dimethylsulfoxide, and 2.5% of polyethylene glycol 1000.

After titers were performed on the serum, the spleen from the mouse with the higher titer was fused with polyethylene glycol 1450 (ATCC.org) to the mouse myeloma SP2-mIL6-hIL21-hTERT cells and plated into 10×96 well plates. After 10 days, the wells were screened by ELISA on plates coated with the acetyl-36-ATDRTRLLAEGKKP-49-C conjugated to chicken ovalbumin. Positive clones were then screened by Western blotting of cell lysates from human embryonic kidney 293T cells transfected with a tetracycline-inducible lentivirus containing the human *KCNJ5* sequence.⁵ Clones which gave single bands of the appropriate molecular mass for *KCNJ5* on Western blots were subcloned using high-density methyl cellulose²⁴ and were isotyped. The use of mice for the generation of monoclonal antibodies was approved by the University of Mississippi Medical Center IACUC.

Immunohistochemistry and Immunofluorescence

Formalin-fixed paraffin-embedded adrenal tissue sections (3 µm) were used for CYP11B2 immunohistochemistry to detect aldosterone synthase expression with a monoclonal antibody (clone 17B) diluted 1:200 as described,²⁵ and *KCNJ5* immunohistochemistry was performed using the *KCNJ5* monoclonal antibody generated herein (clone No. 36-33-5, dilution 1:2000). Double immunofluorescence CYP11B2 and *KCNJ5* staining used an anti-mouse IgG1 Alexa Fluor 488 secondary antibody (to detect CYP11B2 primary antibody) and anti-mouse IgG2B Alexa Fluor 594 (to detect *KCNJ5* antibodies) both diluted 1:200 (Invitrogen). A rabbit anti-PARP (poly-ADP ribose polymerase) monoclonal antibody diluted 1:2000 (Cell Signaling) was used for immunofluorescence staining of cleaved PARP with an anti-rabbit Alexa Fluor 594 secondary antibody diluted 1:200 (Invitrogen).

Scoring Adrenals for Ki67 Proliferation Index and *KCNJ5* Immunostaining

Ki67 immunohistochemistry was performed on formalin-fixed paraffin-embedded adrenal sections (3 µm) using a rabbit monoclonal antibody (clone No. SP6 1:200 dilution, Sigma-Aldrich). The Ki67 proliferation index was assessed as the percentage of the manual count of intense Ki67 stained nuclei relative to the total hematoxylin stained nuclei which were quantified by color segmentation using ImageJ software. Three separate fields of view were used for scoring, and the final proliferation index was calculated as the average of the 3 Ki67 scores.²⁶ To score *KCNJ5* immunostaining intensity in adenomas and paired adjacent cortical tissue, a semi-quantitative

score system was used in which intensity of immunohistochemistry staining was graded 0 to 4 for undetectable, low, moderate, or high²⁷ from a field of view at $\times 20$ magnification acquired from each adrenal sample. Both the Ki67 proliferation index and H scores for CYP11B2 were evaluated by researchers blinded to mutational status and pathological reports of the assessed adrenals (H. Schneider and T. Ann Williams). Adenoma sizes (to determine correlations with Ki67 index) were determined by the pathologist (T. Knösel) as the diameter of the largest nodule.

Statistical Analyses

Statistical analyses were performed using SPSS, version 25.0 and Graphpad Prism version 7.0.

Comparisons between 2 groups were determined using a *t* test or a Mann-Whitney *U* test, multiple comparisons were analyzed by ANOVA with a Bonferroni test or Kruskal-Wallis tests with pairwise comparisons. Pearson correlation coefficients were used to analyze univariate correlations. $P < 0.05$ was considered significant.

Results

Clinical Characteristics of Patients With APA According to Genotype

Genotyping of 72 resected adrenals from patients with an APA, determined 39 APAs with a KCNJ5 mutation (L168R, $n=22$; G151R, $n=16$, and T158A, $n=1$), 5 with a CACNA1D mutation, and 3 and 2 APAs with ATP1A1 or ATP2B3 mutations, respectively. The remaining 23 APAs did not carry a mutation in known hotspots of target genes and were referred to as tumors with no mutation detected (NMD).

Patients with a KCNJ5-mutated APA were younger than patients with an NMD-APA (47.2 years \pm 10.4 versus 57.7 years \pm 11.0; $P=0.001$) with a higher proportion of women than patients with an NMD-APA (82.1% of 39 patients versus 30.4% of 23; $P < 0.001$) or relative to the small group of patients with other somatic APA mutations (10.0% of 10 patients; $P < 0.001$). The largest adenoma diameter at pathology was greater in KCNJ5-mutated APAs (17.0 mm [14.0–24.0]) compared with both NMD-APAs and APAs with other mutations combined (12.0 mm [8.0–25.0], $P=0.019$ and 9.0 mm [7.8–15.3], $P=0.003$, respectively). We noted a lower PAC in KCNJ5-mutated APAs compared with the group of APAs with a mutation in ATP1A1, ATP2B3, and CACNA1D combined (979 pmol/L [500–1470] compared with 1989 pmol/L [1624–3346], $P=0.006$; Table S1 in the [online-only Data Supplement](#)).

Diverse Proliferation in Adenomas With or Without a KCNJ5 Mutation

Ki67 proliferation index was assessed in a subset of adrenals (37 APAs with KCNJ5 mutations; 17 designated NMD and 10 with either a CACNA1D, ATP1A1, or ATP2B3 mutation). Adenoma size was larger in APAs with a KCNJ5 mutation compared with NMD (17.0 mm [14.5–24.5] versus 12.0 mm [8.0–27.5], $P=0.0327$). APAs with a KCNJ5 mutation had a lower proliferation index relative to APAs with NMD (0.9% \pm 0.4 versus 1.2% \pm 0.4, $P=0.011$). The Ki67 proliferation index was positively correlated with adenoma diameter in KCNJ5-mutated APAs ($r=0.4347$, $P=0.0072$) in contrast to the negative linear correlation noted in NMD-APAs ($r=-0.5484$, $P=0.0226$; Figure 1). There was no correlation of adenoma diameter with Ki67 index in the small group of APAs with a

CACNA1D, ATP1A1, or ATP2B3 mutation combined. There was no significant difference in adenoma diameter between APAs with a L168R or a G151R mutation (L168R, 16.0 mm [15.0–27.3] versus G151R, 18.0 mm [14.0–22.0]; $P=0.636$) or in Ki67 score (L168R, 1.0% \pm 0.4 versus G151R, 0.8% \pm 0.4; $P=0.339$).

Effects of KCNJ5 Mutations on Cell Growth in Adrenocortical Cells

Stable HAC15 cell lines expressing KCNJ5 with different genotypes were established using the selection marker puromycin. Sensitivity to puromycin was increased in the presence of verapamil (10 μ mol/L; Figure S1), and the presence of KCNJ5 mutations was confirmed by Sanger sequencing. The cell viability of the KCNJ5-T158A HAC15 cell line was significantly higher compared with control cells (transfected with empty vector) after 24-hour induction with 1 μ g/mL cumate ($P=0.0094$). This effect on cell proliferation was absent in cells with increased transcriptional induction of *KCNJ5-T158A* (10 μ g/mL cumate). KCNJ5-G151R had no apparent effect on adrenocortical proliferation in vitro, whereas decreased proliferation was observed in HAC15 cells with KCNJ5-G151E and L168R mutations ($P < 0.0001$ versus control cells, both comparisons; Figure 2A).

Higher levels of cell death by apoptosis were observed in cells with KCNJ5-G151R, G151E, and L168R mutations ($P < 0.0001$, $P=0.0078$, and $P < 0.0001$ versus control cells, respectively) under the conditions tested (24-hour incubation with 1 μ g/mL cumate). Cells carrying the KCNJ5-T158A mutation did not induce apoptosis under the same conditions (Figure 2B). These observations were consistent with immunofluorescence detection of cleaved PARP, a hallmark of apoptosis, which showed increased numbers cells with positive cleaved PARP staining in the nuclei of *KCNJ5-G151E* and *L168R* transfected cells compared with control cells (Figure S2). HAC15 cells with KCNJ5-T158A and G151R mutations displayed a similar proportion of cleaved-PARP positive cells compared with control cells (Figure S2).

Generation of Monoclonal Antibodies Against Human KCNJ5

There were 100 positive clones from the ELISA screen and of these, 2 clones (No. 33 and No. 68) displayed specific binding to KCNJ5 on Western blots of human embryonic kidney 293T cell lysates transduced with a lentivirus carrying the human *KCNJ5* sequence. Clones No. 33 and No. 68 were subcloned to produce antibodies KCNJ5-33-5 and KCNJ5-68-15, and their specificity was validated by Western blotting (Figure 3A). The 2 clones were isotypized, clone KCNJ5-33-5 was IgG2b, and the KCNJ5-68-15 was IgG2c. Both antibodies were used for immunohistochemistry of formalin-fixed paraffin-embedded sections of resected adrenals from patients with an APA. Analysis of the cortical tissue adjacent to an adenoma demonstrated membrane and cytoplasmic staining with No. 68-15 quite diffuse throughout the cortex compared with predominant plasma membrane staining of zona glomerulosa cells with No. 33-5 (Figure 3B through 3C). Clone No. 33-5 was selected for further immunohistochemistry and immunofluorescence staining.

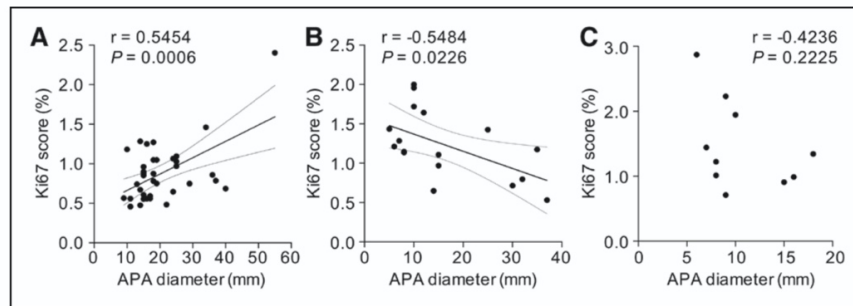


Figure 1. Correlation of Ki67 score with nodule diameter according to genotype. Ki67 score was positively linearly correlated with aldosterone-producing adenoma (APA) diameter in *KCNJ5*-mutated APAs ($r=0.4347$, $P=0.0072$; **A**), whereas a linear negative correlation was observed in the group of tumors with no mutation detected (no mutation detected; $r=-0.5484$, $P=0.0226$; **B**). Ki67 index was not correlated with adenoma diameter in the small group of APAs with a *CACNA1D* [Cav1.3 calcium channel], *ATP1A1*, or *ATP2B3* mutation combined (**C**). Ki67 score was derived using ImageJ software and calculated from the average intense Ki67 nuclei staining count divided by the total nuclei hematoxylin staining count from 3 fields of view. Lines represent the Pearson correlation (thick black line) and 95% CI (thin gray line). When the outlier in **A** is omitted, a positive linear correlation between Ki67 index and APA diameter is still observed ($r=0.5454$, $P=0.0006$).

KCNJ5 Expression in APAs Varies According to Genotype

Immunohistochemistry using the *KCNJ5* No. 33–5 monoclonal antibody was performed on 33 adrenal samples with various APA genotypes (*KCNJ5*, $n=13$; WT, $n=10$; *CACNA1D*, $n=5$; *ATP1A1*, $n=3$; and *ATP2B3*, $n=2$). Adenomas of all adrenals showed positive-immunostaining for *KCNJ5* and *CYP11B2* (Figure 4, Figure S3) with decreased intensity of *KCNJ5* immunostaining in APAs with *KCNJ5* mutations compared with other adenomas (Figure 4). Semi-quantitative H score assessment of *KCNJ5* immunostaining highlighted the decreased *KCNJ5* expression in APAs with a *KCNJ5* mutation (Figure 5A, difference $P<0.0001$ for *KCNJ5*-mutated APAs versus NMD-APAs and APAs with *ATP1A1*, *ATP2B3*, *CACNA1D* mutations combined). There were no apparent differences in *KCNJ5* immunostaining intensity between NMD-APAs versus APAs with *CACNA1D*, *ATP1A1*, and *ATP2B3* mutations (Figure 4, Figure 5A). No differences in intensity of *KCNJ5* immunostaining were apparent between APAs with different *KCNJ5* mutations (*KCNJ5*-G151R, L168R, or T158A; Figure S3).

KCNJ5 immunostaining was lower in all 13 tumors with *KCNJ5* mutations compared with the paired adjacent cortex

(Figure 4A and 4B, Figure 5B). In contrast, the majority of APAs with other genotypes showed either increased or similar *KCNJ5* immunostaining intensity in adenomas (75% of 20 adrenals; Figure 4C, Figure 5B).

Double *KCNJ5*-*CYP11B2* immunofluorescence was performed on APAs of different genotypes. Colocalization of *KCNJ5* with *CYP11B2* was demonstrated in all adrenals, but a decrease of *KCNJ5* immunostaining was evident in *CYP11B2*-positive cells relative to *CYP11B2*-negative cells of the same adenoma carrying a *KCNJ5* mutation (Figure 4D, Figure S4). This difference of *KCNJ5* immunostaining intensity was absent in APAs of other genotypes (Figure S4).

Expression of KCNJ5 in APCCs

KCNJ5 and *CYP11B2* immunohistochemistry and double *KCNJ5*-*CYP11B2* immunofluorescence of APCCs showed moderate to high expression of *KCNJ5* in APCCs ($n=11$; Figure 6A) and the colocalization of the high-level *KCNJ5* and *CYP11B2* immunostaining (Figure 6B).

Discussion

We demonstrate the diverse effects of *KCNJ5* mutations on adrenocortical cell growth. We show an increase in

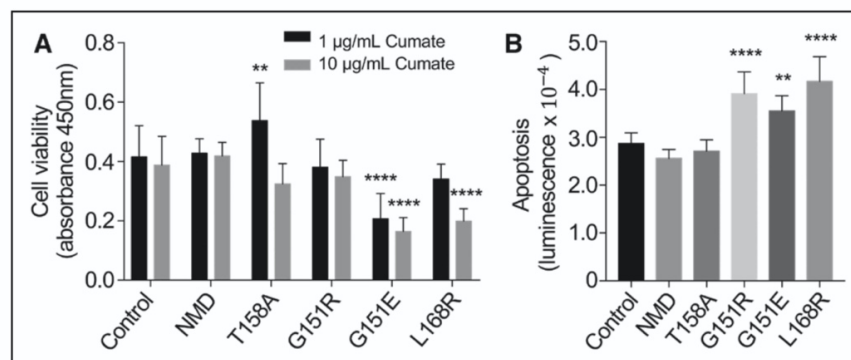


Figure 2. Effects of *KCNJ5* mutants on cell growth in adrenocortical cells. Human adrenocortical cells (HAC15) cells stably transfected with wild-type or mutated forms of *KCNJ5* (T158A, G151R, G151E, or L168R) or empty vector (control) were used to measure cell viability (**A**) or apoptosis (**B**). Cell viability was measured using a WST-1 (water-soluble tetrazolium salts) proliferation assay after 24-hour incubation with either 1 $\mu\text{g}/\text{mL}$ or 10 $\mu\text{g}/\text{mL}$ cumate (black and gray bars, respectively) to induce expression of *KCNJ5* (**A**). Apoptosis was measured using an Annexin V assay after 24-hour incubation with 1 $\mu\text{g}/\text{mL}$ cumate (**B**). Bars represent means of 6 separate experiments, error bars indicate SD. P values were calculated by ANOVA with a post hoc Bonferroni test, **difference ($P<0.01$) from control, **** difference ($P<0.0001$) from control. NMD indicates no mutation detected.

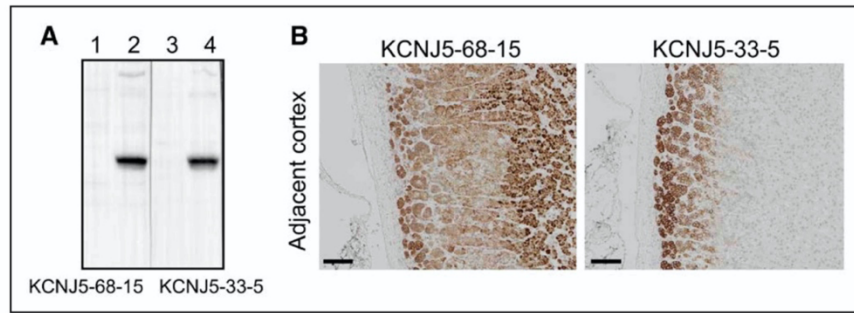


Figure 3. Generation of KCNJ5 monoclonal antibodies. Monoclonal antibodies against KCNJ5 were produced by injection of mice with a synthetic peptide corresponding to the N-terminal portion of KCNJ5 (acetyl-36-ATDRTRLLAEGKPP-49-C). See methods for details. The specificity of antibodies KCNJ5-68-15 and KCNJ5-33-11 was validated by Western blotting of cell lysates of HEK 293T cells transduced with a tetracycline-inducible lentivirus containing the human KCNJ5 sequence (A, uninduced [lanes 1 and 3] and tetracycline-induced [lanes 2 and 4]). KCNJ5 immunohistochemistry of adrenal cortex adjacent to an aldosterone-producing adenoma using KCNJ5-68-15 and KCNJ5-33-5 (B). KCNJ5-68-15 resulted in staining of most of the cortical tissue with evident staining of nuclei (B, left). KCNJ5-33-5 produced intense staining of the zona glomerulosa with clear localization to the plasma membrane (B, right). B, scale bar =100 μ m. KCNJ5 indicates G-protein-coupled inwardly rectifying potassium channel.

adrenocortical cell proliferation with low-level transcriptional induction of KCNJ5-T158A and, under similar conditions, stimulation of apoptosis with KCNJ5-G151R, L168R, and G151E. In adenomas with KCNJ5 mutations, CYP11B2-positive cells display strikingly reduced levels of KCNJ5 expression compared with CYP11B2-negative cells of the

same tumor and compared with CYP11B2-positive cells in APAs of other genotypes. We found decreased KCNJ5 immunostaining in KCNJ5-mutated APAs compared with paired adjacent cortical tissue in agreement with a previous study which also showed the absence of KCNJ5 mutations in the adjacent cortex.²⁸

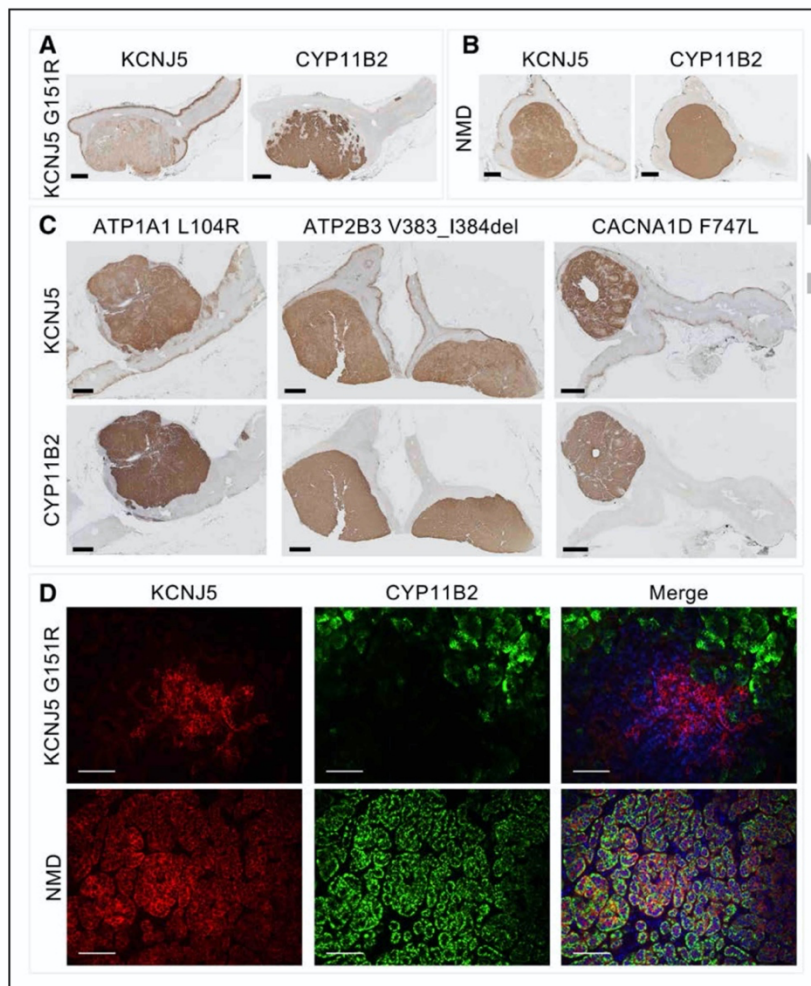


Figure 4. Heterogeneous immunostaining of KCNJ5 in aldosterone-producing adenoma (APA) according to genotype. Immunohistochemical staining of KCNJ5 and CYP11B2 in an APA with a KCNJ5 mutation or in an APA with no mutation detected (NMD) showing decreased KCNJ5 immunostaining in the adenoma with a KCNJ5 mutation (A and B). APAs with ATP1A1, ATP2B3, or CACNA1D mutations displayed intense KCNJ5 immunostaining (C). Double immunofluorescence staining of KCNJ5 and CYP11B2 in an APA with a KCNJ5 mutation compared with a NMD-APA (D). KCNJ5 was intensely expressed in CYP11B2-negative cells in KCNJ5-mutated adenoma, but markedly decreased KCNJ5 immunofluorescence was observed in CYP11B2-positive cells (D, upper). In wild-type APAs, KCNJ5 and CYP11B2 were colocalized to the same cells (D, lower). DAPI staining (blue) was only included in the merged image. A–C, scale bar =2 μ m; D, scale bar =100 μ m. ATP1A1 indicates Na⁺/K⁺ ATPase 1; ATP2B3, Ca²⁺ ATPase 3; CYP11B2, aldosterone synthase; CACNA1D, Cav1.3 Ca²⁺ channel; and KCNJ5, G-protein-coupled inwardly rectifying potassium channel.

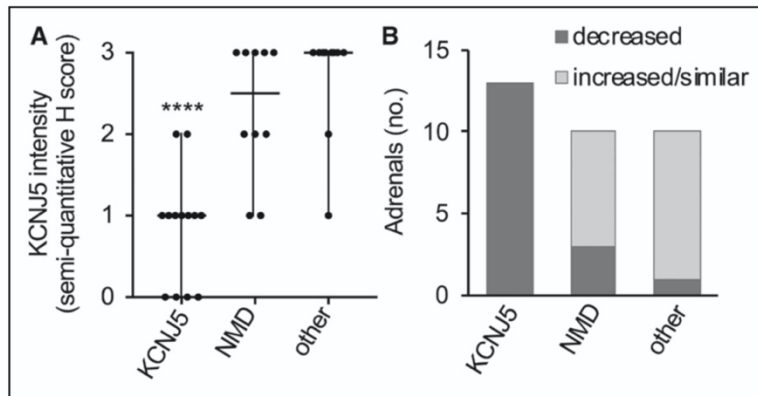


Figure 5. KCNJ5 immunostaining in aldosterone-producing adenomas (APAs) according to genotype. Semi-quantitative H score of KCNJ5 immunohistochemistry in adenomas according to genotype is shown (A). Horizontal Lines represent median, vertical lines represent range (A). *P* value was calculated by the Mann-Whitney *U* test, ****difference ($P < 0.0001$) from no mutation detected (NMD) or from other mutations combined. Relatively lower KCNJ5 immunostaining was noted in all adenomas with a KCNJ5 mutation compared with paired adjacent cortex, whereas 75% of 20 adenomas with other genotypes combined (NMD, $n=10$; *ATP1A1*, $n=3$; *ATP2B2*, $n=2$; and *CACNA1D*, $n=5$) showed either increased or similar expression in APAs compared with paired adjacent cortex (B). NMD, no mutation detected; other, adenomas with *ATP1A1*, *ATP2B3*, and *CACNA1D* mutation.

These observations indicate that only low-level expression of KCNJ5 mutations is compatible with adrenocortical cell survival. KCNJ5 mutations are absent (or at least rarely found) in APCCs which comprise tight nests of zona glomerulosa cells.¹⁷ The cell toxicity of KCNJ5 mutations combined with the high KCNJ5 expression in the zona glomerulosa layer is consistent with the absence of KCNJ5 mutations in APCCs and the particular phenotype of KCNJ5-mutated APAs with a predominance of zona fasciculata cells over zona glomerulosa cells.²⁹⁻³¹

It is unlikely that the differences in intensity of KCNJ5 immunostaining are due to diminished antibody binding to mutated KCNJ5 because the monoclonal antibody was raised against a peptide corresponding to an extracellular N-terminal sequence at positions 36-49 (ATDRTRLLAEGKKP), far removed from the KCNJ5 mutations which are located in or near the channel pore region. Further, KCNJ5 immunohistochemistry with a polyclonal antibody (binding to multiple epitopes) shows a similar reduction of KCNJ5 immunostaining compared with the adjacent cortex.²⁸

As reported in other studies,^{4,12} APAs with KCNJ5 mutations were larger than other APAs, and we show a positive correlation between nodule diameter of tumors with a KCNJ5-G151R or L168R mutation with cell proliferation. The proapoptotic effects of G151R and L168R and the relatively larger adenoma diameter of tumors carrying these mutations

suggests a selective pressure to override apoptosis in these tumors. KCNJ5-mutated APAs have distinct transcriptional profiles compared with other APAs³²⁻³⁴ which may result in the expression of specific prosurvival factors to counteract the proapoptotic effects of KCNJ5-G151R and L168R.³⁵⁻³⁷ Conversely, in NMD-APAs, a decreased Ki67 index was noted with increasing tumor diameter such that NMD-APAs with large tumor diameters displayed relatively lower Ki67 indices. This is probably due to a decline in proliferation rate during the lifespan of the tumor, as described previously for sporadic parathyroid adenomas,³⁸ and potentially explained by the activation of anti-proliferation and proapoptotic mechanisms to self-regulate tumor growth.

KCNJ5 potassium channel mutations associated with PA display a loss of selectivity for potassium ions and aberrant sodium ion conductance.^{2,5} This disturbance in channel conductance appears less severe in with KCNJ5-T158A because human embryonic kidney cells expressing this mutant display an increased permeability ratio for potassium relative to sodium ions compared with cells expressing G151R or L168R.² Transduction of human adrenocortical cells with a lentivirus carrying the cDNA encoding the KCNJ5-T158A channel resulted in a decrease in cell proliferation compared with control cells.⁵ Our data with the higher level of transcriptional induction of KCNJ5 concord with the observations of Oki et al,⁵ but we did observe an increase in cell proliferation when

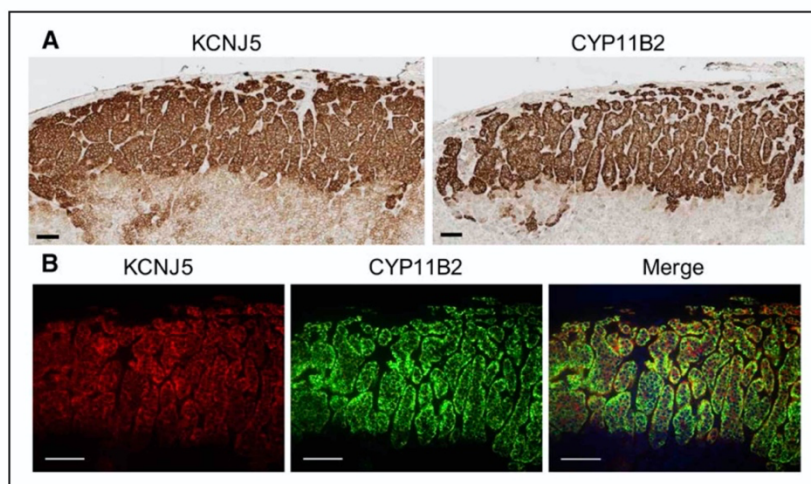


Figure 6. KCNJ5 and CYP11B2 immunostaining of aldosterone-producing cell clusters. Immunohistochemistry (A) and double immunofluorescence (B) showed intense KCNJ5 staining in aldosterone-producing cell clusters and colocalization with CYP11B2. DAPI (blue) was only included in the merged image. Scale bar = 100 μ m. CYP11B2 indicates aldosterone synthase; and KCNJ5, G-protein-coupled inwardly rectifying potassium channel.

the level of induction of *KCNJ5-T158A* gene expression was decreased.

Germline variants of *KCNJ5* cause a familial form of PA called FH type III (familial hyperaldosteronism type III).³⁹ Patients with germline *KCNJ5-T158A* or *G151R* mutations present with a severe form of PA with extensive adrenocortical hyperplasia requiring bilateral adrenalectomy.^{2,16,40} Patients with FH type III with a *KCNJ5-G151E* mutation display a relatively mild, medically-treatable clinical phenotype with apparently normal adrenals from computerized tomography scan results.⁴¹ Patch-clamp electrophysiology of human embryonic kidney 293T cells transfected with *KCNJ5-G151E* and *G151R*, demonstrated the increased sodium ion conductance of the *G151E* mutated channel and cell survival assays established the greater cell lethality induced by *G151E* relative to *G151R*.⁴¹ Our study supports this suggestion because *KCNJ5-G151E*, but not *G151R*, caused a highly significant reduction in the viability of human adrenocortical cells. The increased cell toxicity associated with *KCNJ5-G151E* was inferred to limit adrenocortical cell mass and account for the milder phenotype of carriers of this germline variant⁴¹ probably because only a subset of cells expressing low-levels of the mutated channel can survive and produce excess aldosterone.

Strengths and Limitations of the Study

The strength of our study is the production of stable human adrenocortical cell lines with inducible expression of *KCNJ5* mutations to study the cell growth effects of sporadic and germline *KCNJ5* mutations. A further strength is the analysis of the proliferative status of a large cohort of APAs with genotype data that were homogeneously selected for surgery according to a stringent diagnostic flow chart that included adrenal venous sampling. Finally, we used highly specific monoclonal antibodies to demonstrate by immunohistochemistry and double immunofluorescence the variance in *KCNJ5* and *CYP11B2* expression in APAs according to genotype. A limitation of our study is that genotyping was performed on dissected pieces of adrenal nodule rather than targeted to *CYP11B2* expressing regions. However, we minimized the potential genotyping of a nonfunctional nodule because we performed *CYP11B2* immunohistochemistry of all adrenals included in the study and those with nonfunctional nodules were excluded.

Perspectives

KCNJ5 mutations cause cell lethality to a variable degree according to genotype and expression level. The proliferative function of *KCNJ5* mutations in vivo is challenging to reproduce in vitro because any long-term chronic effects of potential survival factors are difficult to replicate in adrenal cell cultures. Transcriptome studies are planned to identify genes and signaling pathways which enable cell proliferation of adenomas with *KCNJ5* mutations, despite the increased cell lethality caused by their expression, and which limit growth rates of tumors with NMD.

Sources of Funding

This work was supported by the European Research Council under the European Union's Horizon 2020 research and innovation program

(grant agreement No [694913] to M Reincke) and by the Deutsche Forschungsgemeinschaft (DFG, German Research Foundation) Projektnummer: 314061271-TRR 205 to F Beuschlein, M Reincke, and TA Williams; and by DFG grant RE 752/20-1 to M Reincke. This work was also supported by the Else Kröner-Fresenius Stiftung in support of the German Conns Registry-Else-Kröner Hyperaldosteronism Registry (2013_A182 and 2015_A171 to M Reincke). CE Gomez-Sanchez is supported by National Heart, Lung and Blood Institute grant R01 HL27255, the National Institute of General Medical Sciences grant U54 GM115428. Y. Yang is supported by a fellowship from the China Scholarship Council.

Disclosures

None.

References

1. Young WF Jr. Diagnosis and treatment of primary aldosteronism: practical clinical perspectives. *J Intern Med.* 2019;285:126–148. doi: 10.1111/joim.12831
2. Choi M, Scholl UL, Yue P, et al. K+ channel mutations in adrenal aldosterone-producing adenomas and hereditary hypertension. *Science.* 2011;331:768–772. doi: 10.1126/science.1198785
3. Boulkroun S, Beuschlein F, Rossi GP, et al. Prevalence, clinical, and molecular correlates of *KCNJ5* mutations in primary aldosteronism. *Hypertension.* 2012;59:592–598. doi: 10.1161/HYPERTENSIONAHA.111.186478
4. Åkerström T, Crona J, Delgado Verdugo A, et al. Comprehensive resequencing of adrenal aldosterone producing lesions reveal three somatic mutations near the *KCNJ5* potassium channel selectivity filter. *PLoS One.* 2012;7:e41926. doi: 10.1371/journal.pone.0041926
5. Oki K, Plonczynski MW, Luis Lam M, Gomez-Sanchez EP, Gomez-Sanchez CE. Potassium channel mutant *KCNJ5 T158A* expression in HAC-15 cells increases aldosterone synthesis. *Endocrinology.* 2012;153:1774–1782. doi: 10.1210/en.2011-1733.
6. Prada ETA, Burrello J, Reincke M, Williams TA. Old and new concepts in the molecular pathogenesis of primary aldosteronism. *Hypertension.* 2017;70:875–881. doi: 10.1161/HYPERTENSIONAHA.117.10111
7. Perez-Rivas LG, Williams TA, Reincke M. Inherited forms of primary hyperaldosteronism: new genes, new phenotypes and proposition of a new classification. *Exp Clin Endocrinol Diabetes.* 2019;127:93–99. doi: 10.1055/a-0713-0629
8. Nanba K, Omata K, Else T, Beck PCC, Nanba AT, Turcu AF, Miller BS, Giordano TJ, Tomlins SA, Rainey WE. Targeted molecular characterization of aldosterone-producing adenomas in white Americans. *J Clin Endocrinol Metab.* 2018;103:3869–3876. doi: 10.1210/jc.2018-01004
9. Williams TA, Monticone S, Schack VR, et al. Somatic *ATP1A1*, *ATP2B3*, and *KCNJ5* mutations in aldosterone-producing adenomas. *Hypertension.* 2014;63:188–195. doi: 10.1161/HYPERTENSIONAHA.113.01733
10. Fernandes-Rosa FL, Williams TA, Riestler A, et al. Genetic spectrum and clinical correlates of somatic mutations in aldosterone-producing adenoma. *Hypertension.* 2014;64:354–361. doi: 10.1161/HYPERTENSIONAHA.114.03419
11. Zheng FF, Zhu LM, Nie AF, Li XY, Lin JR, Zhang K, Chen J, Zhou WL, Shen ZJ, Zhu YC, Wang JG, Zhu DL, Gao PJ. Clinical characteristics of somatic mutations in Chinese patients with aldosterone-producing adenoma. *Hypertension.* 2015;65:622–628. doi: 10.1161/HYPERTENSIONAHA.114.03346
12. Lenzini L, Rossitto G, Maiolino G, Letizia C, Funder JW, Rossi GP. A meta-analysis of somatic *KCNJ5* K(+) channel mutations in 1636 patients with an aldosterone-producing adenoma. *J Clin Endocrinol Metab.* 2015;100:E1089–E1095. doi: 10.1210/jc.2015-2149
13. Berridge MJ. Calcium signalling and cell proliferation. *Bioessays.* 1995;17:491–500. doi: 10.1002/bies.950170605
14. Miller WL, Auchus RJ. The molecular biology, biochemistry, and physiology of human steroidogenesis and its disorders. *Endocr Rev.* 2011;32:81–151. doi: 10.1210/er.2010-0013
15. Mulatero P, Tauber P, Zennaro MC, et al. *KCNJ5* mutations in European families with nonglucocorticoid remediable familial hyperaldosteronism. *Hypertension.* 2012;59:235–240. doi: 10.1161/HYPERTENSIONAHA.111.183996
16. Geller DS, Zhang J, Wisgerhof MV, Shackleton C, Kashgarian M, Lifton RP. A novel form of human mendelian hypertension featuring nonglucocorticoid-remediable aldosteronism. *J Clin Endocrinol Metab.* 2008;93:3117–3123. doi: 10.1210/jc.2008-0594

17. Nishimoto K, Tomlins SA, Kuick R, Cani AK, Giordano TJ, Hovelson DH, Liu CJ, Sanjanwala AR, Edwards MA, Gomez-Sanchez CE, Nanba K, Rainey WE. Aldosterone-stimulating somatic gene mutations are common in normal adrenal glands. *Proc Natl Acad Sci U S A*. 2015;112:E4591–E4599. doi: 10.1073/pnas.1505529112
18. Yamazaki Y, Nakamura Y, Omata K, Ise K, Tezuka Y, Ono Y, Morimoto R, Nozawa Y, Gomez-Sanchez CE, Tomlins SA, Rainey WE, Ito S, Satoh F, Sasano H. Histopathological classification of cross-sectional image-negative hyperaldosteronism. *J Clin Endocrinol Metab*. 2017;102:1182–1192. doi: 10.1210/jc.2016-2986
19. Funder JW, Carey RM, Mantero F, Murad MH, Reincke M, Shibata H, Stowasser M, Young WF Jr. The management of primary aldosteronism: case detection, diagnosis, and treatment: an endocrine society clinical practice guideline. *J Clin Endocrinol Metab*. 2016;101:1889–1916. doi: 10.1210/jc.2015-4061
20. Williams TA, Reincke M. Management of endocrine disease: diagnosis and management of primary aldosteronism: the endocrine society guideline 2016 revisited. *Eur J Endocrinol*. 2018;179:R19–R29. doi: 10.1530/EJE-17-0990.
21. Yang Y, Burrello J, Burrello A, Eisenhofer G, Peitzsch M, Tetti M, Knösel T, Beuschlein F, Lenders JWM, Mulatero P, Reincke M, Williams TA. Classification of microadenomas in patients with primary aldosteronism by steroid profiling. *J Steroid Biochem Mol Biol*. 2019;189:274–282. doi: 10.1016/j.jsbmb.2019.01.008
22. Bello-Reuss E, Ernest S, Holland OB, Hellmich MR. Role of multidrug resistance P-glycoprotein in the secretion of aldosterone by human adrenal NCI-H295 cells. *Am J Physiol Cell Physiol*. 2000;278:C1256–C1265. doi: 10.1152/ajpcell.2000.278.6.C1256
23. Scholl UI, Abriola L, Zhang C, Reimer EN, Plummer M, Kazmierczak BI, Zhang J, Hoyer D, Merkel JS, Wang W, Lifton RP. Macrolides selectively inhibit mutant KCNJ5 potassium channels that cause aldosterone-producing adenoma. *J Clin Invest*. 2017;127:2739–2750. doi: 10.1172/JCI91733
24. Davis JM. A single-step technique for selecting and cloning hybridomas for monoclonal antibody production. *Methods Enzymol*. 1986;121:307–322. doi: 10.1016/0076-6879(86)21029-0
25. Gomez-Sanchez CE, Qi X, Velarde-Miranda C, Plonczynski MW, Parker CR, Rainey W, Satoh F, Maekawa T, Nakamura Y, Sasano H, Gomez-Sanchez EP. Development of monoclonal antibodies against human CYP11B1 and CYP11B2. *Mol Cell Endocrinol*. 2014;383:111–117. doi: 10.1016/j.mce.2013.11.022
26. Tan GC, Negro G, Pinggera A, et al. Aldosterone-producing adenomas: histopathology-genotype correlation and identification of a novel CACNA1D mutation. *Hypertension*. 2017;70:129–136. doi: 10.1161/HYPERTENSIONAHA.117.09057
27. Fernandes-Rosa FL, Amar L, Tissier F, Bertherat J, Meatchi T, Zennaro MC, Boulkroun S. Functional histopathological markers of aldosterone producing adenoma and somatic KCNJ5 mutations. *Mol Cell Endocrinol*. 2015;408:220–226. doi: 10.1016/j.mce.2015.01.020
28. Boulkroun S, Golib Dzib JF, Samson-Couterie B, Rosa FL, Rickard AJ, Meatchi T, Amar L, Benecke A, Zennaro MC. KCNJ5 mutations in aldosterone producing adenoma and relationship with adrenal cortex remodeling. *Mol Cell Endocrinol*. 2013;371:221–227. doi: 10.1016/j.mce.2013.01.018
29. Azizan EA, Poulsen H, Tuluc P, et al. Somatic mutations in ATP1A1 and CACNA1D underlie a common subtype of adrenal hypertension. *Nat Genet*. 2013;45:1055–1060. doi: 10.1038/ng.2716
30. Dekkers T, ter Meer M, Lenders JW, Hermus AR, Schultze Kool L, Langenhuijsen JF, Nishimoto K, Ogishima T, Mukai K, Azizan EA, Tops B, Deinum J, Küsters B. Adrenal nodularity and somatic mutations in primary aldosteronism: one node is the culprit? *J Clin Endocrinol Metab*. 2014;99:E1341–E1351. doi: 10.1210/jc.2013-4255
31. Monticone S, Castellano I, Versace K, Lucatello B, Veglio F, Gomez-Sanchez CE, Williams TA, Mulatero P. Immunohistochemical, genetic and clinical characterization of sporadic aldosterone-producing adenomas. *Mol Cell Endocrinol*. 2015;411:146–154. doi: 10.1016/j.mce.2015.04.022
32. Azizan EA, Lam BY, Newhouse SJ, Zhou J, Kuc RE, Clarke J, Happerfield L, Marker A, Hoffman GJ, Brown MJ. Microarray, qPCR, and KCNJ5 sequencing of aldosterone-producing adenomas reveal differences in genotype and phenotype between zona glomerulosa- and zona fasciculata-like tumors. *J Clin Endocrinol Metab*. 2012;97:E819–E829. doi: 10.1210/jc.2011-2965
33. Åkerström T, Willenberg HS, Cupisti K, et al. Novel somatic mutations and distinct molecular signature in aldosterone-producing adenomas. *Endocr Relat Cancer*. 2015;22:735–744. doi: 10.1530/ERC-15-0321
34. Backman S, Åkerström T, Maharjan R, Cupisti K, Willenberg HS, Hellman P, Björklund P. RNA sequencing provides novel insights into the transcriptome of aldosterone producing adenomas. *Sci Rep*. 2019;9:6269. doi: 10.1038/s41598-019-41525-2
35. Williams TA, Monticone S, Morello F, Liew CC, Mengozzi G, Pilon C, Asioli S, Sapino A, Veglio F, Mulatero P. Teratocarcinoma-derived growth factor-1 is upregulated in aldosterone-producing adenomas and increases aldosterone secretion and inhibits apoptosis *in vitro*. *Hypertension*. 2010;55:1468–1475. doi: 10.1161/HYPERTENSIONAHA.110.150318
36. Williams TA, Monticone S, Crudo V, Warth R, Veglio F, Mulatero P. Visinin-like 1 is upregulated in aldosterone-producing adenomas with KCNJ5 mutations and protects from calcium-induced apoptosis. *Hypertension*. 2012;59:833–839. doi: 10.1161/HYPERTENSIONAHA.111.188532
37. Shaikh LH, Zhou J, Teo AE, Garg S, Neogi SG, Figg N, Yeo GS, Yu H, Maguire JJ, Zhao W, Bennett MR, Azizan EA, Davenport AP, McKenzie G, Brown MJ. LGR5 activates noncanonical Wnt signaling and inhibits aldosterone production in the human adrenal. *J Clin Endocrinol Metab*. 2015;100:E836–E844. doi: 10.1210/jc.2015-1734
38. Parfitt AM, Braunstein GD, Katz A. Radiation-associated hyperparathyroidism: comparison of adenoma growth rates, inferred from weight and duration of latency, with prevalence of mitosis. *J Clin Endocrinol Metab*. 1993;77:1318–1322. doi: 10.1210/jcem.77.5.8077327
39. Monticone S, Tetti M, Burrello J, Buffolo F, De Giovanni R, Veglio F, Williams TA, Mulatero P. Familial hyperaldosteronism type III. *J Hum Hypertens*. 2017;31:776–781. doi: 10.1038/jhh.2017.34
40. Therien B, Mellinger RC, Caldwell JR, Howard PJ. Primary aldosteronism due to adrenal hyperplasia; occurrence in a boy aged 10 years. *AMA J Dis Child*. 1959;98:90–99.
41. Scholl UI, Nelson-Williams C, Yue P, Grekin R, Wyatt RJ, Dillon MJ, Couch R, Hammer LK, Harley FL, Farhi A, Wang WH, Lifton RP. Hypertension with or without adrenal hyperplasia due to different inherited mutations in the potassium channel KCNJ5. *Proc Natl Acad Sci U S A*. 2012;109:2533–2538. doi: 10.1073/pnas.1121407109

Novelty and Significance

What Is New?

- Ki67 proliferation index is positively correlated with adenoma diameter in KCNJ5-mutated aldosterone-producing adenomas, a negative correlation was noted in tumors with no mutation detected.
- Adrenocortical cell expression of the sporadic and germline KCNJ5-T158A mutation caused cell proliferation at low induction of expression, other KCNJ5 mutations induced apoptosis.
- The zona glomerulosa layer and aldosterone-producing cell clusters adjacent to adenomas show intense KCNJ5 immunostaining.
- KCNJ5-mutated adenomas comprise CYP11B2-positive cells with a marked reduction of KCNJ5 immunostaining compared with CYP11B2-negative cells and aldosterone-producing adenomas of other genotype.

What Is Relevant?

- KCNJ5 mutations in aldosterone-producing adenomas are associated with increased adrenal cell proliferation.
- KCNJ5 mutations may be absent from aldosterone-producing cell clusters due to the high-level of KCNJ5 expression in the zona glomerulosa.

Summary

KCNJ5 mutations induce cell toxicity and their effects on adrenocortical cell growth are determined in part by the expression level of the mutated KCNJ5 potassium channel.

**PRIMARY ALDOSTERONISM: KCNJ5 MUTATIONS AND ADRENOCORTICAL
CELL GROWTH**

Yuhong Yang,¹ Celso E. Gomez-Sanchez,² Diana Jaquin,¹ Elke Tatjana Aristizabal Prada,¹
Lucie S. Meyer,¹ Thomas Knösel,³ Holger Schneider,¹ Felix Beuschlein,^{1,4}
Martin Reincke,¹ Tracy Ann Williams^{1,5}

¹Medizinische Klinik und Poliklinik IV, Klinikum der Universität München, LMU München, Germany

²Endocrine Division, G.V. (Sonny) Montgomery VA Medical Center, University of Mississippi Medical Center, Jackson, MS, USA

³Institute of Pathology, Ludwig-Maximilians-Universität München, Germany

⁴Klinik für Endokrinologie, Diabetologie und Klinische Ernährung, Universitätsspital Zürich, Zürich, Switzerland

⁵Division of Internal Medicine and Hypertension, Department of Medical Sciences, University of Turin, Turin, Italy

Corresponding author:

Tracy Ann Williams
Medizinische Klinik und Poliklinik IV
Klinikum der Universität München
LMU München
Ziemssenstr. 1
D-80336 München
Germany

Tel: +49 89 4400 52941

Fax: +49 89 4400 54428

Email: Tracy.Williams@med.uni-muenchen.de

Key words: aldosterone-producing adenoma, adrenal gland, primary aldosteronism, KCNJ5, growth and apoptosis

Running title: KCNJ5 mutations, growth and apoptosis in primary aldosteronism

BASELINE PARAMETERS	N	APA genotype				Pairwise comparison			
		Total (n=72)	KCNJ5 (n=39)	NMD (n=23)	Other (n=10)	Overall P value	KCNJ5 vs NMD	KCNJ5 vs Other	NMD vs Other
Age (years)	72	51.1 ± 11.4	47.2 ± 10.4	57.7 ± 11.0	51.1 ± 10.4	0.002	0.001	0.907	0.319
Sex (Women)	40	40 (55.5%)	32 (82.1%)	7 (30.4%)	1 (10.0%)	<0.001	<0.001	<0.001	0.382
BMI (kg/m ²)	72	27.0 ± 4.8	26.2 ± 4.8	27.4 ± 5.2	28.9 ± 3.1	0.238	NA	NA	NA
Known duration of hypertension (months)	72	120 [49-180]	104 [47-180]	125 [72-192]	107 [33-236]	0.568	NA	NA	NA
Aldosterone (pmol/L)	72	1158 [665-2201]	979 [500-1470]	1331 [754-2913]	1989 [1624-3346]	0.005	0.204	0.006	0.325
DRC (mU/L)	72	3.6 [2.1-9.9]	3.2 [2.0-9.3]	4.3 [2.4-8.3]	8.8 [3.4-21.1]	0.150	NA	NA	NA
ARR_DRC	72	254 [132-546]	247 [115-487]	259 [172-659]	361 [82-664]	0.551	NA	NA	NA
Lowest serum K ⁺ (mmol/L)	72	3.1 ± 0.5	3.0 ± 0.5	3.3 ± 0.5	2.9 ± 0.3	0.102	NA	NA	NA
Systolic BP (mmHg)	72	150.0 ± 17.2	149.4 ± 16.8	152.3 ± 17.9	147.1 ± 18.1	0.688	NA	NA	NA
Diastolic BP (mmHg)	72	94.0 ± 11.4	94.2 ± 10.8	93.4 ± 11.9	95.0 ± 13.5	0.936	NA	NA	NA
Antihypertensive medication (DDD)	71	2.0 [1.3-3.7]	2.0 [1.3-3.7]	2.0 [0.9-3.0]	3.3 [1.4-7.4]	0.200	NA	NA	NA
Largest nodule diameter at pathology (mm)	72	15.0 [10.0-21.3]	17.0 [14.0-24.0]	12.0 [8.0-25.0]	9.0 [7.8-15.3]	0.001	0.019	0.003	0.662

Table S1. Clinical characteristics of patients with PA according to APA genotype

Quantitative normally distributed variables are expressed as means ± SD and quantitative non-normally distributed variables are reported as medians [IQR]. Categorical variables are presented as absolute numbers and percentages. *P* values are calculated using Chi-square and Fisher's exact tests or ANOVA followed by Bonferroni tests or Kruskal-Wallis tests with pairwise comparisons as appropriate. APA, aldosterone-producing adenoma; ARR, aldosterone-to-renin ratio; BMI, body mass index; BP, blood pressure; DDD, defined daily dose; DRC, direct renin concentration; K⁺, potassium ions; N, number; NA, not applicable; NMD, no mutation detected. *NMD indicates absence of somatic APA mutations in *KCNJ5*, *CACNA1D*, *ATP1A1* and *ATP2B3*; "Other" indicates APA mutations in *CACNA1D*, *ATP1A1* or *ATP2B3*. The defined daily dose is the assumed average maintenance dose per day for a drug used for its main indication in adults according to ATC/DDD Index 2018 https://www.whocc.no/atc_ddd_index/

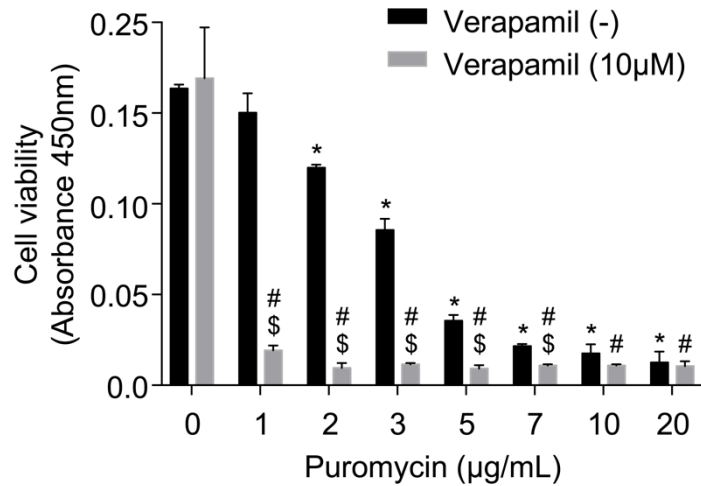


Figure S1: Cell viability of HAC15 cell in response to treatment with puromycin and verapamil.

A dose-response of cell viability to increasing concentrations of puromycin was measured after

96 h with a WST-1 assay. HAC15 cells were markedly more responsive to puromycin in the presence of verapamil (10 µM) which was used to inhibit the P glycoprotein. Bars indicate the mean of 3 separate experiments, error bars represent SD. *P* values were calculated using ANOVA with a post hoc Bonferroni test. *Difference ($P < 0.05$) versus absence of puromycin and verapamil; #Difference ($P < 0.05$) versus absence of puromycin and presence of verapamil (10 µM); \$Difference ($P < 0.05$) absence versus presence verapamil (10 µM) at indicated concentration of puromycin.

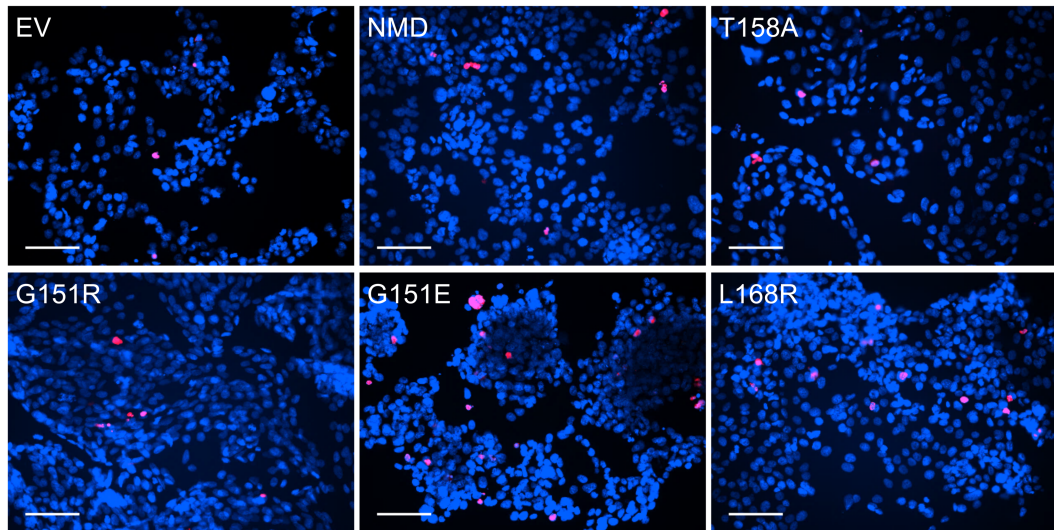


Figure S2: Apoptosis in HAC15 cell lines expressing different *KCNJ5* mutants

HAC15 cell lines stably expressing wild type or *KCNJ5* mutants or empty vector were incubated with cumate (10 $\mu\text{g}/\text{mL}$) for 12 hours and cell nuclei with cleaved PARP immunostaining (red) were visualized by immunofluorescence. Scale bar = 100 μm . EV, empty vector; NMD, no mutation detected.

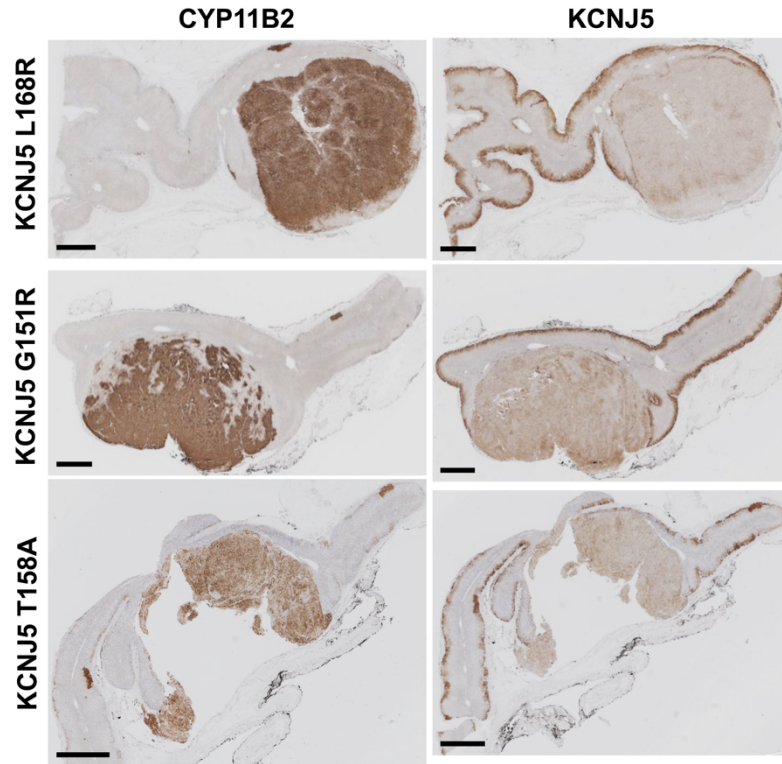


Figure S3: CYP11B2 and KCNJ5 immunohistochemistry in APAs with different *KCNJ5* mutations

KCNJ5 showed similarly low expression in adenomas harboring KCNJ5-L168R (upper panel), KCNJ5-G151R (middle panel), and KCNJ5-T158A (lower panel) mutations. Scale bar = 2 mm.

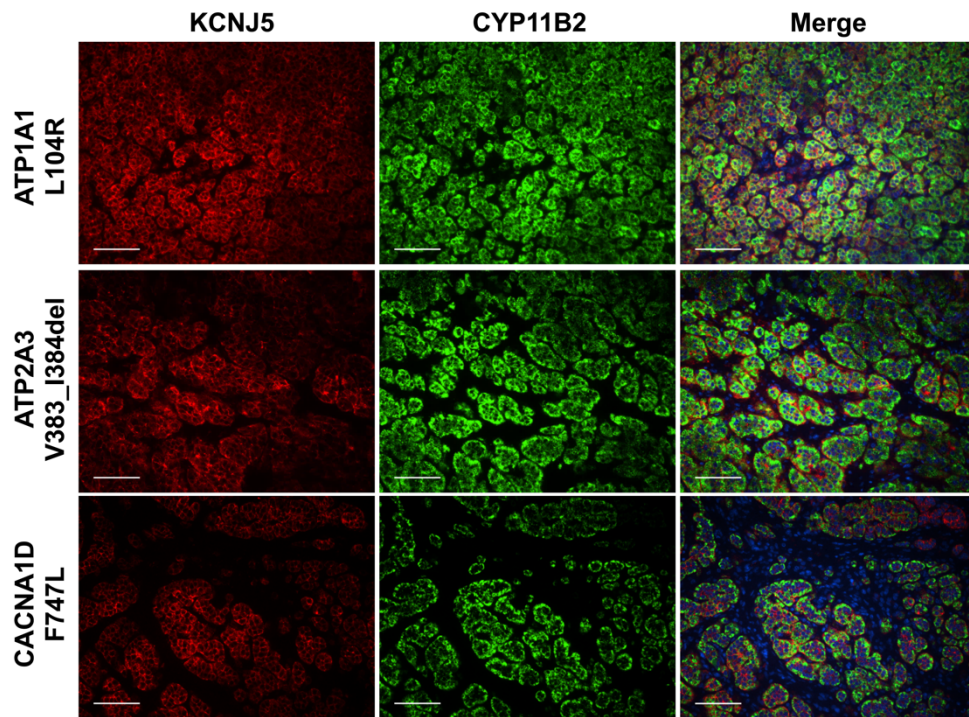


Figure S4: Double KCNJ5-CYP11B2 immunofluorescence of APAs with *ATP1A1*, *ATP2B3*, or *CACNA1D* mutations

KCNJ5 and CYP11B2 were co-localized in adenomas with *ATP1A1* (upper panel), *ATP2B3* (middle panel), or *CACNA1D* mutations (lower panel). Scale bar = 100 μ m.

10. References

1. Arnold J. Ein Beitrag zu der feineren Structur und dem Chemismus der Nebennieren. *Virchows Archiv*. 1866;35:64-107.
2. Vinson GP. Functional zonation of the adult mammalian adrenal cortex. *Front Neurosci*. 2016;10:238.
3. Hattangady NG, Olala LO, Bollag WB, Rainey WE. Acute and chronic regulation of aldosterone production. *Mol Cell Endocrinol*. 2012;350:151-62.
4. Mornet E, Dupont J, Vitek A, White PC. Characterization of two genes encoding human steroid 11 beta-hydroxylase (P-450(11) beta). *J Biol Chem*. 1989;264:20961-7.
5. Schiffer L, Anderko S, Hannemann F, Eiden-Plach A, Bernhardt R. The CYP11B subfamily. *J Steroid Biochem Mol Biol*. 2015;151:38-51.
6. Enberg U, Volpe C, Höög A, Wedell A, Farnebo L, Thorén M, Hamberger B. Postoperative differentiation between unilateral adrenal adenoma and bilateral adrenal hyperplasia in primary aldosteronism by mRNA expression of the gene CYP11B2. *Eur J Endocrinol*. 2004;151:73-85.
7. Gomez-Sanchez CE, Qi X, Velarde-Miranda C, Plonczynski MW, Parker CR, Rainey W, Satoh F, Maekawa T, Nakamura Y, Sasano H, Gomez-Sanchez EP. Development of monoclonal antibodies against human CYP11B1 and CYP11B2. *Mol Cell Endocrinol*. 2014;383:111-7.
8. Nanba K, Vaidya A, Williams GH, Zheng I, Else T, Rainey WE. Age-related autonomous aldosteronism. *Circulation*. 2017;136:347-55.
9. Nishimoto K, Nakagawa K, Li D, Kosaka T, Oya M, Mikami S, Shibata H, Itoh H, Mitani F, Yamazaki T, Ogishima T, Suematsu M, Mukai K. Adrenocortical zonation in humans under normal and pathological conditions. *J Clin Endocrinol Metab*. 2010;95:2296-305.
10. Williams TA, Gomez-Sanchez CE, Rainey WE, Giordano TJ, Lam AK, Marker A, Mete O, Yamazaki Y, Zerbini MCN, Beuschlein F, Satoh F, Burrello J, Schneider H, Lenders JWM, Mulatero P, Castellano I, Knösel T, Papotti M, Saeger W, Sasano H, Reincke M. International histopathology consensus for unilateral primary aldosteronism. *J Clin Endocrinol Metab*. 2021;106:42-54.
11. Conn JW. Primary aldosteronism. *J Lab Clin Med*. 1955;45:661-4.
12. Mulatero P, Stowasser M, Loh KC, Fardella CE, Gordon RD, Mosso L, Gomez-Sanchez CE, Veglio F, Young WF, Jr. Increased diagnosis of primary aldosteronism, including surgically correctable forms, in centers from five continents. *J Clin Endocrinol Metab*. 2004;89:1045-50.
13. Käyser SC, Dekkers T, Groenewoud HJ, van der Wilt GJ, Carel Bakx J, van der Wel MC, Hermus AR, Lenders JW, Deinum J. Study heterogeneity and estimation of prevalence of primary aldosteronism: a systematic review and meta-regression analysis. *J Clin Endocrinol Metab*. 2016;101:2826-35.
14. Yang Y, Reincke M, Williams TA. Prevalence, diagnosis and outcomes of treatment for primary aldosteronism. *Best Pract Res Clin Endocrinol Metab*. 2020;34:101365.
15. Monticone S, D'Ascenzo F, Moretti C, Williams TA, Veglio F, Gaita F, Mulatero P. Cardiovascular events and target organ damage in primary aldosteronism compared with essential hypertension: a systematic review and meta-analysis. *Lancet Diabetes Endocrinol*. 2018;6:41-50.

-
16. Young WF, Jr. Diagnosis and treatment of primary aldosteronism: practical clinical perspectives. *J Intern Med.* 2019;285:126-48.
 17. Funder JW, Carey RM, Mantero F, Murad MH, Reincke M, Shibata H, Stowasser M, Young WF, Jr. The management of primary aldosteronism: case detection, diagnosis, and treatment: an endocrine society clinical practice guideline. *J Clin Endocrinol Metab.* 2016;101:1889-916.
 18. Kempers MJ, Lenders JW, van Outheusden L, van der Wilt GJ, Schultze Kool LJ, Hermus AR, Deinum J. Systematic review: diagnostic procedures to differentiate unilateral from bilateral adrenal abnormality in primary aldosteronism. *Ann Intern Med.* 2009;151:329-37.
 19. Lim V, Guo Q, Grant CS, Thompson GB, Richards ML, Farley DR, Young WF, Jr. Accuracy of adrenal imaging and adrenal venous sampling in predicting surgical cure of primary aldosteronism. *J Clin Endocrinol Metab.* 2014;99:2712-9.
 20. Dekkers T, Prejbisz A, Kool LJS, Groenewoud H, Velema M, Spiering W, Kolodziejczyk-Kruk S, Arntz M, Kadziela J, Langenhuijsen JF, Kerstens MN, van den Meiracker AH, van den Born BJ, Sweep F, Hermus A, Januszewicz A, Ligthart-Naber AF, Makai P, van der Wilt GJ, Lenders JWM, Deinum J, SPARTACUS Investigators. Adrenal vein sampling versus CT scan to determine treatment in primary aldosteronism: an outcome-based randomised diagnostic trial. *Lancet Diabetes Endocrinol.* 2016;4:739-46.
 21. Williams TA, Burrello J, Sechi LA, Fardella CE, Matrozova J, Adolf C, Baudrand R, Bernardi S, Beuschlein F, Catena C, Dumas M, Fallo F, Giacchetti G, Heinrich DA, Saint-Hilary G, Jansen PM, Januszewicz A, Kocjan T, Nishikawa T, Quinkler M, Satoh F, Umakoshi H, Widimsky J, Jr., Hahner S, Douma S, Stowasser M, Mulatero P, Reincke M. Computed tomography and adrenal venous sampling in the diagnosis of unilateral primary aldosteronism. *Hypertension.* 2018;72:641-9.
 22. Rossi GP, Auchus RJ, Brown M, Lenders JW, Naruse M, Plouin PF, Satoh F, Young WF, Jr. An expert consensus statement on use of adrenal vein sampling for the subtyping of primary aldosteronism. *Hypertension.* 2014;63:151-60.
 23. Monticone S, Viola A, Rossato D, Veglio F, Reincke M, Gomez-Sanchez C, Mulatero P. Adrenal vein sampling in primary aldosteronism: towards a standardised protocol. *Lancet Diabetes Endocrinol.* 2015;3:296-303.
 24. Williams TA, Lenders JWM, Mulatero P, Burrello J, Rottenkolber M, Adolf C, Satoh F, Amar L, Quinkler M, Deinum J, Beuschlein F, Kitamoto KK, Pham U, Morimoto R, Umakoshi H, Prejbisz A, Kocjan T, Naruse M, Stowasser M, Nishikawa T, Young WF, Jr., Gomez-Sanchez CE, Funder JW, Reincke M, Primary Aldosteronism Surgery Outcome (PASO) investigators. Outcomes after adrenalectomy for unilateral primary aldosteronism: an international consensus on outcome measures and analysis of remission rates in an international cohort. *Lancet Diabetes Endocrinol.* 2017;5:689-99.
 25. Goupil R, Wolley M, Ahmed AH, Gordon RD, Stowasser M. Does concomitant autonomous adrenal cortisol overproduction have the potential to confound the interpretation of adrenal venous sampling in primary aldosteronism? *Clin Endocrinol (Oxf).* 2015;83:456-61.
 26. Raman PB, Sharma DC, Dorfman RI, Gabilove JL. Biosynthesis of C-18-oxygenated steroids by an aldosterone-secreting human adrenal tumor. Metabolism of [4-14C] progesterone, [1,2-3H]11-deoxycorticosterone, and [4-14C] pregnenolone. *Biochemistry.* 1965;4:1376-85.

-
27. Gordon RD, Hamlet SM, Tunny TJ, Gomez-Sanchez CE, Jayasinghe LS. Distinguishing aldosterone-producing adenoma from other forms of hyperaldosteronism and lateralizing the tumour pre-operatively. *Clin Exp Pharmacol Physiol*. 1986;13:325-8.
28. Ulick S, Chu MD. Hypersecretion of a new corticosteroid, 18-hydroxycortisol in two types of adrenocortical hypertension. *Clin Exp Hypertens A*. 1982;4:1771-7.
29. Mulatero P, di Cella SM, Monticone S, Schiavone D, Manzo M, Mengozzi G, Rabbia F, Terzolo M, Gomez-Sanchez EP, Gomez-Sanchez CE, Veglio F. 18-hydroxycorticosterone, 18-hydroxycortisol, and 18-oxocortisol in the diagnosis of primary aldosteronism and its subtypes. *J Clin Endocrinol Metab*. 2012;97:881-9.
30. Keevil BG. LC-MS/MS analysis of steroids in the clinical laboratory. *Clin Biochem*. 2016;49:989-97.
31. Vogeser M, Parhofer KG. Liquid chromatography tandem-mass spectrometry (LC-MS/MS)-technique and applications in endocrinology. *Exp Clin Endocrinol Diabetes*. 2007;115:559-70.
32. Peitzsch M, Dekkers T, Haase M, Sweep FC, Quack I, Antoch G, Siegert G, Lenders JW, Deinum J, Willenberg HS, Eisenhofer G. An LC-MS/MS method for steroid profiling during adrenal venous sampling for investigation of primary aldosteronism. *J Steroid Biochem Mol Biol*. 2015;145:75-84.
33. Eisenhofer G, Dekkers T, Peitzsch M, Dietz AS, Bidlingmaier M, Treitl M, Williams TA, Bornstein SR, Haase M, Rump LC, Willenberg HS, Beuschlein F, Deinum J, Lenders JW, Reincke M. Mass spectrometry-based adrenal and peripheral venous steroid profiling for subtyping primary aldosteronism. *Clin Chem*. 2016;62:514-24.
34. Turcu AF, Wannachalee T, Tsodikov A, Nanba AT, Ren J, Shields JJ, O'Day PJ, Giacherio D, Rainey WE, Auchus RJ. Comprehensive analysis of steroid biomarkers for guiding primary aldosteronism subtyping. *Hypertension*. 2020;75:183-92.
35. Satoh F, Morimoto R, Ono Y, Iwakura Y, Omata K, Kudo M, Takase K, Seiji K, Sasamoto H, Honma S, Okuyama M, Yamashita K, Gomez-Sanchez CE, Rainey WE, Arai Y, Sasano H, Nakamura Y, Ito S. Measurement of peripheral plasma 18-oxocortisol can discriminate unilateral adenoma from bilateral diseases in patients with primary aldosteronism. *Hypertension*. 2015;65:1096-102.
36. Hundemer GL, Curhan GC, Yozamp N, Wang M, Vaidya A. Cardiometabolic outcomes and mortality in medically treated primary aldosteronism: a retrospective cohort study. *Lancet Diabetes Endocrinol*. 2018;6:51-9.
37. Rossi GP, Maiolino G, Flego A, Belfiore A, Bernini G, Fabris B, Ferri C, Giacchetti G, Letizia C, Maccario M, Mallamaci F, Muiesan ML, Mannelli M, Negro A, Palumbo G, Parenti G, Rossi E, Mantero F, PAPY Study Investigators. Adrenalectomy lowers incident atrial fibrillation in primary aldosteronism patients at long term. *Hypertension*. 2018;71:585-91.
38. Lifton RP, Dluhy RG, Powers M, Rich GM, Gutkin M, Fallo F, Gill JR, Jr., Feld L, Ganguly A, Laidlaw JC, et al. Hereditary hypertension caused by chimaeric gene duplications and ectopic expression of aldosterone synthase. *Nat Genet*. 1992;2:66-74.
39. Lifton RP, Dluhy RG, Powers M, Rich GM, Cook S, Ulick S, Lalouel JM. A chimaeric 11 beta-hydroxylase/aldosterone synthase gene causes glucocorticoid-remediable aldosteronism and human hypertension. *Nature*. 1992;355:262-5.

-
40. Scholl UI, Stölting G, Schewe J, Thiel A, Tan H, Nelson-Williams C, Vichot AA, Jin SC, Loring E, Untiet V, Yoo T, Choi J, Xu S, Wu A, Kirchner M, Mertins P, Rump LC, Onder AM, Gamble C, McKenney D, Lash RW, Jones DP, Chune G, Gagliardi P, Choi M, Gordon R, Stowasser M, Fahlke C, Lifton RP. CLCN2 chloride channel mutations in familial hyperaldosteronism type II. *Nat Genet.* 2018;50:349-54.
41. Fernandes-Rosa FL, Daniil G, Orozco IJ, Göppner C, El Zein R, Jain V, Boulkroun S, Jeunemaitre X, Amar L, Lefebvre H, Schwarzmayr T, Strom TM, Jentsch TJ, Zennaro MC. A gain-of-function mutation in the CLCN2 chloride channel gene causes primary aldosteronism. *Nat Genet.* 2018;50:355-61.
42. Scholl UI, Nelson-Williams C, Yue P, Grekin R, Wyatt RJ, Dillon MJ, Couch R, Hammer LK, Harley FL, Farhi A, Wang WH, Lifton RP. Hypertension with or without adrenal hyperplasia due to different inherited mutations in the potassium channel KCNJ5. *Proc Natl Acad Sci U S A.* 2012;109:2533-8.
43. Scholl UI, Stölting G, Nelson-Williams C, Vichot AA, Choi M, Loring E, Prasad ML, Goh G, Carling T, Juhlin CC, Quack I, Rump LC, Thiel A, Lande M, Frazier BG, Rasoulpour M, Bowlin DL, Sethna CB, Trachtman H, Fahlke C, Lifton RP. Recurrent gain of function mutation in calcium channel CACNA1H causes early-onset hypertension with primary aldosteronism. *Elife.* 2015;4:e06315.
44. Scholl UI, Goh G, Stölting G, de Oliveira RC, Choi M, Overton JD, Fonseca AL, Korah R, Starker LF, Kunstman JW, Prasad ML, Hartung EA, Mauras N, Benson MR, Brady T, Shapiro JR, Loring E, Nelson-Williams C, Libutti SK, Mane S, Hellman P, Westin G, Åkerström G, Björklund P, Carling T, Fahlke C, Hidalgo P, Lifton RP. Somatic and germline CACNA1D calcium channel mutations in aldosterone-producing adenomas and primary aldosteronism. *Nat Genet.* 2013;45:1050-4.
45. Choi M, Scholl UI, Yue P, Björklund P, Zhao B, Nelson-Williams C, Ji W, Cho Y, Patel A, Men CJ, Lolis E, Wisgerhof MV, Geller DS, Mane S, Hellman P, Westin G, Åkerström G, Wang W, Carling T, Lifton RP. K⁺ channel mutations in adrenal aldosterone-producing adenomas and hereditary hypertension. *Science.* 2011;331:768-72.
46. Azizan EA, Poulsen H, Tuluc P, Zhou J, Clausen MV, Lieb A, Maniero C, Garg S, Bochukova EG, Zhao W, Shaikh LH, Brighton CA, Teo AE, Davenport AP, Dekkers T, Tops B, Küsters B, Ceral J, Yeo GS, Neogi SG, McFarlane I, Rosenfeld N, Marass F, Hadfield J, Margas W, Chaggar K, Solar M, Deinum J, Dolphin AC, Farooqi IS, Striessnig J, Nissen P, Brown MJ. Somatic mutations in ATP1A1 and CACNA1D underlie a common subtype of adrenal hypertension. *Nat Genet.* 2013;45:1055-60.
47. Nanba K, Blinder AR, Rege J, Hattangady NG, Else T, Liu CJ, Tomlins SA, Vats P, Kumar-Sinha C, Giordano TJ, Rainey WE. Somatic CACNA1H mutation as a cause of aldosterone-producing adenoma. *Hypertension.* 2020;75:645-9.
48. Dutta RK, Arnesen T, Heie A, Walz M, Alesina P, Söderkvist P, Gimm O. A somatic mutation in CLCN2 identified in a sporadic aldosterone-producing adenoma. *Eur J Endocrinol.* 2019;181:K37-K41.
49. Beuschlein F, Boulkroun S, Osswald A, Wieland T, Nielsen HN, Lichtenauer UD, Penton D, Schack VR, Amar L, Fischer E, Walther A, Tauber P, Schwarzmayr T, Diener S, Graf E, Allolio B, Samson-Couterie B, Benecke A, Quinkler M, Fallo F, Plouin PF, Mantero F, Meitinger T, Mulatero P, Jeunemaitre X, Warth R, Vilsen B, Zennaro MC, Strom TM, Reincke M. Somatic mutations in

-
- ATP1A1 and ATP2B3 lead to aldosterone-producing adenomas and secondary hypertension. *Nat Genet.* 2013;45:440-4, 4e1-2.
50. Oki K, Plonczynski MW, Luis Lam M, Gomez-Sanchez EP, Gomez-Sanchez CE. Potassium channel mutant KCNJ5 T158A expression in HAC-15 cells increases aldosterone synthesis. *Endocrinology.* 2012;153:1774-82.
51. Nanba K, Omata K, Else T, Beck PCC, Nanba AT, Turcu AF, Miller BS, Giordano TJ, Tomlins SA, Rainey WE. Targeted molecular characterization of aldosterone-producing adenomas in white Americans. *J Clin Endocrinol Metab.* 2018;103:3869-76.
52. Nanba K, Omata K, Gomez-Sanchez CE, Stratakis CA, Demidowich AP, Suzuki M, Thompson LDR, Cohen DL, Luther JM, Gellert L, Vaidya A, Barletta JA, Else T, Giordano TJ, Tomlins SA, Rainey WE. Genetic characteristics of aldosterone-producing adenomas in blacks. *Hypertension.* 2019;73:885-92.
53. De Sousa K, Boulkroun S, Baron S, Nanba K, Wack M, Rainey WE, Rocha A, Giscos-Douriez I, Meatchi T, Amar L, Travers S, Fernandes-Rosa FL, Zennaro MC. Genetic, cellular, and molecular heterogeneity in adrenals with aldosterone-producing adenoma. *Hypertension.* 2020;75:1034-44.
54. Nanba K, Yamazaki Y, Bick N, Onodera K, Tezuka Y, Omata K, Ono Y, Blinder AR, Tomlins SA, Rainey WE, Satoh F, Sasano H. Prevalence of somatic mutations in aldosterone-producing adenomas in Japanese patients. *J Clin Endocrinol Metab.* 2020;105:dga595.
55. Lenzini L, Rossitto G, Maiolino G, Letizia C, Funder JW, Rossi GP. A meta-analysis of somatic KCNJ5 K(+) channel mutations in 1636 patients with an aldosterone-producing adenoma. *J Clin Endocrinol Metab.* 2015;100:E1089-95.
56. Seidel E, Schewe J, Scholl UI. Genetic causes of primary aldosteronism. *Exp Mol Med.* 2019;51:1-12.
57. Williams TA, Monticone S, Schack VR, Stindl J, Burrello J, Buffolo F, Annaratone L, Castellano I, Beuschlein F, Reincke M, Lucatello B, Ronconi V, Fallo F, Bernini G, Maccario M, Giacchetti G, Veglio F, Warth R, Vilsen B, Mulatero P. Somatic ATP1A1, ATP2B3, and KCNJ5 mutations in aldosterone-producing adenomas. *Hypertension.* 2014;63:188-95.
58. Mulatero P, Tauber P, Zennaro MC, Monticone S, Lang K, Beuschlein F, Fischer E, Tizzani D, Pallauf A, Viola A, Amar L, Williams TA, Strom TM, Graf E, Bandulik S, Penton D, Plouin PF, Warth R, Allolio B, Jeunemaitre X, Veglio F, Reincke M. KCNJ5 mutations in European families with nonglucocorticoid remediable familial hyperaldosteronism. *Hypertension.* 2012;59:235-40.
59. Scholl UI, Abriola L, Zhang C, Reimer EN, Plummer M, Kazmierczak BI, Zhang J, Hoyer D, Merkel JS, Wang W, Lifton RP. Macrolides selectively inhibit mutant KCNJ5 potassium channels that cause aldosterone-producing adenoma. *J Clin Invest.* 2017;127:2739-50.
60. Caroccia B, Prisco S, Seccia TM, Piazza M, Maiolino G, Rossi GP. Macrolides blunt aldosterone biosynthesis: a proof-of-concept study in KCNJ5 mutated adenoma cells ex vivo. *Hypertension.* 2017;70:1238-42.
61. Fernandes-Rosa FL, Williams TA, Riester A, Steichen O, Beuschlein F, Boulkroun S, Strom TM, Monticone S, Amar L, Meatchi T, Mantero F, Cicala MV, Quinkler M, Fallo F, Allolio B, Bernini G, Maccario M, Giacchetti G, Jeunemaitre X, Mulatero P, Reincke M, Zennaro MC. Genetic spectrum and clinical correlates of somatic mutations in aldosterone-producing adenoma. *Hypertension.* 2014;64:354-61.

-
62. Scholl UI, Healy JM, Thiel A, Fonseca AL, Brown TC, Kunstman JW, Horne MJ, Dietrich D, Riemer J, Kücüköylü S, Reimer EN, Reis AC, Goh G, Kristiansen G, Mahajan A, Korah R, Lifton RP, Prasad ML, Carling T. Novel somatic mutations in primary hyperaldosteronism are related to the clinical, radiological and pathological phenotype. *Clin Endocrinol (Oxf)*. 2015;83:779-89.
63. Åkerström T, Maharjan R, Sven Willenberg H, Cupisti K, Ip J, Moser A, Stålberg P, Robinson B, Alexander Iwen K, Dralle H, Walz MK, Lehnert H, Sidhu S, Gomez-Sanchez C, Hellman P, Björklund P. Activating mutations in CTNNB1 in aldosterone producing adenomas. *Sci Rep*. 2016;6:19546.
64. Kim AC, Reuter AL, Zubair M, Else T, Serecky K, Bingham NC, Lavery GG, Parker KL, Hammer GD. Targeted disruption of beta-catenin in Sf1-expressing cells impairs development and maintenance of the adrenal cortex. *Development*. 2008;135:2593-602.
65. Pignatti E, Leng S, Yuchi Y, Borges KS, Guagliardo NA, Shah MS, Ruiz-Babot G, Kariywasam D, Taketo MM, Miao J, Barrett PQ, Carlone DL, Breault DT. Beta-catenin causes adrenal hyperplasia by blocking zonal transdifferentiation. *Cell Rep*. 2020;31:107524.
66. Berthon A, Drelon C, Ragazzon B, Boulkroun S, Tissier F, Amar L, Samson-Couterie B, Zenaro MC, Plouin PF, Skah S, Plateroti M, Lefèbvre H, Sahut-Barnola I, Batisse-Lignier M, Assié G, Lefrançois-Martinez AM, Bertherat J, Martinez A, Val P. WNT/ β -catenin signalling is activated in aldosterone-producing adenomas and controls aldosterone production. *Hum Mol Genet*. 2014;23:889-905.
67. Gordon RD, Klemm SA, Tunny TJ, Stowasser M. Primary aldosteronism: hypertension with a genetic basis. *Lancet*. 1992;340:159-61.
68. Nakamura Y, Kitada M, Satoh F, Maekawa T, Morimoto R, Yamazaki Y, Ise K, Gomez-Sanchez CE, Ito S, Arai Y, Dezawa M, Sasano H. Intratumoral heterogeneity of steroidogenesis in aldosterone-producing adenoma revealed by intensive double- and triple-immunostaining for CYP11B2/B1 and CYP17. *Mol Cell Endocrinol*. 2016;422:57-63.
69. Nakamura Y, Maekawa T, Felizola SJ, Satoh F, Qi X, Velarde-Miranda C, Plonczynski MW, Ise K, Kikuchi K, Rainey WE, Gomez-Sanchez EP, Gomez-Sanchez CE, Sasano H. Adrenal CYP11B1/2 expression in primary aldosteronism: immunohistochemical analysis using novel monoclonal antibodies. *Mol Cell Endocrinol*. 2014;392:73-9.
70. Yamazaki Y, Omata K, Tezuka Y, Ono Y, Morimoto R, Adachi Y, Ise K, Nakamura Y, Gomez-Sanchez CE, Shibahara Y, Kitamoto T, Nishikawa T, Ito S, Satoh F, Sasano H. Tumor cell subtypes based on the intracellular hormonal activity in KCNJ5-mutated aldosterone-producing adenoma. *Hypertension*. 2018;72:632-40.
71. Tan GC, Negro G, Pinggera A, Tizen Laim NMS, Mohamed Rose I, Ceral J, Ryska A, Chin LK, Kamaruddin NA, Mohd Mokhtar N, AR AJ, Sukor N, Solar M, Striessnig J, Brown MJ, Azizan EA. Aldosterone-producing adenomas: histopathology-genotype correlation and identification of a novel CACNA1D mutation. *Hypertension*. 2017;70:129-36.
72. Inoue K, Yamazaki Y, Kitamoto T, Hirose R, Saito J, Omura M, Sasano H, Nishikawa T. Aldosterone suppression by dexamethasone in patients with KCNJ5-mutated aldosterone-producing adenoma. *J Clin Endocrinol Metab*. 2018;103:3477-85.
73. Williams TA, Peitzsch M, Dietz AS, Dekkers T, Bidlingmaier M, Riester A, Treitl M, Rhayem Y, Beuschlein F, Lenders JW, Deinum J, Eisenhofer G, Reincke M. Genotype-specific steroid profiles associated with aldosterone-producing adenomas. *Hypertension*. 2016;67:139-45.

-
74. Meyer LS, Wang X, Sušnik E, Burrello J, Burrello A, Castellano I, Eisenhofer G, Fallo F, Kline GA, Knosel T, Kocjan T, Lenders JWM, Mulatero P, Naruse M, Nishikawa T, Peitzsch M, Rump LC, Beuschlein F, Hahner S, Gomez-Sanchez CE, Reincke M, Williams TA. Immunohistopathology and steroid profiles associated with biochemical outcomes after adrenalectomy for unilateral primary aldosteronism. *Hypertension*. 2018;72:650-7.
75. Nishimoto K, Tomlins SA, Kuick R, Cani AK, Giordano TJ, Hovelson DH, Liu CJ, Sanjanwala AR, Edwards MA, Gomez-Sanchez CE, Nanba K, Rainey WE. Aldosterone-stimulating somatic gene mutations are common in normal adrenal glands. *Proc Natl Acad Sci U S A*. 2015;112:E4591-9.
76. Nishimoto K, Seki T, Kurihara I, Yokota K, Omura M, Nishikawa T, Shibata H, Kosaka T, Oya M, Suematsu M, Mukai K. Case report: nodule development from subcapsular aldosterone-producing cell clusters causes hyperaldosteronism. *J Clin Endocrinol Metab*. 2016;101:6-9.
77. Vouillarmet J, Fernandes-Rosa F, Graeppi-Dulac J, Lantelme P, Decaussin-Petrucci M, Thivolet C, Peix JL, Boulkroun S, Clauser E, Zennaro MC. Aldosterone-producing adenoma with a somatic KCNJ5 mutation revealing APC-dependent familial adenomatous polyposis. *J Clin Endocrinol Metab*. 2016;101:3874-8.
78. Casamassimi A, Federico A, Rienzo M, Esposito S, Ciccodicola A. Transcriptome profiling in human diseases: new advances and perspectives. *Int J Mol Sci*. 2017;18:1652.
79. Pease J, Sooknanan R. A rapid, directional RNA-seq library preparation workflow for Illumina® sequencing. *Nature Methods*. 2012;9:i-ii.
80. Anamika K, Verma S, Jere A, Desai A. Transcriptomic profiling using next generation sequencing - advances, advantages, and challenges. In: Kulski JK, editor. *Next generation sequencing - advances, applications and challenges*. IntechOpen; 2016.
81. Aristizabal Prada ET, Castellano I, Sušnik E, Yang Y, Meyer LS, Tetti M, Beuschlein F, Reincke M, Williams TA. Comparative genomics and transcriptome profiling in primary aldosteronism. *Int J Mol Sci*. 2018;19:1124.
82. Williams TA, Monticone S, Crudo V, Warth R, Veglio F, Mulatero P. Visinin-like 1 is upregulated in aldosterone-producing adenomas with KCNJ5 mutations and protects from calcium-induced apoptosis. *Hypertension*. 2012;59:833-9.
83. Kobuke K, Oki K, Gomez-Sanchez CE, Gomez-Sanchez EP, Ohno H, Itcho K, Yoshii Y, Yoneda M, Hattori N. Calneuron 1 increased Ca²⁺ in the endoplasmic reticulum and aldosterone production in aldosterone-producing adenoma. *Hypertension*. 2018;71:125-33.
84. Ye P, Mariniello B, Mantero F, Shibata H, Rainey WE. G-protein-coupled receptors in aldosterone-producing adenomas: a potential cause of hyperaldosteronism. *J Endocrinol*. 2007;195:39-48.
85. Maniero C, Garg S, Zhao W, Johnson TI, Zhou J, Gurnell M, Brown MJ. NEFM (Neurofilament Medium) polypeptide, a marker for zona glomerulosa cells in human adrenal, inhibits D1R (Dopamine D1 Receptor)-mediated secretion of aldosterone. *Hypertension*. 2017;70:357-64.
86. Williams TA, Monticone S, Morello F, Liew CC, Mengozzi G, Pilon C, Asioli S, Sapino A, Veglio F, Mulatero P. Teratocarcinoma-derived growth factor-1 is upregulated in aldosterone-producing adenomas and increases aldosterone secretion and inhibits apoptosis in vitro. *Hypertension*. 2010;55:1468-75.

-
87. Teo AE, Garg S, Johnson TI, Zhao W, Zhou J, Gomez-Sanchez CE, Gurnell M, Brown MJ. Physiological and pathological roles in human adrenal of the glomeruli-defining matrix protein NPNT (Nephronectin). *Hypertension*. 2017;69:1207-16.
88. Wang T, Rainey WE. Human adrenocortical carcinoma cell lines. *Mol Cell Endocrinol*. 2012;351:58-65.
89. Gazdar AF, Oie HK, Shackleton CH, Chen TR, Triche TJ, Myers CE, Chrousos GP, Brennan MF, Stein CA, La Rocca RV. Establishment and characterization of a human adrenocortical carcinoma cell line that expresses multiple pathways of steroid biosynthesis. *Cancer Res*. 1990;50:5488-96.
90. Rainey WE, Saner K, Schimmer BP. Adrenocortical cell lines. *Mol Cell Endocrinol*. 2004;228:23-38.
91. Wang T, Rowland JG, Parmar J, Nesterova M, Seki T, Rainey WE. Comparison of aldosterone production among human adrenocortical cell lines. *Horm Metab Res*. 2012;44:245-50.
92. Parmar J, Key RE, Rainey WE. Development of an adrenocorticotropin-responsive human adrenocortical carcinoma cell line. *J Clin Endocrinol Metab*. 2008;93:4542-6.
93. Belavgeni A, Bornstein SR, von Mässenhausen A, Tonnus W, Stumpf J, Meyer C, Othmar E, Latk M, Kanczkowski W, Kroiss M, Hantel C, Hugo C, Fassnacht M, Ziegler CG, Schally AV, Krone NP, Linkermann A. Exquisite sensitivity of adrenocortical carcinomas to induction of ferroptosis. *Proc Natl Acad Sci U S A*. 2019;116:22269-74.
94. Weigand I, Schreiner J, Röhrig F, Sun N, Landwehr LS, Urlaub H, Kendl S, Kiseljak-Vassiliades K, Wierman ME, Angeli JPF, Walch A, Sbiera S, Fassnacht M, Kroiss M. Active steroid hormone synthesis renders adrenocortical cells highly susceptible to type II ferroptosis induction. *Cell Death Dis*. 2020;11:192.
95. Dixon SJ, Lemberg KM, Lamprecht MR, Skouta R, Zaitsev EM, Gleason CE, Patel DN, Bauer AJ, Cantley AM, Yang WS, Morrison B, 3rd, Stockwell BR. Ferroptosis: an iron-dependent form of nonapoptotic cell death. *Cell*. 2012;149:1060-72.
96. Galluzzi L, Vitale I, Aaronson SA, Abrams JM, Adam D, Agostinis P, Alnemri ES, Altucci L, Amelio I, Andrews DW, Annicchiarico-Petruzzelli M, Antonov AV, Arama E, Baehrecke EH, Barlev NA, Bazan NG, Bernassola F, Bertrand MJM, Bianchi K, Blagosklonny MV, Blomgren K, Borner C, Boya P, Brenner C, Campanella M, Candi E, Carmona-Gutierrez D, Cecconi F, Chan FK, Chandel NS, Cheng EH, Chipuk JE, Cidlowski JA, Ciechanover A, Cohen GM, Conrad M, Cubillos-Ruiz JR, Czabotar PE, D'Angiolella V, Dawson TM, Dawson VL, De Laurenzi V, De Maria R, Debatin KM, DeBerardinis RJ, Deshmukh M, Di Daniele N, Di Virgilio F, Dixit VM, Dixon SJ, Duckett CS, Dynlacht BD, El-Deiry WS, Elrod JW, Fimia GM, Fulda S, Garcia-Saez AJ, Garg AD, Garrido C, Gavathiotis E, Golstein P, Gottlieb E, Green DR, Greene LA, Gronemeyer H, Gross A, Hajnoczky G, Hardwick JM, Harris IS, Hengartner MO, Hetz C, Ichijo H, Jaattela M, Joseph B, Jost PJ, Juin PP, Kaiser WJ, Karin M, Kaufmann T, Kepp O, Kimchi A, Kitsis RN, Klionsky DJ, Knight RA, Kumar S, Lee SW, Lemasters JJ, Levine B, Linkermann A, Lipton SA, Lockshin RA, Lopez-Otin C, Lowe SW, Luedde T, Lugli E, MacFarlane M, Madeo F, Malewicz M, Malorni W, Manic G, Marine JC, Martin SJ, Martinou JC, Medema JP, Mehlen P, Meier P, Melino S, Miao EA, Molkenkin JD, Moll UM, Munoz-Pinedo C, Nagata S, Nunez G, Oberst A, Oren M, Overholtzer M, Pagano M, Panaretakis T, Pasparakis M, Penninger JM, Pereira DM, Pervaiz S, Peter ME, Piacentini M, Pinton P, Prehn JHM, Puthalakath H, Rabinovich GA, Rehm M, Rizzuto R, Rodrigues CMP, Rubinsztein DC, Rudel T, Ryan KM, Sayan E, Scorrano L, Shao F, Shi Y, Silke J,

Simon HU, Sistigu A, Stockwell BR, Strasser A, Szabadkai G, Tait SWG, Tang D, Tavernarakis N, Thorburn A, Tsujimoto Y, Turk B, Vanden Berghe T, Vandenabeele P, Vander Heiden MG, Villunger A, Virgin HW, Vousden KH, Vucic D, Wagner EF, Walczak H, Wallach D, Wang Y, Wells JA, Wood W, Yuan J, Zakeri Z, Zhivotovsky B, Zitvogel L, Melino G, Kroemer G. Molecular mechanisms of cell death: recommendations of the nomenclature committee on cell death 2018. *Cell Death Differ.* 2018;25:486-541.

97. Yang Y, Burrello J, Burrello A, Eisenhofer G, Peitzsch M, Tetti M, Knösel T, Beuschlein F, Lenders JWM, Mulatero P, Reincke M, Williams TA. Classification of microadenomas in patients with primary aldosteronism by steroid profiling. *J Steroid Biochem Mol Biol.* 2019;189:274-82.

98. Yang Y, Tetti M, Vohra T, Adolf C, Seissler J, Hristov M, Belavgeni A, Bidlingmaier M, Linkermann A, Mulatero P, Beuschlein F, Reincke M, Williams TA. *BEX1* is differentially expressed in aldosterone-producing adenomas and protects human adrenocortical cells from ferroptosis. *Hypertension.* 2021. [Epub ahead of print].

99. Yang Y, Gomez-Sanchez CE, Jaquin D, Aristizabal Prada ET, Meyer LS, Knösel T, Schneider H, Beuschlein F, Reincke M, Williams TA. Primary aldosteronism: *KCNJ5* mutations and adrenocortical cell growth. *Hypertension.* 2019;74:809-16.

Acknowledgements

I would like to express my gratitude to all the people who have provided me with kind and precious support during the journey of obtaining my doctoral degree.

I would like to thank my supervisor **Prof. Dr. Martin Reincke** for providing me the opportunity to work in his lab and the possibility to obtain my doctoral degree focusing on the research field of primary aldosteronism. I genuinely thank for his unreserved support and insightful suggestions of my doctoral project.

I am extremely thankful to **Dr. Tracy Ann Williams** for her co-supervision of my doctoral project and valuable guidance and care throughout my doctoral training. I have truly learned a lot from her mentorship, not only about research but also about the attitude and working style to make things perfect. I genuinely thank her for her encouragement and support to advance my English and all kinds of skills required in research. I consider myself extremely fortunate that I got the opportunity to work in her research group. It has been a wonderful and enriching experience.

I am thankful to my Thesis Advisory Committee members, **Prof. Dr. Jacques Lenders** and **Prof. Dr. Celso E. Gomez Sanchez**, for their time and consideration and their insightful suggestions for my thesis project.

I would like to thank **Prof. Dr. Paolo Mulatero** for providing patient data and samples from Turin and for his kindness to give me help and support.

I thank **Lucie Meyer** for being a helpful and co-operative colleague. She is always willing to offer help, share information and knowledge, and be a good listener whenever I have difficulties. It has been a pleasant experience to have her around throughout my doctoral training.

I would like to thank **Isabella-Sabrina Kinker, Diana Jaquin, Petra Rank, Youssra Mohammed Ahmed, Eva Sušnik** and **Brigitte Mauracher** for their technical assistance and support.

I would like to thank **Dr. Twinkle Vohra, Dr. Holger Schneider,** and **Siyuan Gong** for their valuable scientific discussions.

I would like to thank **Dr. Jacopo Burrello** for his statistical assistances.

I would like to thank **Dr. Mattina Tetti, Nina Nirschl** and **Lisa Sturm** for the collection and management of patient data and samples.

I would like to thank **Dr. Dunja Reiss** and **Dr. Stefanie Meyer** for their help in all the administrative works.

I am grateful to **China Scholarship Council** for funding a considerable period of my doctoral training.

I am thankful to **CRC/TRR 205** for funding our project and providing me with scientific trainings, and I also thank **Eva Spickenheuer** and **Dr. Nicole Bechmann** for organizing these wonderful scientific trainings.

I would also like to thank **Theodora Astalaki, Nicolas Meese, Wei Zhang, Xiao Wang, Yao Meng, Sicheng Tang, Yichen Zhang, Ru Zhang, Jing Ju** and **Xiao Chen** for their generous help and for a delightful time in the department.

Finally, I would like to thank my family, my beloved parents, husband and brother, who have always loved me and supported me unconditionally, and given me a lot of confidence throughout

these years. I appreciated all the help from my husband who was also pursuing the doctoral degree in medicine and has given me a lot of technical advices and inspiring ideas.